รายงานสรุปความก้าวหน้าของโครงการในรอบ 3 ปี

โครงการวิจัย: การศึกษาตัวเร่งปฏิกิริยาสำหรับใช้ในอุตสาหกรรมปิโตรเคมีและใช้กำจัดมลพิษทางอากาศ

A study of catalysts for petrochemical industry and for air pollution abatement

(สัญญาเลขที่ RTA/02/2540)

โดย ศ.ดร. ปิยะสาร ประเสริฐธรรม

จุฬาลงกรณ์มหาวิทยาลัย

สัญญาเลขที่ RTA/02/2540.

โครงการวิจัย: การศึกษาตัวเร่งปฏิกิริยาสำหรับใช้ในอุตสาหกรรมปิโตรเคมีและใช้กำจัดมลพิษทางอากาศ

A study of catalysts for petrochemical industry and for air pollution abatement

รายงานสรุปความก้าวหน้าของโครงการในรอบ 3 ปี

ชื่อหัวหน้าโครงการ ศ.ดร. ปิยะสาร ประเสริฐธรรม

รายงานในช่วงเวลาตั้งแต่วันที่ 1 ธันวาคม พ.ศ. 2541 **ถึง** 30 พฤศจิกายน พ.ศ. 2543

1. กิจกรรมที่ได้ดำเนินการ

1.1 ด้านการประสานงานระหว่างผู้ดำเนินการ

- เนื่องจากคณะผู้ดำเนินการประกอบด้วยอาจารย์จากหลายสถาบัน ดังนั้นการปรึกษางานจึงทำด้วยวิธีต่อไปนี้

- อ.ดร. นุรักษ์ กฤษดานุรักษ์ จากมหาวิทยาลัยขอนแก่น ใช้การติดต่อทางโทรศัพท์ และเดินทางมาจุฬาลงกรณ์มหาวิทยาลัย
- ผศ.ดร. ชาคริต ทองอุไร จากมหาวิทยาลัยสงขลานครินทร์ ใช้การติดต่อทางโทรศัพท์ และเดินทางมาจุฬาลงกรณ์มหาวิทยาลัย
- อ.ดร. วรากรณ์ ธนะกุลรังสรรค์ จากสถาบันเทคโนโลยีราชมงคล วิทยาเขตเทคนิค-กรุงเทพ ใช้การติดต่อทางโทรศัพท์ และเดินทางมาจุฬาลงกรณ์มหาวิทยาลัย

1.2 ด้านการเข้าร่วมประชุมทางวิชาการระดับนานาชาติ

1.2.1 การสัมมนาทางวิชาการ 15th Canadian Symposium on Catalysis" ที่ประเทศคานาดา ในวันที่ 17-20 พฤษภาคม พ.ศ. 2541

1. "Effect of NO on Coke Formation for Propane and Propene Conversion via Cu/Na-ZSM-5 Catalyst"

2. "Determination of Coke Propagation on Metal and Support of Pt/Al2O3 by Using Schulz-Flory Distribution Theory"
3. "Comparative Study of Coke Deposition on Pt Catalysts in Reactions with and with out Oxygen"

1.2.2 Regional Symposium on Chemical Engineering ณ ประเทศมาเลเซีย (2540)

1. "Determination of high temperature coke deposition on metal active sites of propane dehydrogenation catalysts"
2. "Adsorption study on Cu/ZSM-5 of NO Reduction by Hydrocarbon using Transient Technique"

1.2.3 Regional Symposium on Chemical Engineering ณ ประเทศฟิลิปปินส์ (2541)

1. "The Effect of NO on Coke Formation over Pt Catalyst in NO Reduction by Propene under Lean-Burn Condition"
2. "Determination of Coke Propagation on Metal and Support of Pt/Al_2O_3 by Using Schulz-Flory Distribution Theory"

1.2.4 Miami 2nd World Congress on Environmental Catalysis ณ ประเทศสหรัฐอเมริกา (2541)

1. "Removal of Automotive Emissions By Co/Pd Three-way Catalysts"
2. "Relationship Between Coke Formation , Hydrocarbon and NO Conversion on Selective Catalytic Reduction of NO by Propene on Cu/Na –ZSM-5 with Excess Oxygen",
3. "Role of NO Propene and NO Conversion over Pt/ Al_2O_3 Catalyst under Lean-Burn Condition at low temperature"

1.2.5 The 8th Congress of Asian Pacific Conference of Chemical Engineering ที่เมืองโซล ประเทศเกาหลี ระหว่างวันที่ 16 – 19 สิงหาคม พ.ศ. 2542

1. "Influence of Fe and Zn loading method over MFI- type zeolite catalysts on toluene methylation"
2. "Aromatization of light paraffins over metal-containing MFI-type catalysts"
3. "Catalytic cracking of n-octane over Y-type zeolite catalyst"
4. "Isomerization of n-Hexane over beta zeolite"

1.2.6 งานประชุมทางวิชาการระดับนานาชาติ The Regional Symposium on Chemical Engineering 1999 ที่จังหวัดสงขลา ระหว่างวันที่ 22 – 24 พฤศจิกายน พ.ศ. 2542

1. "Synergistic effect in catalytic hydrogenation on modified supported nickel catalyst by platinum"
2. "Oxidation of C_3H_8, C_3H_6 and CO over V-Mg-O/TiO_2 catalyst"

3. "Oxidation of C_3H_8, C_3H_6 and CO over Co-Mg-O/TiO_2 catalyst"
4. "The use of infrared-spectroscopy in studies of metal oxide surfaces: experience on experimental procedure"
5. "Dehydrogenation of propane in a palladium membrane reactor"
6. "Oxidative dehydrogenation of butane in a ceramic membrane reactor"

1.2.7 การสัมมนาทางวิชาการ 2nd Asia Pacific Congress on Catalysis APCAT 2000" ที่ประเทศออสเตรเรีย ในวันที่ 31 มกราคม – 3 กุมภาพันธ์ พ.ศ. 2543

1. "Activation of acetylene selective hydrogenation catalysis using oxygen containing compound"
2. "Influence of Fe or Zn loading method over MFI type zeolite catalysts on toluene methylation"
3. "Determination of coke propagation on metal and support of Pt/Al_2O_3 using Schulz-Flory distribution theory"
4. "Effect of Lantana on SiO_2-supported Pd catalyst over catalytic coversion of ethanol to syngas"
5. "Non oxidative methane coupling over Co-ion exchanged Y type zeolite"

1.3 การประชุมทางวิชาการระดับนานาชาติที่กำลังจะเข้าร่วม

1.3.1 งานประชุมทางวิชาการระดับนานาชาติ The Regional Symposium on Chemical Engineering 2000 ที่ National University of Singapore ระหว่างวันที่ 10 – 12 ธันวาคม พ.ศ. 2543

1. "Ethanol and 1-propanol oxidation over supported cobolt oxide catalyst"
2. "Monocyclopentadienyl Metallocene catalyst with methylaluminoxane as cocatalyst for styrene polymerization"
3. "Kinetics of Liquid Phase Synthesis of Ethyl *tert*-Butyl Ether from *tert*-Butyl Alcohol and Ethanol Catalyzed by β-Zeolite"

1.3.2 งานประชุมวิชาการระดับนานาชาติ Bangkok International Conference on Catalysis จัดที่ โรงแรมมณฑียรริเวอร์ไซด์ วันที่ 7-9 มกราคม 2544

1. "Design of Electrode Catalyst for Solid Oxide Fuel Cell Type Reactor"
2. "Application of a palladium membrane reactor to the dehydrogenation of ethylbenzene to styrene"
3. "Cumene synthesis from benzene and isopropanol over zeolite"

4. "Oxidation of alcohol's to aldehyde over V-MgO/TiO_2 catalyst"
5. "Effect of the preparation with O_2 and/or O_2-containing compounds on the catalytic performance of Pd-Ag/Al_2O_3 for the selective hydrogenation of acetylene"

1.4 การเสนอผลงานในที่ประชุมวิชาการในประเทศไทย

1.4.1 การประชุมทางวิชาการวิศวกรรมเคมีและเคมีประยุกต์แห่งประเทศไทย ครั้งที่ 8 ณ มหาวิทยาลัยมหิดล วันที่ 17 – 18 ธันวาคม พ.ศ. 2541

1. "Role of External Electron Donor in Supported Ziegler-Natta Catalyst on Isotacticity of Polypropylene"
2. "ผลของตัวรองรับที่มีต่อคุณสมบัติในการออกซิเดชันของโคบอลต์ออกไซด์"
3. "ผลของลำดับการเติมทังสเตนบนตัวเร่งปฏิกิริยาวานาเดียมออกไซด์บนตัวรองรับไททาเนียมออกไซด์ที่ใช้ในการเลือกกำจัดแก๊สไนตริกออกไซด์"
4. "บทบาทความเป็นกรดของพื้นผิวตัวเร่งปฏิกิริยาวานาเดียม (V) ออกไซด์บนไททาเนียม (IV) ออกไซด์ต่อความว่องไวในการเกิดปฏิกิริยาการเลือกรีดิวซ์ไนตริกออกไซด์ด้วยแอมมอเนีย"
5. "คุณสมบัติในการออกซิเดชันของตัวเร่งปฏิกิริยาวาเนเดียมแมกนีเซียออกไซด์บนตัวรองรับไทเทเนียมออกไซด์"

1.4.2 การประชุมทางวิชาการครั้งที่ 37 ณ มหาวิทยาลัยเกษตรศาสตร์ วันที่ 23 กุมภาพันธ์ พ.ศ. 2542

1. "Dehydrogenation of Propane in a Palladium Membrane Reactor: ii) Determination of the rate law for the dehydrogenation of propane on Pt-Sn-K/Al_2O_3 catalyst"

1.4.3 การประชุมทางวิชาการครั้งที่ 38 ณ มหาวิทยาลัยเกษตรศาสตร์ วันที่ 1-4 กุมภาพันธ์ พ.ศ. 2543

1. "การศึกษาปฏิกิริยาออกซิเดทีฟดีไฮโดรจีเนชันของบิวเทนในเครื่องปฏิกรณ์แบบอินเนอร์ทเมมเบรน"

1.4.4 การประชุมทางวิชาการวิศวกรรมเคมีและเคมีประยุกต์แห่งประเทศไทย ครั้งที่ 10 ณ BITECH วันที่ 24-25 ตุลาคม พ.ศ. 2543

1. "Photocatalytic Decomposition of 2-propanol over TiO_2 catalyst"
2. "Surface basicity characterization using probe molecule adsorption"
3. "การผลิตซินดิโอแทคติคพอลิสไตรีนโดยใช้ไตรเอทิลอะลูมินัมเป็นสารกระตุ้น"

2. ผลงาน

2.1 บทความวิจัยในวารสารระดับนานาชาติ จำนวน 18 ผลงาน

1. "Determination of coke Deposition on Metal Active sites of Propane Dehydrogenation Catalysts" *Stud. Surf. Sci. Catal.* vol. 111 (1997) 153. (เอกสารแนบ 1)
2. "Comparative study of Coke Deposition on Catalysts in Reactions with and without oxygen" *Res.Chem.Intermed.* Vol. 24 No 5 (1998) 605. (เอกสารแนบ 2)
3. "Role of Pt and Alumina during the oxidation of Coke Deposits on Propane Dehydrogenation Catalysts" *Korean Journal of Chemical Engineering*, vol. 15(1998) 486. (เอกสารแนบ 3)
4. "Transient study of the effect of residual cation in in Cu/ZSM-5 for SCR of NO by hydrocarbon" *Chemical Engineering Science* vol. 55 (2000) 2249. (เอกสารแนบ 4)
5. "Influence of Fe or Zn loading Methane, over MFI Type Zeolite Catalysts on Toluene Methylation," *Korean Journal of Chemical Engineering* vol. 17 (2000) 414. (เอกสารแนบ 5)
6. "Activation of Pd-Ag Catalyst for selective hydrogenation of acetylene via nitrous oxide addition," *Reaction Kinetics and Catalysis Letters* vol. 70 (2000) 125. (เอกสารแนบ 6)
7. "Coke formation over Pt-Sn-K/Al_2O_3 in C_3, C_5, C_5-C_8 alkane dehydrogenation" *Chemical Engineering Journal* vol. 77(2000) 215. (เอกสารแนบ 7)
8. "Oxidative Coupling of Methane in a Ceramic Membrane Uniform oxygen Permeation Pattern, *J. Chin. Inst. Chem. Engrs*, vol. 31 (2000) 19. (เอกสารแนบ 8)
9. "Kinetics for the dehydrogenation of propane on Pt-Sn-K/Al2O3 catalyst" *Journal of Chemical Engineering of Japan* vol. 33 No. 3 (2000) 529. (เอกสารแนบ 9)
10. "Dependence of hydrogen pressure on the permeation rate of hydrogen through a composite palladium membranes" *Journal of Chemical Engineering of Japan* vol. 33 No. 2 (2000) 330. (เอกสารแนบ 10)
11. "The effect of direction of hydrogen permeation on the rate through a composite palladium membrane" *Journal of Membrane Science* vol. 175 (2000) 19. (เอกสารแนบ 11)
12. "Synthesis of large-surface area silica-modified titania ultrafine particles by the glycothermal method" *J. of Materials Science Letters* vol. 19 (2000) 1439. (เอกสารแนบ 12)
13. " Selective Oxidation of Ethanol and 1-Proponol over V-Mg-O/TiO_2 catalyst", Chemistry Letter (2000) 968-969. (เอกสารแนบ 13)
14. "Deactivation of the metal and acedic function for Pt, Pt-Sn, Pt-Sn-K using physically mixed catalyst" *Korean J. of Chem. Eng.* vol. 17 (2000) 548. (เอกสารแนบ 14)

15. "Activation of Acetylene Selective Hydrogenation Catalysts using oxygen containing Compounds" *Catalysis Today* (accepted 29 August 2000). (เอกสารแนบ 15)
16. "Effect of organic solvents on the thermal stability of porous silica-modified alumina powders prepared via one pot solvothermal synthesis" *Inorg. Chem. Commu.* (accepted Aug 16, 2000). (เอกสารแนบ 16)
17. "Effect of Pd on the stability improvement of Cu/H-MFI for NO removal under hydrothermal pretreatment condition" *J. Molecular Catalysis* (accepted September 30, 2000). (เอกสารแนบ 17)
18. Isomerization of n-hexane over Pt ion exchanged β zeolite. Reaction Kinetics and Catalysis Letters 2000 (accepted October, 2000) (เอกสารแนบ 18)

2.2 จำนวนผลงานที่อยู่ในขั้นตอนการแก้ไข จำนวน 5 ผลงาน

1. "Selective oxidation of achohols over Co-Mg-O catalyst" นำเสนอในวารสาร Journal of the Chinese Institute of Chemical Engineers ขณะนี้อยู่ในขั้นตอนการพิจารณาต้นฉบับที่ผ่านการแก้ไขแล้ว
2. " The catalytic performance for NO elimination of Co- and Cu-species in MFI zeolite and the effect of high temperature calcination on the state of copper" เสนอในวารสาร Microporous and Mesoporous Material ขณะนี้อยู่ในขั้นตอนการพิจารณาต้นฉบับที่ผ่านการแก้ไขแล้ว
3. "Cooperative effect of Pt and alumina on catalyst deactivation for dehydrogenation reaction" เสนอในวารสาร Reaction Kinetics and Catalysis Letters ขณะนี้อยู่ในขั้นตอนการแก้ไข
4. "Role of Sn and K on Hydrogen Spillover on Pt/γ-Al_2O_3 Catalyst" นำเสนอในวารสาร Journal of the Chinese Institute of Chemical Engineers ขณะนี้อยู่ในขั้นตอนการแก้ไข
5. "Effect of organic solvent on the synthesis of silica modified titanium (IV) oxide นำเสนอในวารสาร Journal of the Chemical Engineering of Japan ขณะนี้อยู่ในขั้นตอนการแก้ไข

2.3 ผลงานที่อยู่ระหว่างการพิจารณา จำนวน 3 ผลงาน

1. "Effect of pretreatment of O_2 and O_2-containing compounds on the catalytic performance of Pd-Ag/Al_2O_3 for acetylene dehydrogenation" เสนอในวารสาร Applied Catalysis A เมื่อ 9 กันยายน 2543
2. "The nature and distribution of coke on the metal sites and the support sites for Pt, Pt-Sn and Pt-Sn-K catalysts applied a physical mixture" เสนอในวารสาร Canadian Journal of Chemical Engineering เมื่อ 20 กรกฎาคม 2543

3. "Application of Ceramic Membrane Reactor to Oxidative Dehydrogenation of *n*-Butane" นำเสนอในวารสาร Chemical Engineering Journal เมื่อ 2 ตุลาคม 2543

2.5 จำนวนนิสิตที่จบ

2.5.1 ดุษฎีบัณฑิต สำเร็จการศึกษาแล้ว 3 คน

1. นาย นครินทร์ มงคลศิริ
2. นาย ธนา พูลทรัพย์สวัสดิ์
3. น.ส. สุนีย์ ศรีหิรัญพัลลภ

2.5.2 มหาบัณฑิต สำเร็จการศึกษาแล้ว 21 คน

1. น.ส. ภาวิณี สินทรโก
2. น.ส. สุภาภรณ์ ขอบุญส่งเสริม
3. น.ส. พูนทรัพย์ ตรีภพนาถกูล
4. นาย อาทิตย์ เนรมิตตกพงษ์
5. นาย เกรียงศักดิ์ ไกรวัฒนวงศ์
6. น.ส. หฤทัย ตั้งอุดมวงษา
7. น.ส. อรวรรณ กนกรัตนา
8. น.ส. นิษฐกานต์ ฉัตรเท
9. น.ส. วิไลวรรณ เยื้องสวัสดิกูล
10. นางสาว ระพีพรรณ เล็กเลิศสุนทร
11. นาย นิพนธ์ คนองชัยยศ
12. นางสาว วนิดา ยังวนิชเศรษฐ
13. นางสาว เพียงพร ล้ออัศจรรย์
14. นางสาว วราภรณ์ มากพูน
15. นาย วิโรจน์ จรลีชาญชัย
16. นาย ศักดิ์ชัย กิตติเกิดกุลชัย
17. นาย สุวัฒน์ ลิ้มตระกูล
18. นางสาว ภูริดา พิมานมาศ
19. นาย พงศ์พรหม เฉลิมวรรณพงศ์
20. นาย ศิพิระ กุหลาบแก้ว
21. นางสาว สุดศิริ เหมศรี

2.6 จำนวนผู้ช่วยศาสตราจารย์ที่ได้

1. ดร. ธราธร มงคลศรี
2. ดร. นุรักษ์ กฤษดานุรักษ์
3. ดร. สุทธิชัย อัสสะบำรุงรัตน์

2.7 จำนวนรองศาสตราจารย์

ผศ.ดร. ธราธร มงคลศรี ได้ยื่นเอกสารเพื่อขอรับการพิจารณาตำแหน่งรองศาตราจารย์เมื่อวันที่ 2 มิถุนายน 2543

2.8 การจัดสัมมนาทางวิชาการ

1. ได้มีการจัดสัมมนาทางวิชาการเมื่อวันที่ 27 พฤศจิกายน พ.ศ. 2541 โดยการสัมมนามีหัวข้อว่า "Recent Development of Catalysis in Thailand" ซึ่งจัดที่ชั้นที่ 12 อาคาร 4 คณะวิศวกรรมศาสตร์ จุฬาลงกรณ์มหาวิทยาลัย
2. ได้มีการจัดสัมมนาทางวิชาการในหัวข้อ "ตัวเร่งปฏิกิริยากับสิ่งแวดล้อม" เมื่อวันที่ 29 พฤศจิกายน 2542 ณ ห้อง 209 ตึก 3 คณะวิศวกรรมศาสตร์ จุฬาลงกรณ์มหาวิทยาลัย
3. ได้มีการจัดสัมมนาทางวิชาการเมื่อวันที่ 6 ตุลาคม พ.ศ. 2543 โดยการสัมมนามีหัวข้อว่า "ตัวเร่งปฏิกิริยากับอุตสาหกรรมปิโตรเคมี" ซึ่งจัดที่ชั้นที่ห้อง 209 ตึก 3 คณะวิศวกรรมศาสตร์ จุฬาลงกรณ์มหาวิทยาลัย

2.9 สรุปผลงาน

ตารางที่ 1 สรุปผลงานตามข้อเสนอโครงการและผลงานในปัจจุบันประจำปี พ.ศ. 2541 - 2543

ผลงาน	ข้อเสนอ	ผลงาน
1. บทความลงวารสารระดับนานาชาติ	17	18 + (5)[1] + (3)[2]
2. ประชุมทางวิชาการระดับนานาชาติ	-	33
3. ประชุมทางวิชาการระดับชาติ	-	10
4. ดุษฎีบัณฑิต	3	3
5. มหาบัณฑิต	21	21
6. รองศาสตราจารย์	1	(1)[3]
7. ผู้ช่วยศาสตราจารย์	2	3
8. การจัดสัมมนาทางวิชาการ	3	3

หมายเหตุ [1] จำนวนบทความลงวารสารระดับนานาชาติที่อยู่ในขั้นตอนการแก้ไข (revised manuscripts)

[2] จำนวนบทความลงวารสารระดับนานาชาติที่อยู่ในขั้นตอนการพิจารณา

[3] ยื่นเอกสารเพื่อขอตำแหน่งรองศาสตราจารย์เมื่อวันที่ 9 มิถุนายน 2543 ขณะนี้อยู่ในขั้นตอนการพิจารณา

ลงนาม .....

(ศ.ดร. ปิยะสาร ประเสริฐธรรม)

หัวหน้าโครงการ

Catalyst Deactivation 1997
C.H. Bartholomew and G.A. Fuentes, editors

Determination of Coke Deposition on Metal Active Sites of Propane Dehydrogenation Catalysts

P.Praserthdam*, T.Mongkhonsi, S.Kunatippapong, B.Jaikaew and N.Lim

Petrochemical Engineering Laboratory, Department of Chemical Engineering,
Faculty of Engineering, Chulalongkorn University, Bangkok 10330 THAILAND.
e-mail : fengpps@chulkn.car.chula.ac.th

Sn and alkali metals (Li, Na and K) can reduce coke covering on the Pt active site of a propane dehydrogenation catalyst, Pt/γ-Al_2O_3. The role of the alkali metals is to increase excess mobile electrons of the catalyst surface. Sn and Sn-alkali metal promoted catalysts show higher excess mobile electrons than unpromoted ones. The excess mobile electrons enhance hydrogen spillover on the catalyst surface, thus reducing the amount of coke deposits.

1. INTRODUCTION

Coking is a common deactivation mode in hydrocarbon conversion processes, involving the deposition of carbonaceous materials on the catalyst surface. Materials deposit may include elemental carbon, high molecular weight polymer and polycyclic aromatics [1,2]. Coke formation involves the metallic and acidic functions of the catalyst with the steps of dehydrogenation, condensation, alkylation and cyclization [3]. The structure of coke is rather complex, containing several different growth forms, which can be grouped into amorphous, filamentous and graphitic platelets [4-6]. The surface on which coke is deposited and their effects on coking can also vary widely. Most metallic catalysts are supported and the metal, the support and metal-support interaction can affect the coking.

The thermodynamics of the dehydrogenation reaction of propane to propene are such that it is desirable to operate at high temperature and low pressure. But these conditions are the conditions that favour coke formation. Therefore, there are many attempts trying to improve the performance of the present catalyst, based on Pt/γ-Al_2O_3, and to develop new catalyst compositions that yield the desired results. Sn and alkali metals are examples of promoter that can increase catalyst resistance to coking [7-11].

In the present work, the effect of Sn and the alkali metals (Li, Na and K) is presented. The main objective is to clarify their role in enhancing coking resistance of the resulting catalyst.

2. EXPERIMENT

Pt/γ-Al_2O_3 (0.3wt%Pt), Pt-Sn/γ-Al_2O_3 (0.3wt%Pt, 0.3wt%Sn), Pt-Sn-Li/γ-Al_2O_3 (0.3wt%Pt, 0.3wt%Sn, 0.6wt%Li), Pt-Sn-Na/γ-Al_2O_3 (0.3wt%Pt, 0.3wt%Sn, 0.6%wtNa), and

Pt-Sn-K/γ-Al_2O_3 (0.3wt%Pt, 0.3wt%Sn, 0.6wt%K) were used in the research. The catalysts were prepared by a conventional dry impregnation method using H_2PtCl_6, $SnCl_2$ and alkali metal nitrates as salt precursors. All chemicals used are normally analytical grade.

Coked catalyst was prepared from the dehydrogenation reaction of C_3H_8 to C_3H_6. 0.1 mg of the catalyst was packed in a quartz reactor. 20% C_3H_8, balanced with N_2 was used as reactant gas. To study the effect of H_2, H_2 was mixed with the reactant gas at a Hydrogen/Hydrocarbon (H/HC) ratio equal to 1. All gas reactants were supplied by Thai Industrial Gas Co.Ltd. and were passed through oxygen and moisture traps before entering the reactor. The reaction was performed at near atmospheric pressure with gas hourly space velocity (GHSV) 25000 hr^{-1}.

Temperature programmed oxidation (TPO) was performed by burning the obtained coked catalyst in 1%O_2 in an He atmosphere. The heating rate was 10°C/min. CO_2 produced was measured using a gas chromatograph equipped with a TCD and an on-line gas sampling valve.

To measure the amount of metal active sites, a CO adsorption technique was used. In the case of fresh or coked samples, the measurement was performed by monitoring the amount of CO adsorbed at room temperature. The % active site covered by coke was defined as (active site lost due to coke coverage)/(active site of fresh catalyst) x 100

The electrical conductivities of all catalyst samples were measured using a Philips PM 6303 automatic RCL meter. The catalyst was first ground to a fine powder and packed into a die. Then the sample was reduced with H_2 for 1 hour. At the end of the reduction period, the powder was pressed at 13.3 MPa for 5 min. The measurement was performed under these condition. This measurement was used only for qualitative guidance.

3. RESULTS AND DISCUSSION

3.1. Temperature programmed oxidation and metal active site measurement

Figure 1 shows the TPO profiles of 0.3%Pt/γ-Al_2O_3, 0.3%Pt-0.3%Sn/γ-Al_2O_3 and 0.3%Pt-0.3%Sn-0.6%Li/γ-Al_2O_3 catalysts. Each sample shows a TPO peak around 460°C. In addition, a small peak around 100°C was observed for all catalysts used in this work. For the same operating conditions, the amount of coke deposit can be arranged in the following order: Sn-promoted > unpromoted > Sn-Li-promoted. However, when based on propane conversion, the following order was found ; unpromoted > Sn-promoted > Sn-Li-promoted. Sn-Na- or Sn-K-promoted catalysts also have less coke than unpromoted and Sn-promoted.

BET surface area and metal active site measured by CO adsorption of the promoted and unpromoted fresh catalysts are shown in Table 1. The addition of Sn significantly reduced the

Table 1 BET surface area and metal active site

Catalyst	Surface area (m^2/g cat)	Metal active site (site/g cat)
γ-Al_2O_3	316	-
0.3%Pt/γ-Al_2O_3	366	1.63×10^{18}
0.3%Pt-0.3%Sn/γ-Al_2O_3	351	0.73×10^{18}
0.3%Pt-0.3%Sn-0.6%Li/γ-Al_2O_3	282	1.17×10^{18}
0.3%Pt-0.3%Sn-0.6%Na/γ-Al_2O_3	289	1.53×10^{18}
0.3%Pt-0.3%Sn-0.6%K/γ-Al_2O_3	304	1.50×10^{18}

number of surface Pt atom. In this case, more than half of the surface Pt atoms disappear. However, the incorporation of the alkali metals can the increase number of surface Pt atoms again. The percentage of metal active site covered by coke is shown in Figure 2. The figure demonstrates that in the low reaction temperature region ,*i.e.* < 550°C, Sn does reduce coke deposits on the metal active site. At higher reaction temperatures, however, adding only Sn does not yield any benefit. The addition of alkali metals to Sn-promoted catalysts significantly increases the metal surface available in both low and high reaction temperature regions.

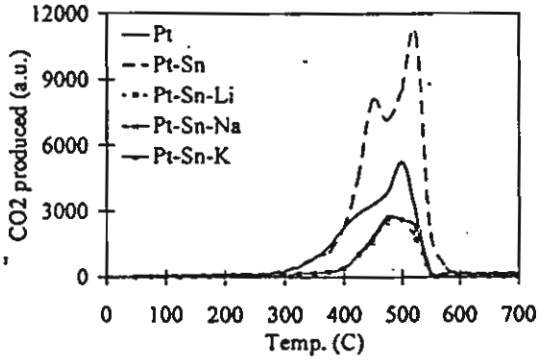

Figure 1 Effect of Sn and alkali metals on TPO spectra. Reaction Temperature 600°C.

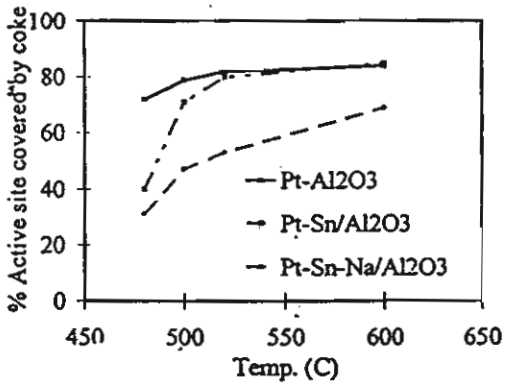

Figure 2 Total coke deposited on the metal active site of various catalysts at different reaction temperatures. H/HC = 0

The effect of hydrogen partial pressure on % active site covered by coke is shown in Figure 3. For Pt/γ-Al_2O_3 catalyst, H_2 decreases coke deposits only in the initial period. On the other hand, on Sn or Sn-Na promoted samples, higher H_2 pressure results in less coke on the metal active sites throughout the reaction period. This underlines the role of Sn and the alkali metals in enhancing the activity of H_2 in the coke elimination process. It should be noted here that coke can cover a fraction of the metal active sites, in accordance with the literature [12,13].

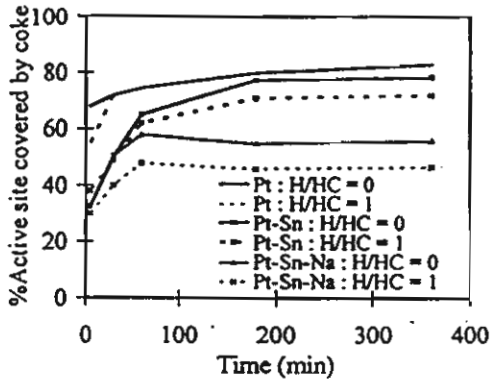

Figure 3 Coke deposit on the metal active site of 0.3%Pt/γ-Al_2O_3, 0.3%Pt-0.3%Sn/γ-Al_2O_3 and 0.3%Pt-0.3%Sn-0.6%Na/γ-Al_2O_3 catalysts at reaction temperature 500°C, H/HC = 0,1.

3.2 Electrical conductivity

Table 2 shows electrical conductivity data of the catalysts and the support. A is the electrical conductivity of alumina. B is the electrical conductivity of Sn and alkali metals promoted alumina. C is the electrical conductivity of Pt catalyst while D is the electrical conductivity of Pt-Sn catalyst. E is the electrical conductivity of Pt-Sn-Alkali metals catalyst. The data shows that the addition of metal to alumina increases electrical conductivity. The addition of Sn to Pt catalyst augments electrical conductivity approximately three times. Further incorporation of the alkali metals results in an order of magnitude further increases.

Since electrical conductivity reflects the mobility of electrons in the bulk solid (14), the data in Table 2 can be used to compare the amount of mobile electrons in each sample. Table 3 shows the amount of excess mobile electrons (in conductivity unit) of the catalysts shown in table 2. The value (B-A) is the electrical conductivity of 0.3wt%Sn added to γ-Al_2O_3 support. The value (D-C) is the electrical conductivity of 0.3wt%Sn added to 0.3%Pt/γ-Al_2O_3 catalyst. If Sn does not have any electronic effect on the Pt site, the value (B-A) should be equal to the value (D-C). The calculation, however, clearly indicates that 0.3wt%Sn loaded on 0.3%Pt/γ-Al_2O_3 catalyst does provide more mobile electrons to the catalyst than its presence on γ-Al_2O_3 support. The addition of alkali metals also shows an interesting result. The value (E-D) is the increase in electrical conductivity of 0.3%Pt-0.3%Sn/γ-Al_2O_3 after 0.6wt% of the alkali metals was added. The result demonstrates that the alkali metals greatly increase the amount of the excess mobile electrons in the bulk catalysts.

By decreasing the amount of coke, Sn functions by creating an ensemble effect and forming a solid solution with Pt in electron-rich Pt sites [15]. The proposed synergistic model for Sn addition is exhibited in Figure 4. The presence of Sn on Pt surface results in a dilution in the number of large active ensembles of Pt. Thus, it is more difficult for coke molecules to deposit on the metal surface. In addition, Sn also provides some additional electron to Pt site. Not only do the alkali metals not only act as electron donors to Pt [16], but their addition also decreases the acidity of the catalyst, which results in less coke forming on the support. Moreover, the alkali metals also promote hydrogen spillover, which can eliminate some coke already formed on the metal site. The alkali metals also act as textural promoters by reducing

Pt-Sn alloy formation. The synergistic mechanism model for Sn and the alkali metal addition are shown in Figure 5.

Table 2 Electrical conductivity data of catalysts and support

Code	Catalyst	Electrical conductivity ($Ohm^{-1}cm^{-1}$)
A	γ-Al_2O_3	2.15×10^{-6}
B	0.3%Sn/γ-Al_2O_3	3.05×10^{-6}
	0.6%Li/γ-Al_2O_3	5.58×10^{-6}
	0.6%Na/γ-Al_2O_3	5.23×10^{-6}
	0.6%K/γ-Al_2O_3	4.04×10^{-6}
C	0.3%Pt/γ-Al_2O_3	3.25×10^{-6}
D	0.3%Pt-0.3%Sn/γ-Al_2O_3	9.43×10^{-6}
E	0.3%Pt-0.3%Sn-0.6%Li/γ-Al_2O_3	20.3×10^{-6}
	0.3%Pt-0.3%Sn-0.6%Na/γ-Al_2O_3	26.6×10^{-6}
	0.3%Pt-0.3%Sn-0.6%K/γ-Al_2O_3	74.7×10^{-6}

Table 3 Amount of excess mobile electrons on the surface of bulk catalysts (in conductivity units)

Catalysts	Equations	excess mobile electrons ($Ohm^{-1}cm^{-1}$)
0.3%Pt-0.3%Sn/γ-Al_2O_3	(D-C) - (B-A)	5.28×10^{-6}
0.3%Pt-0.3%Sn-0.6%Li/γ-Al_2O_3	(E-D) - (B-A)	7.44×10^{-6}
0.3%Pt-0.3%Sn-0.6%Na/γ-Al_2O_3	(E-D) - (B-A)	14.1×10^{-6}
0.3%Pt-0.3%Sn-0.6%K/γ-Al_2O_3	(E-D) - (B-A)	63.4×10^{-6}

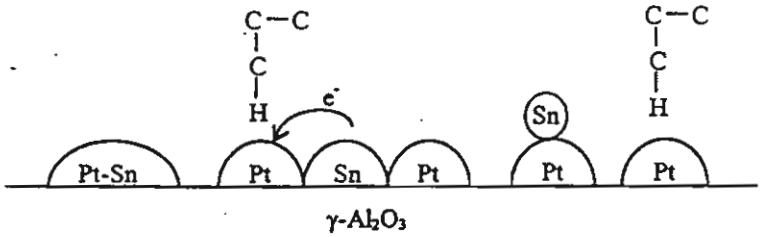

Figure 4 Synergistic mechanism model for Sn addition

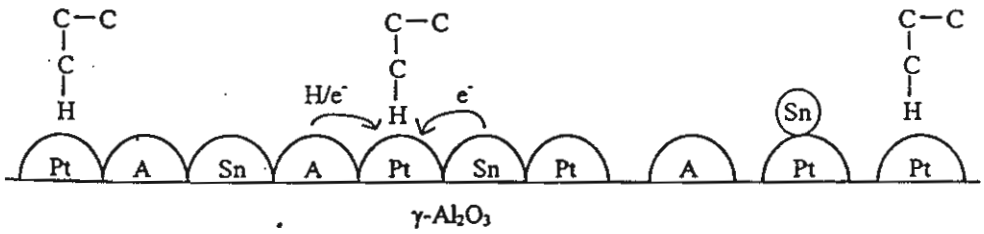

Figure 5 Synergistic mechanism model for Sn and alkali metal (A) addition

4. CONCLUSIONS

Test results reveal that the addition of only Sn or Sn + alkali metals (Li, Na and K) can reduce coke covering on Pt active sites of propane dehydrogenation catalyst, Pt/γ-Al_2O_3. Sn reduces the coke coverage area on the metal active site by creating an ensemble effect and providing additional electrons to Pt atoms. The role of the alkali metals is to increase excess mobile electrons of the catalyst surface and reduce Pt-Sn alloy formation. Sn and Sn-Alkali metal promoted catalysts show higher excess mobile electrons than the unpromoted ones. The additional excess mobile electrons enhance hydrogen spillover on the catalyst surface, thus, reducing the amount of coke deposits on the catalyst surface.

REFERENCES

1. F.Caruso, E.L.Jablonski, J.M.Graw and J.M.Parera, Appl. Catal., 51 (1989) 195.
2. B.C.Gates, J.R..Katzer and G.C.Schuit, Chemistry of Catalytic Processes, McGraw Hill, New York, 1979.
3. J.M.Parera, R.J.Venderone and C.A.Querini in Catalyst Deactivation 1987, B.Delmon and G.F.Froment (eds.), p135, Amsterdam, 1987.
4. H.B.Palmer and C.F.Cullis, Chemistry and Physics of Carbons (vol. 1) p265, Dekker, New York, 1965.
5. R.T.K.Baker and P.S.Harris, Chemistry and Physics of Carbons (vol. 14) p83, Dekker, New York, 1978.
6. B.W.Gainey, U.S. Energy Research and Development Admin. Report. GA-Al 3982, UC-77.
7. J.Barbier in B.Delmon and G.F.Froment (eds.), Catalyst Deactivation 1987 p135, Amsterdam, 1987.
8. J.Barbier, P.Marecot, N.Martin, L.Elassal and R.Maurel in Catalyst Deactivation 1987, B.Delmon and G.F.Froment (eds.),p135, Amsterdam, 1987.
9. R.D.Corright and J.A.Dumesic, J.Catal., 157 (1995) 576.
10. O.A.Barias, A.Holmen and E.A.Blekkan, J.Catal., 158 (1996) 1.
11. S.de Migues, A.Castro, O.Scelza, J.L.G.Fierro and J.Sorin, Catal. Lett., 36 (1996) 201.
12. J.Barbier, G.corro, P.Marecot, J.P.Bournonville and J.P.Frank, React. Kinet. Catal. Lett., 28 (1985) 245.
13. J.Barbier, E.Churin, J.M.Parera and Riviere, React. Kinet. Catal. Lett., 29 (1985) 323.
14. F.W.Sears, M.W.Zemansky and H.D.Yound, University Physics, 5th ed. p784, Addison-Wesley Publishing Company 1981.
15. R..Burch, J. Catal., 71 (1981) 348.
16. J.Oudar, in J. Oudar (ed.), Deactivation and Poisoning of Catalysts, New York, Dekker, 1986.

Res. Chem. Intermed., Vol. 24, No. 5, pp. 605-612 (1998)

COMPARATIVE STUDY OF COKE DEPOSITION ON CATALYSTS IN REACTIONS WITH AND WITHOUT OXYGEN

P. PRASERTHDAM, C. CHAISUK and P. KANCHANAWANICHKUN
Petrochemical Research Laboratory, Department of Chemical Engineering, Chulalongkorn University, Bangkok 10330, Thailand

Received 1 December 1997; accepted 27 November 1997

Abstract—Two types of catalysts, i.e. Pt/γ Al_2O_3 and Cu/Na-ZSM-5, were used to investigate the catalyst activity and amount of coke formation on the spent catalysts. The reactions of particular interest were the hydrocarbon oxidation and the SCR of NO with and without O_2. Propane and propene were used as the hydrocarbon sources. The reaction conditions were as follows: reaction temperature = 170-500°C, GHSV = 4,000 hr^{-1}, TOS = 2 hr, feed composition depending on each reaction, but the composition of gases were fixed as HC = 3,000 ppm, NO = 1,000 ppm and O_2 = 2.5%, using He balance. It was found that both the case of Pt/γ Al_2O_3 and the case of Cu/Na-ZSM-5, propene provided higher conversion and coke deposition than propane in the presence or the absence of O_2 and/or NO. For Pt/γ Al_2O_3 catalyst, in case of the absence of oxygen reactions, the propene conversion dropped more rapidly than the propane conversion. Finally the reaction of propene gave a lower percent of hydrocarbon conversion than the reaction of propane. Additionally, propene had a higher percent selectivity of coke formation for the reaction with the absence of oxygen, but propane had a higher percent selectivity of coke formation for the reaction with the presence of oxygen. For Cu/Na-ZSM-5, in the system with absence and presence of oxygen, the addition of oxygen caused a significant change in % coke selectivity. With the presence of NO_x, the percent conversion of both propane and propene decreased and that the % coke selectivity of propane decreased, whereas that of in propene increased.

INTRODUCTION

Coke deposition is an important deactivation mode in the hydrocarbon conversion process In general, most researchers [1-5] have emphasized only coke formation in reducing atmospheres e.g. dehydrogenation, cracking, reforming etc. Nevertheless, in oxidizing atmospheres, coke deposition can also take place on the catalyst surface. Therefore, in the present work, it is set up to compare the amount of coke formed on Pt/Al_2O_3 and Cu/Na-ZSM-5 catalysts for reactions with the absence and presence of oxygen. The catalytic activity and the amount of coke on the spent Pt/Al_2O_3 and Cu/Na-ZSM-5 catalysts were investigated for reactions with oxygen, *i.e.* hydrocarbon combustion and reduction of NO_X, and without oxygen, *i.e.* dehydrogenation or aromatization and reduction of NO_X. Propane and propene were used as the hydrocarbon sources for all four reactions.

EXPERIMENTAL

Pt/Al_2O_3 (0.3 wt.% Pt) catalyst in this study was prepared by a dry impregnation method using H_2PtCl_6 as the salt precursor. The parent Na-ZSM-5 zeolite with Si/Al ratio of 50 was hydrothermally synthesized from gel and decant solution in an autoclave. The structure of ZSM-5 was confirmed by X-ray diffraction (XRD). Cu/Na-ZSM-5 zeolite was prepared by exchanging Cu^{2+} into Na-ZSM-5 sample in the aqueous solution. The catalytic reactions were carried out at atmospheric pressure in a fixed bed reactor. A 0.5 g of catalyst was packed in a quartz tube reactor. In the case of Cu/Na-ZSM-5, before the reaction, the catalyst was heated under He flow from room temperature to 500°C in 1 hr., and held for 1 hr. before being cooled down. In the case of Pt/Al_2O_3, the catalyst was reduced to 500°C for 1 hr using hydrogen as the reductant gas. The 50 cc./min. of mixed gas feed consisting of 100 ppm NO, 3000 ppm hydrocarbon, 2.5% vol. oxygen and He was introduced to the reactor at a space velocity of 4000 hr^{-1}. The temperatures of the reaction with and without oxygen were 170°C and 350°C (in the case of Pt/Al_2O_3) or 500 °C (in the case of Cu/Na-ZSM-5) respectively. The outlet gases were analyzed by SHIMADZU GC-8APT gas chromatograph with MS-5A column for nitrogen, oxygen and carbon monoxide and with SHIMADZU GC-8AIT porapak QS column for carbon dioxide, propane and propene. Coke deposited on the catalysts was characterized by temperature programmed oxidation (TPO). Before starting the TPO, 0.5 g of the spent catalysts was heated to 130°C at 10°C/min. under He atmosphere and held for 3 hr. The heat treatment removed any air and water that was adsorbed on the catalyst. Then the pretreated sample was heated from 50°C to 700°C with a heating rate of 5°C/min. then in a 30 cc./min. stream of 1% O_2 in helium gas. The carbon dioxide formed was determined by SHIMADZU GC-8AIT gas chromatograph using a thermal conductivity detector with parapak QS column. The percentage of carbon in coke can be calculated from TPO curves. CO_2 area is divided by a internal time in which CO_2 flows through the sampling loop (1 cc.). The rate of CO_2 formation is, hence, obtained. The area under the curve of CO_2 formation rate versus time gives the value of total CO_2 formation. Finally, this value is converted to milligram carbon or percentage of carbon by using a calibration curve.

RESULTS AND DISCUSSION

For the Case of Pt/Al_2O_3

The experimental results were shown in Table 1, Figure 1 and Figure 2. In all four reactions, it was observed that the reactions with propene as a reactant gave a larger percent of hydrocarbon conversion in the initial interval of time on stream and also

Table 1
Hydrocarbon conversion, amount of coke and coke selectivity of 0.3% Pt/Al_2O_3.

Reaction	Reactant	Temperature (°C)	% HC conversion (at 5 min.)	% Carbon in coke	% Selectivity of coke formation
HC	Propane	350	59.36	0.17	0.22
	Propene	350	98.88	0.32	0.27
HC+NO	Propane	350	46.17	0.13	0.19
	Propene	350	66.14	0.16	0.34
$HC+O_2$	Propane	170	11.71	0.13	1.13
	Propene	170	100.00	0.48	0.29
$HC+NO+O_2$	Propane	170	5.59	0.12	1.07
	Propene	170	40.12	0.33	0.54

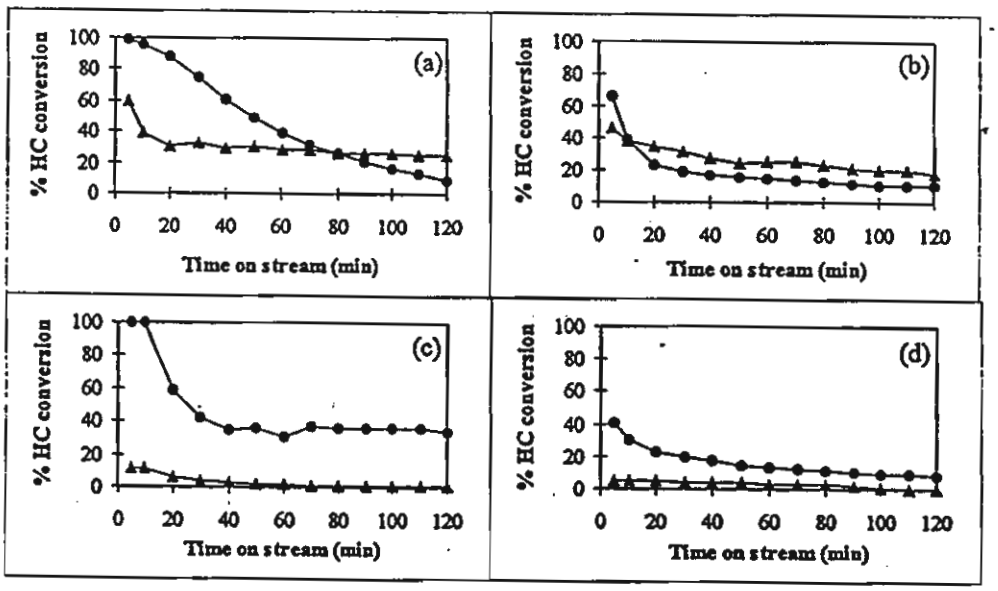

Figure 1. Relationship between % HC conversion versus time on stream. (a) Feed: 3000 ppm HC + He balance, Temperature = 350°C. (b) Feed: 3000 ppm HC + 1000 ppm NO + He balance, Temperature = 350°C. (c) Feed: 3000 ppm HC + 2.5 vol.% O_2 + He balance, Temperature = 170°C. (d) Feed: 3000 ppm HC + 1000 ppm NO + 2.5 vol.% O_2 + He balance, Temperature = 170°C.: (♦) Propane, (●) Propene.

had a larger amount of coke than the reactions with propane as a reactant. However, in the dehydrogenation reaction and NO_x reduction under the absence of oxygen condition, the propene conversion dropped more rapidly than the propane

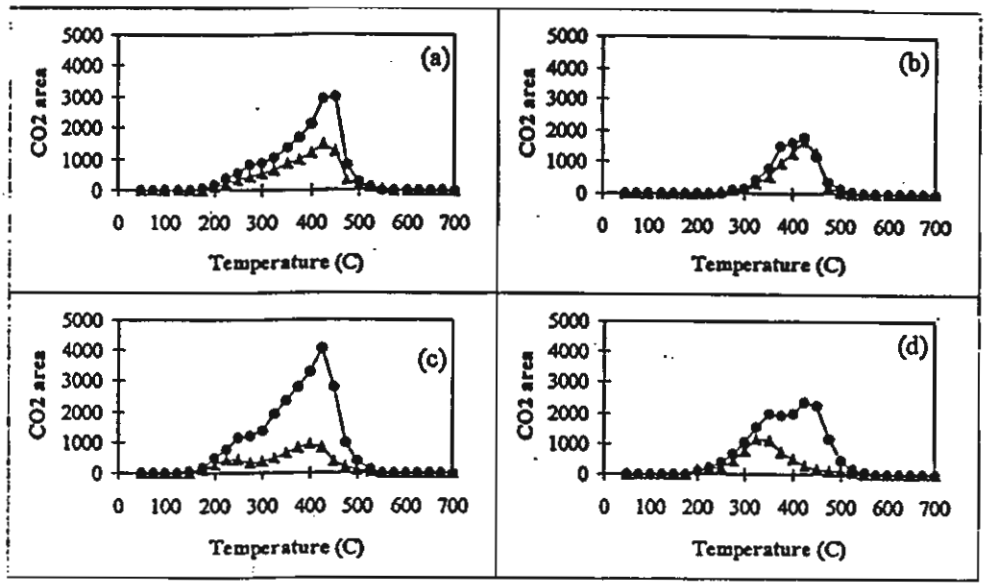

Figure 2. TPO profiles of 0.3 g coked catalyst from reaction. (a) Dehydrogenation, Temperature = 350°C. (b) Reduction of NO_x under absence of oxygen condition, Temperature = 350°C. (c) Combustion, Temperature = 170°C. (d) Reduction of NO_x under absence of oxygen condition, Temperature = 170°C.: (♦) Propane, (●) Propene.

conversion. Finally the reaction of propene gave a lower percent of hydrocarbon conversion than the reaction of propane. It meant that propene is more active than propane [6]. Since propene reacted more, there was more opportunity to convert to coke precursor. Additionally, it was clarified that the product of propene from the reaction with the absence of oxygen, propadiene which is converted irreversibly to ethylidyne leading to coke deposition [7,8], was more reactive than propene [6]. Thus the catalysts in the reaction using propene as a reactant were rapidly covered by carbonaceous deposits. The TPO profiles of 0.3% Pt/Al_2O_3 catalysts are indicated in Figure 2. Each sample showed a TPO peak around 425°C except the TPO profiles of spent catalyst from reduction of NO_X in the presence of oxygen condition. This TPO profiles showed a TPO peak at a temperature of around 325°C for the reaction with propane as a reactant and two peaks at the temperature around 325°C and 425°C for that with propene as a reactant. Barbier *et al.* [3] suggested that the first peak is the coke on metal and the second peak is the coke on the support. In this paper, we define the selectivity of coke formation as the ratio of carbon atom in coke to carbon atom of feed hydrocarbon converted. It was found that propene had a higher percent of selectivity of coke formation for the reaction with the absence of oxygen, but propane had a higher percent of selectivity of coke

formation for the reaction with the presence of oxygen. Under the presence of oxygen, it suggested that coke is formed in parallel with carbon dioxide formation. Propene or coke precursor is more effectively reacted with oxygen to carbon dioxide [9]. Additionally, for the reaction with the presence of oxygen using propane as a reactant, it was observed that the reaction with the absence of NO gave a higher percent of selectivity of coke formation than the reaction with the presence of NO. On the other hand, in the case of propene, the reactant with the presence of NO gave higher percent selectivity of coke formation. It suggests that propane or propene is first reacted with adsorbed oxygen to be converted to intermediates [10,11]. In the case of propane [10,11], these intermediates are preferably reacted with NO which result in, when NO was added in feed, propane producing less selectively of coke formation. However, in the case of propene [12], NO hardly reacted with the intermediates but it preferred to dissociate into dinitrogen. Thus, since the dissociation of NO hinders the reaction of carbon dioxide formation, the intermediates prefer produce coke rather than carbon dioxide for the case of the presence of NO reaction.

For the Case of Cu/Na-ZSM-5

The experimental results were summarized in Figure 3. It was found that the propene conversion was higher than that of propane. This is particularly obvious for the reaction with the presence of oxygen and absence of NO_x as shown in Figure 3(b). Propane conversion was only 10 % ,whereas propene conversion is about 100 %. Figure 3(c),(d) (reduction of NO_x with and without O_2) exhibited the effect of NO_x on the reaction. It was found that the % of propene conversion decreased when NO_x was added, however the % of propene conversion was still higher than that of propane. It means that propene is more active than propane [6]. The temperature program oxidation (TPO) results were shown in Figure 4. It was found that the amount of coke from the four reactions of propene was greater than propane over Cu/Na-ZSM-5 zeolite. The results in Table 2 can suggest that in aromatization, the percentage of propene conversion was greater than that of propane; however, on the other hand, the % coke selectivity of propene was less than that of propane, because propene was converted to product more than to coke while propane formed product less than coke. In the system with absence and presence of oxygen it was found that the addition of oxygen caused a significant change in % of coke selectivity [13-15]. With the presence of NO_x, it was found that the percent conversion of both propane and propene decrease and that the % of coke selectivity of propane decreased whereas that of in propene increased. From this result in the case of propene, we can propose that NO_x was adsorbed on the surface of the catalyst to form an intermediate which is strongly adsorbed and, hence, the desorption rate is slow [16-21]. As a result, the intermediate can not selectively form the product but can be further

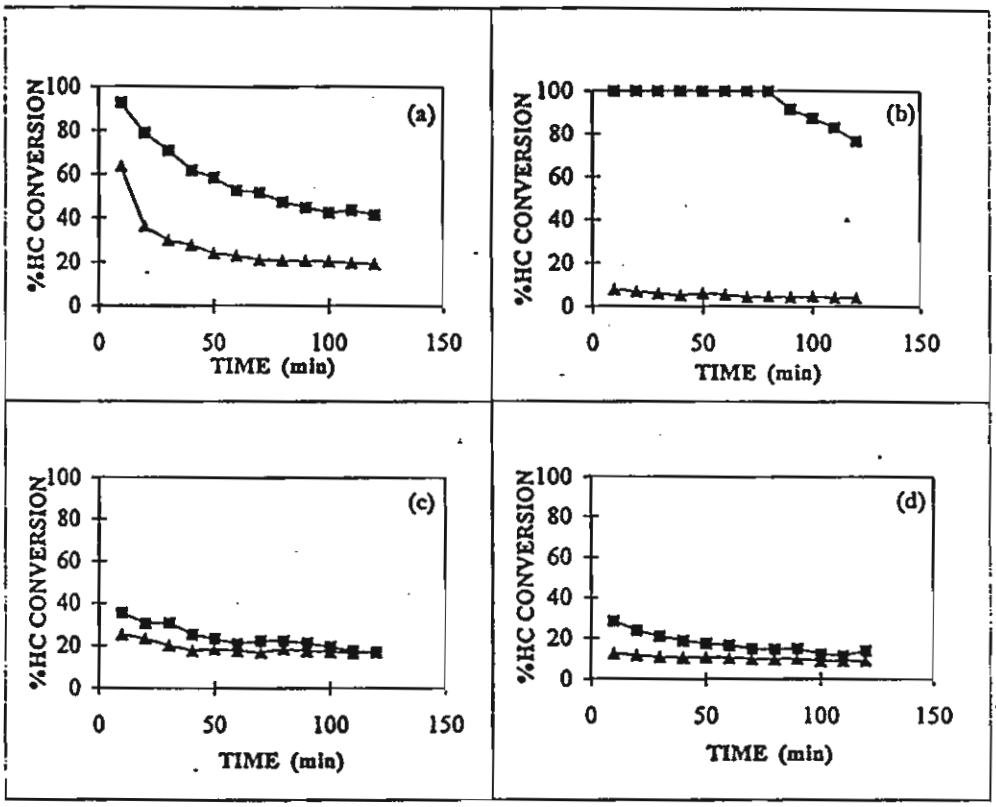

Figure 3. Relationship between % HC conversion versus time over 1.58% Cu/Na-ZSM-5; (a) Feed: 3000 ppm HC + He balance, Temperature = 500°C. (b) Feed: 3000 ppm HC + 2.5 vol.% O_2 + He balance, Temperature = 170°C. (c) Feed: 3000 ppm HC + 1000 ppm NO + He balance, Temperature = 500°C. (d) Feed: 3000 ppm HC + 1000 ppm NO + 2.5 vol.% O_2 + He balance, Temperature = 170°C: (▲) C_3H_8, (■) C_3H_6

converted to coke.

CONCLUSION

Both in the case of Pt/γ Al_2O_3 and in the case of Cu/Na-ZSM-5, propene provided both higher conversion and coke deposition than propane in the presence or the absence of O_2 and/or NO. For Pt/γ Al_2O_3 catalyst, in the case of the absence of oxygen reactions, the propene conversion dropped more rapidly than the propane conversion. Finally, the reaction of propene gave a lower percentage of hydrocarbon conversion than the reaction of propane. Additionally, propene had a higher

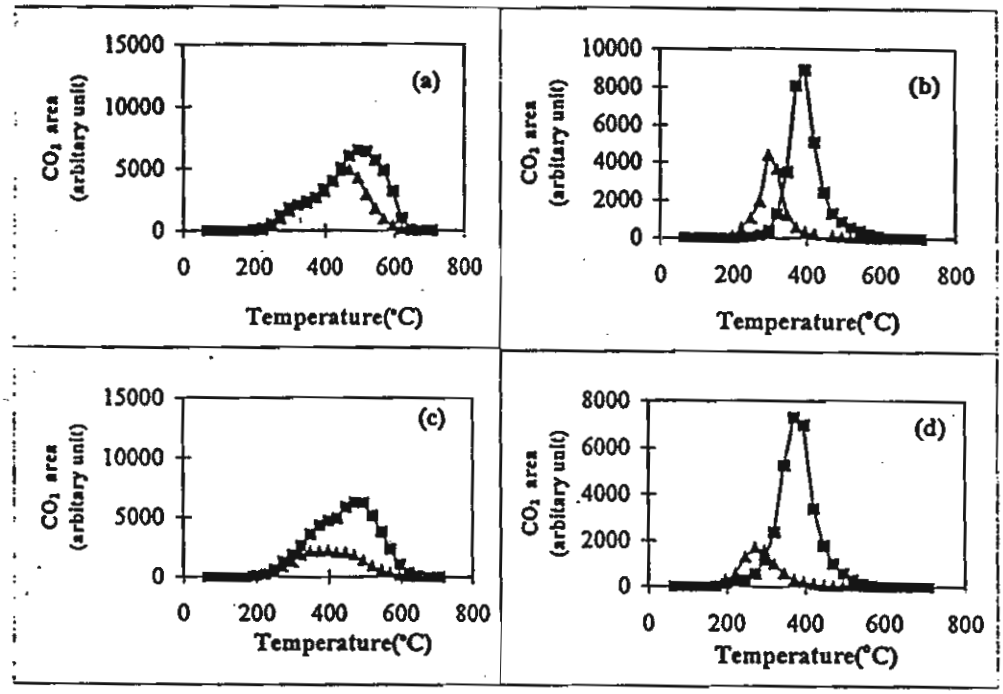

Figure 4. TPO curve of 1.58% Cu/Na-ZSM-5 after the reaction; (a) HC at 500 °C, (b) HC+O_2 at 170 °C, (c) HC+NO at 500 °C, (d) HC+NO+O_2 at 170 °C; (▲) C_3H_8, (■) C_3H_6; In the case of propene (b,d), amount of coked catalyst for TPO is five times than that of propane.

Table 2
Percentage HC conversion and selectivity of coke over 1.58%Cu/Na-ZSM-5

Reaction	Reactant	Temperature (°C)	% HC conversion (at 5 min.)	% Carbon in coke	% Selectivity of coke formation
HC	propane	500	75	0.45	0.74
	propene	500	98	0.68	0.51
HC+O_2	propane	170	9	0.17	1.43
	propene	170	100	2.03	0.86
HC+NO_x	propane	500	26	0.25	0.45
	propene	500	38	0.67	1.51
HC+NO_x+O_2	propane	170	15	0.10	0.39
	propene	170	38	1.82	2.80

percentage of selectivity of coke formation for the reaction with the absence of oxygen but propane had higher percent selectivity of coke formation for the reaction with the presence of oxygen. For Cu/Na-ZSM-5, in the system with absence and presence of oxygen, the addition of oxygen caused a significant change in the % of coke selectivity. With the presence of NO_x, the percent conversion of both propane and propene decreased and that of the % coke selectivity of propane decreased, whereas that in propene increased.

REFERENCES

1. W.G. Appleby, J.W. Gibson, and G.M. Good, *I & EC Process Design and Development* 1, 102 (1962).
2. J.N. Beltramini, E.E. Martinelli, E.J. Churin, N.S. Figoli, and J.M. Parera, *Applied Catalysis* 7, 43 (1983).
3. J. Barbies, *Catalyst Deactivation* 1 (1987).
4. J. Biswas, P.G. Gray, and D.D. Do, *Applied Catalysis* 32, 249 (1987).
5. Mikael Larsson, Magnus Hulten, Edd A Blekkan, and Bengt Andersson, *Journal of Catalysis* 164, 44 (1996).
6. Morrison and Boyd, *Organic Chemistry (sixth edition)*: 122, 287, 410. .
7. Gabor A. Somorjai, *Introduction to Surface Chemistry and Catalysis*: 420.
8. B.J. McIntyre, M. Salmeron, and G.A. Somorjai, *Journal of Catalysis* 164, 184 (1996).
9. R. Burch and T.C. Watling, *Catalysis Letters* 43, 19 (1997).
10. Motoi Sasaki, Hideaki Hamada, Yoshiaki Kintaichi, and Takehiko Ito, *Catalysis Letters 15*, 297 (1992).
11. Megumu Inaba, Yoshiaki Kintaichi, and Hideaki Hamada, *Catalysis Letters* 36, 223 (1996).
12. R. Burch, P.J. Millington, and A.P. Walker, *Applied Catalysis* B4, 65 (1994).
13. J.L. d' Itri and W.M.H. Sachtler, *Catal. Lett.*. 15, 289 (1992).
14. H. Hamada, Y. Kintaichi, M. Sasaki, T. Ito, and M. Tabata, *Appl. Catal*. 64, L1 (1990).
15. A.Yu Stakheev, C.W. Lee, S.P. Park, and P.J.Chong, *Progess in Zeolite and Microporous Materials.*, Vol 105 , 1579 (1997).
16. H. Hamada, Y. Kintaichi, M. Sasaki, M. Tabata, and T. Ito, *Appl. Catal.*, 70, L15 (1991).
17. C.J. Bennett, P.S. Bennett, S.E. Golunski, J.W. Hayes, and A.P. Walliker, *Appl. Catal. A*, 86 L1 (1992).
18. R.Burch and P.J. Millington , *Appl. Catal B:Env*, 2. 101 (1993).
19. M. Iwamoto, H. Yahiro, H. Khin, M.Watanabe, J Gue, M. Konno, T. Chikabisa and T. Murayama, *Appl. Catal* B5., L1 (1994).
20. Chikafumi Yokotama and Makoto Misono, *Journal of Catalysis.*160, 95 (1996).
21. Janos Szanyi and Mark T. Paffett, *Journal of Catalysis.*164 232 (1996).

Korean J. Chem. Eng., 15(5), 486-490 (1998)

ROLES OF Pt AND ALUMINA DURING THE COMBUSTION OF COKE DEPOSITS ON PROPANE DEHYDROGENATION CATALYSTS

Tharathon Mongkhonsi†, Piyasan Prasertdham, Atchara Saengpoo, Nonglak Pinitniyom and Bualom Jaikaew

Department of Chemical Engineering, Faculty of Engineering, Chulalongkorn University, Bangkok 10330, Thailand
(*Received 2 November 1997 • accepted 26 June 1998*)

Table 1. Catalyst composition, surface area and Pt active site

Catalysts	wt% of metal loading					Surface area	Pt active site
	Pt	Sn	Li	Na	K	m^2/g cat	molecule CO/g cat
$Pt/\gamma\text{-}Al_2O_3$	0.3	-	-	-	-	330	5.55×10^{18}
$Pt\text{-}Sn/\gamma\text{-}Al_2O_3$	0.304	0.292	-	-	-	320	3.17×10^{18}
$Pt\text{-}Sn\text{-}Li/\gamma\text{-}Al_2O_3$	0.299	0.266	0.528	-	-	248	3.26×10^{18}
$Pt\text{-}Sn\text{-}Na/\gamma\text{-}Al_2O_3$	0.288	0.269	-	0.590	-	289	4.26×10^{18}
$Pt\text{-}Sn\text{-}K/\gamma\text{-}Al_2O_3$	0.283	0.311	-	-	0.577	304	4.17×10^{18}

by CO adsorption technique on the basis that one CO molecule is adsorbed per one Pt atom [Biswas et al., 1987]. The actual catalyst compositions, surface areas and number of Pt active sites of fresh samples are reported in Table 1. The catalysts were coked using the dehydrogenation reaction of propane to propene at different reaction temperatures and H_2/HC ratios. 20% vol C_3H_8 balanced with N_2 was used as reactant gas. In order to change H_2/HC ratio, an appropriate amount of N_2 was replaced by H_2. All results reported here are based on the following reference conditions unless otherwise stated: reaction temperature 600 °C, time on stream 40 minutes, H_2/HC=0. The reactor was operated at atmospheric pressure and the gas hourly space velocity (GHSV) was 25,000 hr^{-1}. Coke deposited on the catalyst was studied by Temperature Programmed Oxidation (TPO). Thermogravimetric analysis (TGA), Shimadzu model TG-50, was also used to cross check some TPO results. In the TPO experiment, 1% O_2 in He was used as the oxidizing gas. About 90 mg of coked catalyst sample was used in each experiment unless otherwise stated. The coked catalyst sample was packed in a quartz tube, supported by glass wool and burnt at a constant heating rate of 5 °C/min from 50 °C to 700 °C. The effluent gas was directed to a gas chromatograph Shimadzu model GC-8A equipped with a 1 ml gas sampling loop and a thermal conductivity detector. The gas sampling was performed every 5 minutes (or 25 °C). Our experience on TGA and results reported in some literatures [e. g. Barbier et al., 1980, 1985] have shown that the main TPO peaks usually distance from the adjacent peak(s) by about 100 °C. Therefore, this sample interval is considered appropriate. In addition, it can be seen later that there are other factors affecting locations of TPO peaks apart from C/H ratio of coke.

Separation of coke from the coked catalysts was achieved by dissolving the coked catalyst sample in a warm mixture of HCl and HNO_3. $\gamma\text{-}Al_2O_3$ and Pt can dissolve in this acid solution, but SiO_2 which is present as the major impurity (up to about 20 wt%) cannot dissolve in this manner. Several drops of HF have to be added to the solution to dissolve the remaining SiO_2 particle but coke. Separation of coke from the solution was performed by using a centrifuge. After each centrifuge, the clear solution was pipetted out and distilled water was added instead. This step was to wash any remaining acid and dissolve solid from the coke sample. The centrifugal and washing steps were repeated until most of the acids added were removed. The obtained coke sample then was dried in air at 110 °C overnight. Further details of experimental system and experimental procedures are described elsewhere [Atchara, 1995; Bualom, 1995; Nonglak, 1996].

RESULTS AND DISCUSSION

Effects of H_2/HC ratio and reaction temperature are shown in Figs. 1 and 2, respectively. From the TPO spectra, despite the differences in H_2/HC ratio and reaction temperature, we can categorise coke into three groups. The first group appears in a very small amount and burns around 110 °C (in the small boxed area). Since this coke appears in a very small amount, there will be no further discussion on this coke. The second coke is the one that can be removed at around 450 °C and the last one must use temperatures higher than 450 °C. Location of the second coke on the coked catalyst was determined by the CO adsorption technique. The CO adsorption results obtained from coked catalysts regenerated at different temperature show that burning the coked catalyst at 450 °C can recover all Pt active

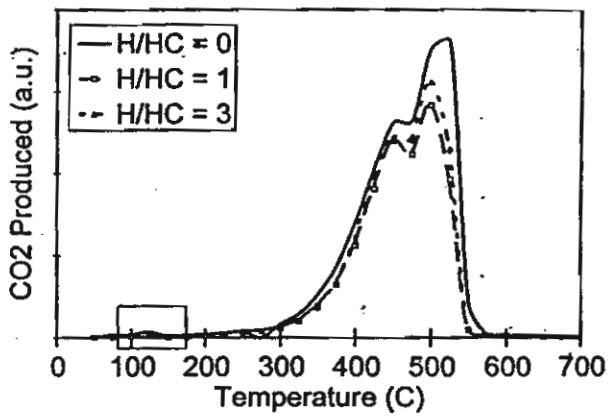

Fig. 1. TPO spectra of $Pt\text{-}Sn/\gamma\text{-}Al_2O_3$ at different H_2/HC ratios.

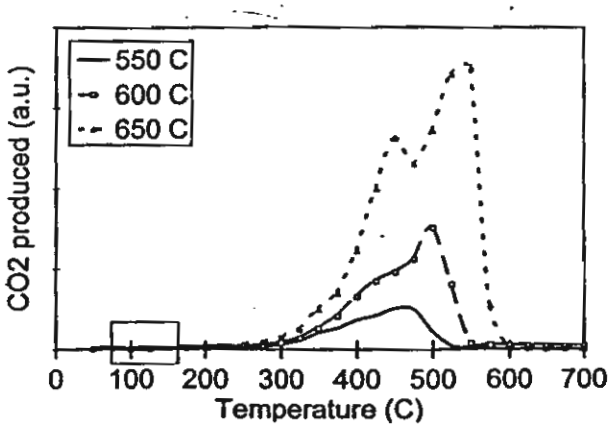

Fig. 2. TPO spectra of $Pt\text{-}Sn/\gamma\text{-}Al_2O_3$ at different reaction temperatures.

es. The TPO spectra of the coked catalyst regenerated at ·0 °C (not shown here) did not show the peak of the sec- d coke while the peak of the third coke still remained. ierefore, it can be identified that the second coke is the ke on metal site and the last is the coke on alumina sup- t. The TPO results clearly show that both H_2/HC ratio and ction temperature can alter the amount of coke formed. The rning characteristic of the coke on the coked catalysts is "l the same. Reaction temperature rather than H_2/HC ratio a stronger effect on the amount of coke. The slight shift of PO peaks in both figures is the effect of the amount of coke n each sample. The sample with a larger amount of coke ex- its a higher temperature of TPO peak for the same group coke.

Fig. 3 shows TPO spectra of coked Pt-Sn/γ-Al_2O_3 after be- used at different time on stream. The TPO peak of the coke the metal site still appears around 450 °C and seems not depend on the total amount of coke. The location of the eak of coke on the support shifts to a higher temperature the total amount of coke increases. At a high coke con- t the peaks of the coke on the metal site and on the sup- ort lump together into one large peak.

The effect of promoters (Sn, Li, Na, K) on propene yield demonstrated in Fig. 4. Fig. 4 shows that addition of Sn o the Pt catalyst significantly enhances propene yield. Addi- on of Li, Na and K further increases yield of propene. TPO ectra of the unpromoted and promoted catalysts are shown Fig. 5. Despite the differences in catalyst compositions and

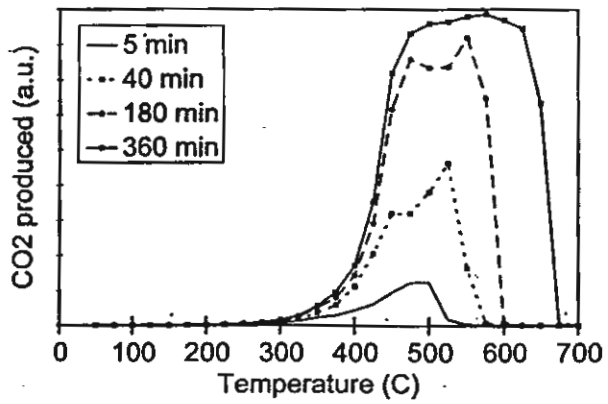

g. 3. TPO spectra of Pt-Sn/γ-Al_2O_3 at different time on stream.

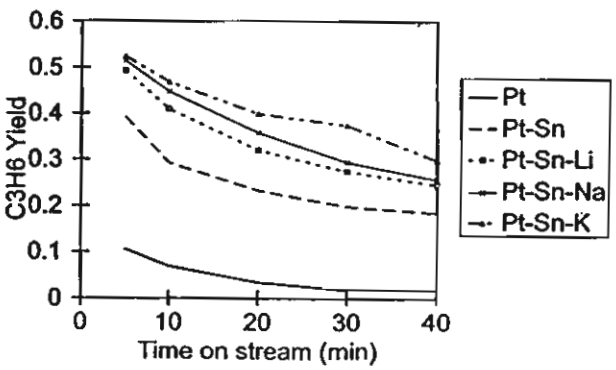

ig. 4. Effect of promoters on propene yield.

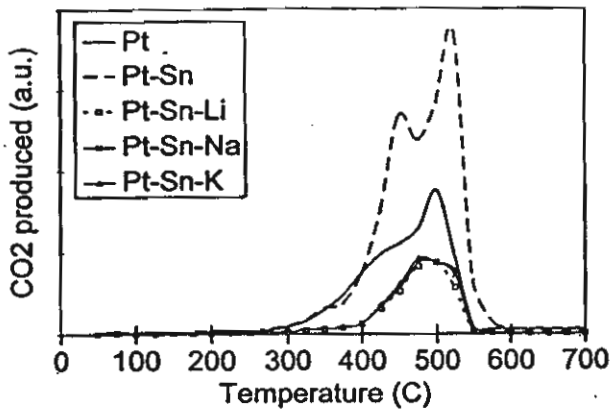

Fig. 5. Effect of promoters on TPO spectra of Pt based catalyst.

reaction conditions, all TPO spectra exhibit similar behaviour. It is found that Pt-Sn catalyst produced more coke per unit mass of catalyst more than the unpromoted one. This is because propane conversion is higher on Pt-Sn catalyst, and if propane conversion is taken into account it will be found that selectivity to coke on Pt-Sn catalyst is lower. Addition of alkali metals suppresses the formation and accumulation of coke on metal sites and catalyst support by reducing acidity of the catalyst surface. However, no significant effect on locations of TPO peaks is observed.

The roles of Pt and γ-Al_2O_3 during coke combustion were clarified by separating the coke from the coked catalyst and performing a TPO study on the carbonaceous compound obtained. Since the results shown previously indicate that the structure of coke formed does not likely to depend on reaction condition and catalyst composition, only the coke formed on Pt-Sn/γ-Al_2O_3 at the reference condition was studied. Fig. 6 demonstrates the comparison between TPO spectra of the coked catalyst and the coke sample. The figure shows that the absence of the metal and the support has an obvious effect on the characteristics of coke combustion. Only one CO_2 evolution peak was detected from the coke sample. This peak also appears at a higher combustion temperature than that of the coked catalyst. This result suggests that the appearance of two CO_2 evolution peaks of the coked catalyst relates to the

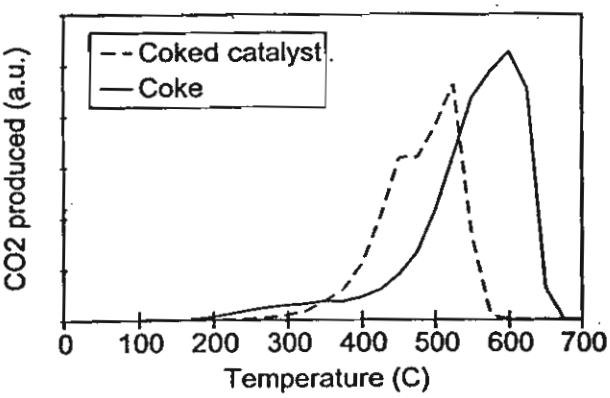

Fig. 6. Comparison between TPO spectra of coked Pt-Sn/γ-Al_2O_3 catalyst and coke separated from Pt-Sn/γ-Al_2O_3 catalyst.

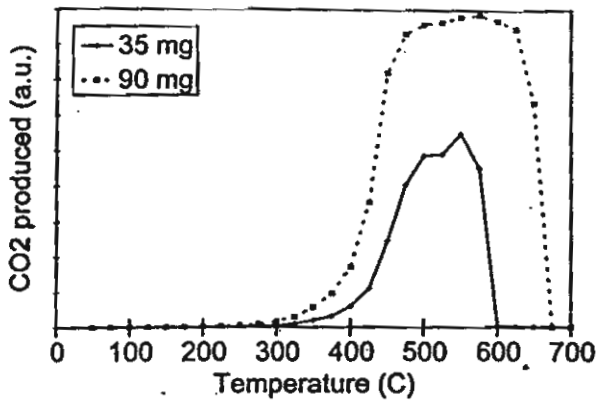

Fig. 7. Effect of weight of coked catalyst (Pt-Sn/γ-Al_2O_3) on TPO profiles.

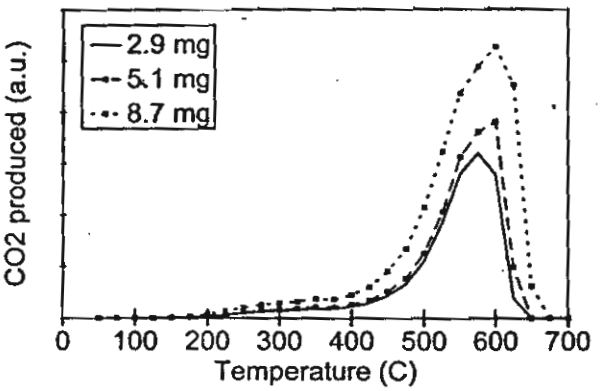

Fig. 8. Effect of weight of coke separated from coked Pt-Sn/γ-Al_2O_3 on TPO profiles.

presence of the metal and the support. The high surface area and porosity of the support promote the combustion of coke by increasing coke surface area contact to oxygen. In addition, Pt may also be involved in the combustion process by acting as a catalyst since CO_2 evolved from the coked catalyst at a lower temperature than the coke sample.

The effect of sample weight on the resolution of TPO spectra is shown in Fig. 7. TPO spectra of 90 mg coked catalyst sample show only one large peak but it cannot be determined whether it consists of only one large peak or several small peaks lumped together. Using a smaller sample amount shows a different result, *i.e.*, better resolution. Here, when the amount of coked catalyst sample was reduced to 35 mg a shoulder near 500 °C becomes distinct from the peak at 550 °C.

Fig. 8 shows TPO spectra of a coke sample by using different sample weights. The spectrum patterns do not show any obvious difference. Only one combustion peak can be observed independent from sample weight. When the TPO spectrum of the coke sample is superimposed on the TPO spectrum of coked catalyst (Fig. 6), one can see that the coke on the catalyst can be burned off at a lower temperature. This result provides further support for the hypothesis that both the metal site (in this case Pt) and the support should play some role in coke burning process.

CONCLUSIONS

At least three groups of coke can be present on the Pt based dehydrogenation catalyst. The first group, which appears in a very small amount, is the coke that can be removed at a temperature only around 110 °C. The second group, the amount of which increases with time on stream but up to a limit, can be burned using higher combustion temperatures, *i.e.*, >450 °C. These two groups are determined to be the coke that deposits on metal sites. The third coke, which keeps increasing with time on stream and can be removed by using further higher temperature, *i.e.*, 550 °C, is the coke that deposits on alumina support. Experiments also show that changing dehydrogenation reaction temperature, variation of H_2/HC ratios, addition of Sn or alkali metals (Li, Na and K) significantly affect mainly the amount of each coke formed.

TPO is a powerful technique widely used in coke characterization. However, one must be careful in interpreting the obtained spectra since the amount of sample used can lead to a different explanation. An optimal sample weight which is a compromise between sensitivity and resolution of the technique should be determined.

ACKNOWLEDGEMENT

T. Mongkhonsi and P. Praserthdam wish to acknowledge The Thailand Research Fund (TRF) for their support.

REFERENCES

Atchara Saengpoo, "Combustion of Coke on Dehydrogenation Catalysts", M. Eng. Theses, Chulalongkorn University (1995).

Barbier, J. B., Corro, G. and Zhang, Y., "Coke Formation on Platinum-Alumina Catalyst of Wide Varying Dispersion", *Appl. Catal.*, 13, 245 (1985).

Barbier, J. B., Marecot, P., Martin, N., Elassal, L. and Maurel, R., "Selective Poisoning by Coke Formation on Pt/Al_2O_3", Catalyst Deactivation (Delmon, B. and Froment, G. F. eds), Elsevier, Amsterdam, p.53 (1980).

Bartholdy, J., Zenthen, P. and Masooth, F. E., "Temperature-Programmed Oxidation Studies of Aged Hydroprocessing Catalysts", *Appl. Catal. A*, 129, 33 (1995).

Biswas, J., Gray, P. G. and Do, D. D., "The Reformer Line-out Phenomenon and Its Fundamental Importance to Catalyst Deactivation", *Appl. Catal.*, 32, 249 (1987).

Bualom Jaikaew, "Effect of Alkali Metals in Dehydrogenation Catalysts for Coke Reduction", M. Eng. Theses, Chulalongkorn University (1995).

Carlos, L. P. and Jose, M. P., "Comparison of Coke Burning on Catalysts Coked in a Commercial Plant and in the Laboratory", *Ind. Eng. Chem. Res.*, 28, 1785 (1989).

Larsson, M., Hulten, M., Blekkan, E. and Andersson, B., "The Effect of Reaction Conditions and Time on Stream on the Coke Formed During Propane Dehydrogenation", *J. Catal.*, 164, 44 (1996).

Liwu, L., Tao, Z., Jingling, Z. and Zhusheng, Z., "Dynamic

Process of Carbon Deposition on Pt and Pt-Sn Catalysts for Alkane Dehydrogenation", *Appl. Catal.*, **67**, 11 (1990).

Marecot, P., Akhachane, A. and Barbier, J., "Coke Deposition on Supported Palladium Catalysts", *Catal. Lett.*, **36**, 37 (1996).

Nonglak Pinitniyom, "Characterization of Coke on Dehydrogenation Catalysts", M. Eng. Theses, Chulalongkorn University (1996).

Pieck, C. L., Jablonski, E. L., Verderone, R. J. and Parera, J. M., "Selective Regeneration of Catalytic Functions of Pt-Re-S/Al_2O_3-Cl During Coke Burning", *Appl. Catal.*, **56**, 1 (1989).

Querini, C. A. and Fung, S. C., "Coke Characterisation by Temperature Programmed Techniques", *Catal. Today*, **37**, 277 (1997).

Querini, C. A. and Fung, S. C., "Temperature-Programmed Oxidation Technique: Kinetics of Coke-O_2 Reaction on Supported Metal Catalysts", *Appl. Catal. A*, **117**, 53 (1994).

Reyes, P., Oportus, M., Pecchi, G., Frety, R. and Moraweck, B., "Influence of the Nature of the Platinum Precursor on the Surface Properties and Catalytic Activity of Alumina-Supported Catalysts", *Catal. Lett.*, **37**, 193 (1996).

Silipoln Kunatippapong, "Determination of Irreversible Coke Deposition of Platinum Active Site of Propane Dehydrogenation Catalyst", D. Eng. Theses, Chulalongkorn University (1995).

Tao, Z., Jingling, Z. and Liwu, L., "Relation Between Surface Structure and Carbon Deposition on Pt/Al_2O_3 and Pt-Sn/Al_2O_3 Catalysts", Studies in Surface Science and Catalyst, Elsevier, Amsterdam, **34**, 143 (1991).

PERGAMON

Chemical Engineering Science 55 (2000) 2249–2256

Chemical Engineering Science

Transient study of the effect of residual cations in Cu/ZSM-5 for SCR of NO by hydrocarbon

Nakarin Mongkolsiri[a], Piyasan Praserthdam[a,*], P.L. Silveston[b], R.R. Hudgins[b]

[a]*Department of Chemical Engineering, Chulalongkorn University, Bangkok, 10330, Thailand*
[b]*Department of Chemical Engineering, University of Waterloo, Ontario, Canada, N2L 3G1*

Received 4 December 1997; accepted 16 August 1999

Abstract

A step change technique was used to investigate individual reactions in the reduction of NO by hydrocarbon on Na-ZSM-5, H-ZSM-5, Cu/Na-ZSM-5 and Cu/H-ZSM-5 catalysts. Na-ZSM-5 is not active in NO decomposition and NO reduction by propane both in the presence and in the absence of oxygen. On the other hand, H-ZSM-5 is active in the oxidation of NO to NO_2 and in the reduction of NO. Zeolite does not adsorb NO but preferentially adsorbs O_2 which, subsequently, reacts with NO in the gas phase to produce NO_2. In the absence of oxygen, Cu/H-ZSM-5 is more active than Cu/Na-ZSM-5 in both the decomposition of NO and the reduction of NO by propane since Cu/H-ZSM-5 can produce more NO_2 in the absence of oxygen. Differences in the Cu/H and Cu/Na forms of ZSM-5 result from residual H^+ or Na^+ in these zeolites. These residual cations either affect catalytic sites directly or control the Cu^+/Cu^{2+} ratios. Differences in these ratios were observed.

Keywords: SCR of NO; Transient experiments; NO oxidation; Cu-exchanged ZSM-5

1. Introduction

The selective catalytic reduction (SCR) of NO by hydrocarbon has been a topic of interest during the last decade (Held, Konig, Richter & Puppe, 1990; Iwamoto & Hamada, 1991). Unlike the reaction over conventional three-way catalysts normally used on gasoline engine exhaust, SCR of NO by hydrocarbon can occur even under a highly oxidizing atmosphere. Consequently, this reduction may be promising for the removal of NO from diesel and other lean burn engines. A number of catalysts have been proposed in literature; however, among them, Cu/ZSM-5 is one of the most active ones. It has been the most widely studied.

In general, Cu/ZSM-5 zeolite can be prepared by ion-exchanging Cu ion with either the Na- or H- forms of ZSM-5. The choice of the primary form of ZSM-5 used by a researcher seems to be arbitrary. Na-ZSM-5 is used because it can be exchanged with Cu ion more easily than the H^+ form. In other cases, H-ZSM-5 is used in order to avoid the effect of Na^+ ion (Shelef, 1995). Although overexchanged Cu/ZSM-5, the most active catalyst for SCR of NO by hydrocarbon (Iwamoto, Mizuno & Yahiro, 1992), has a degree of Cu^{2+} exchange above 100%, based on the assumption that one Cu^{2+} ion exchanges with two Na^+ ions or two protons, this sample retains a significant amount of cations on the surface (Shelef, 1995). This was confirmed by Zhang, Leo, Salofim and Hu (1995) who found that some Na^+ ion still existed in 165% Cu-exchanged ZSM-5. Therefore, there should be some residual Na^+ ions left in Cu/Na-ZSM-5 whereas some protons should still remain in Cu/H-ZSM-5. These residual ions could result in different activities between Cu/ZSM-5 zeolites formed from the H^+ and Na^+. Alternatively, they could result in different Cu^+/Cu^{2+} ratios which would then affect activity.

In order to study the effect of the residual ions, the activities of Na-ZSM-5, H-ZSM-5, Cu/Na-ZSM-5 and Cu/H-ZSM-5 for NO removal in the absence and presence of oxygen were investigated by transient methods. The performance of these catalysts was compared for the various reactions making up the reduction process. In addition, the state of copper on Cu-ZSM-5 catalysts was characterized.

* Corresponding author.

0009-2509/00/$ - see front matter
PII: S0009-2509(99)00476-5

2. Experimental

The parent Na-ZSM-5 zeolite was synthesized by the method described elsewhere (Inui et al., 1984). The given zeolite was analysed by XRD to confirm the structure of ZSM-5. Na-ZSM-5 was exchanged with ammonium nitrate solution at 80°C twice and then calcined in air at 540°C for 3.5 h in order to form H-ZSM-5. Cu/ZSM-5 was prepared by exchanging either Na-ZSM-5 or H-ZSM-5 with a copper (II) nitrate solution overnight by controlling the pH of the solution at about 9. The solid obtained was washed with fresh batches of deionized water 5 times. Finally, the catalysts were dried at 110°C in an oven overnight and then calcined in air at 540°C for 3.5 h. The catalyst powder was pelletized using a press. Then the zeolite pellet was crushed into a granular form and sieved to select a particle size between 10 and 20 mesh. This granular sample was used in the experiments of this study.

The GC switching valve was modified to alternate flows of reactant or inert gas passing through the reactor. A 10 mm diameter quartz tube reactor was filled with 1.2 g of catalyst and also glass beads to reduce void volume as much as possible. This bed of catalyst was pretreated in N_2 at 400°C for 1 h before use. The reactor operated at 300–400°C. Outlet gas was passed through a specially designed IR gas cell (Khodadadi, 1994) placed in a FT-IR (Mattson Galaxy series 5022) to continuously measure the composition of the outlet stream. The FT-IR measured NO, NO_2, N_2O, CO_2 and propane simultaneously but neither N_2 nor O_2 could be detected. The band of each gas used in this study is summarized in Table 1. No other species besides those mentioned in Table 1 were detected, of course, with the exception of water. From a blank test, the retention time for a total gas flow of around 50 ml/min at 350°C was approximately 12 s from the switching valve to the detector.

The amount of total Cu, Al, Si and Na in catalysts was determined by AAS and XRF methods. Tetrahedral alumina in ZSM-5 zeolite was investigated by Al NMR. Cu^{1+} sites on the Cu/ZSM-5 surface were quantified by CO adsorption (Iwamoto, Yahiro, Tanda, Mizuno, Mine & Kagawa, 1991). For this measurement, 0.2 g of the catalyst sample was packed in an 4 mm stainless-steel tube. The catalyst bed was pretreated in 50 ml/min of He at 450°C for 1 h. Then, the catalyst bed was cooled to room temperature for adsorption. Injections of 0.2 ml of CO to the bed were carried out until adsorption was complete. Unabsorbed CO downstream of the catalyst bed was detected by TCD. Further details of equipment and procedure are found in a Ph.D. Thesis (Mongkolsiri, 1998).

3. Results and discussion

Amounts of total copper and Na in the catalysts used in this study were determined and the result shown in Table 2. In order to avoid the effect of copper content on the activities of catalysts, the same amount of copper was loaded into the Cu/Na-ZSM-5 and Cu-H-ZSM-5 samples. Na was not found in H-ZSM-5 and there was very little in Cu/H-ZSM-5. However, a significant amount of Na was detected in Cu/Na-ZSM-5. Because of the remaining Na in the Cu/Na-ZSM-5, we expect that the Cu/H-ZSM-5 will contain significant residual protons as well.

The signals of NO absorbance with time following a switch from a N_2 to a NO feed to the reactor are shown in Fig. 1 for various catalysts. It is likely that Na-ZSM-5 and H-ZSM-5 are not active for direct decomposition of NO because the retention time and trend of the NO response were similar to those from a blank experiment. Moreover, only NO was observed for these samples. With the Cu-loaded zeolites, N_2O and NO_2 are seen. It is known that Cu/ZSM-5 shows a remarkably high activity for NO decomposition (Iwamoto, 1991,1994). Although both N_2 and O_2 are the main products of the decomposition, these cannot be detected by IR measurement. NO_2 and N_2O are intermediate or side products in decomposition reaction. There are both similarities and differences between transient responses over Cu/Na-ZSM-5 and Cu/H-ZSM-5. The absorbance signal first appeared at about the same time in both experiments; however, the retention time indicated by these signals was much longer than the time for the experiment without catalyst or with the Na-ZSM-5 and H-ZSM-5 samples. The signal for N_2O overshot the steady-state level

Table 1
IR band of gases used for transient studies[a]

Gas species	Appearance peak (cm^{-1})
NO	1905(xl), 1850(l)
NO_2	1630(xl), 1600(xl), 1750(l), 1263(l)
N_2O	2225(xl), 1290(l)
C_3H_8	2970
CO_2	2362

[a]*Note*: xl = extra large, l = large.

Table 2
Si/Al, Na/Al, Cu/Al weight ratio and Cu and Na contents in catalysts

Catalyst	Si/Al	Na/Al	Cu/Al	Cu content (wt%)	Na content (wt%)
Na-ZSM-5	40.4	0.79	—	—	1.84
H-ZSM-5	40.0	—	—	—	—
Cu/Na-ZSM-5	37.2	0.15	0.42	1.06	0.38
Cu/H-ZSM-5	39.0	0.04	0.44	1.09	< 0.09

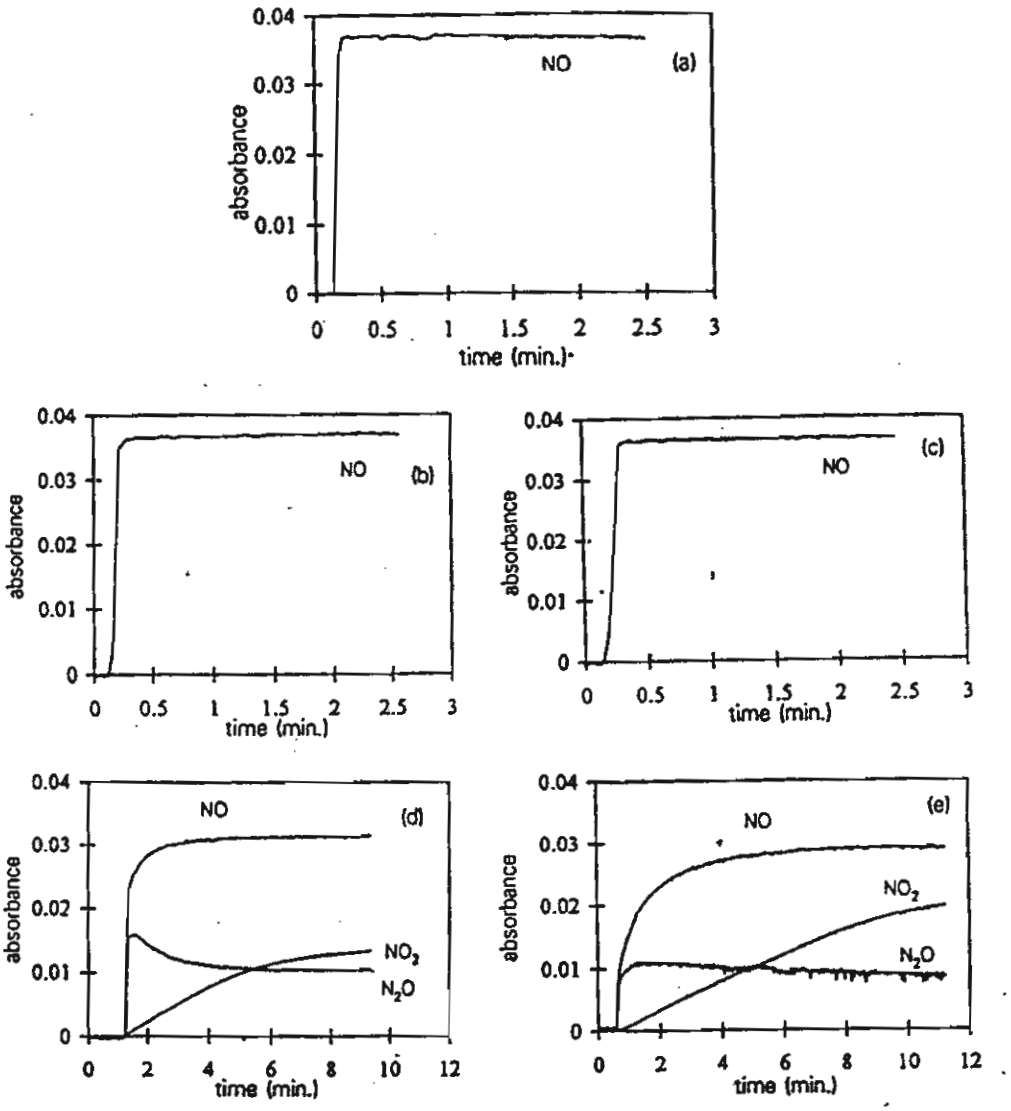

Fig. 1. Absorbance of gaseous species after switching from N_2 to 1.2% NO + N_2 350°C over (a) without catalyst; (b) Na-ZSM-5; (c) H-ZSM-5; (d) Cu/Na-ZSM-5; (e) Cu/H-ZSM-5.

in the first few minutes and then gradually decreased to this level. By contrast, NO_2 signal increased slowly after appearing in the reactor outlet. These phenomena were also observed by Li and Hall (1990) and Iwamoto et al. (1992). Pirone, Ciambelli, Morrette and Russo (1996) mentioned that at a temperature below 300°C NO disproportionation to N_2O and NO_2 occurs in parallel with NO decomposition. Furthermore, O_2 formed by NO decomposition might further oxidize NO to produce NO_2 (Iwamoto, 1991). NO consumption seems to be slightly greater for Cu/H-ZSM-5 than for Cu/Na-ZSM-5. In addition, the experiment on Cu/H-ZSM-5 produced more NO_2 whereas the one on Cu/Na-ZSM-5 produced more N_2O.

Fig. 2 shows results of a step change from N_2 gas to a gas mixture of 0.5% NO + 12% O_2. NO_2 formation in homogeneous NO oxidation at 25°C (Fig. 2a) was more than that at 350°C (Fig. 2b). This indicates that NO can be oxidized in the gas phase but preferably at a low temperature and that the net homogeneous oxidation rate decreases as the temperature increases because the reverse reaction becomes important. Occurrence of this homogeneous reaction was also reported by Chajar, Primet, Praliaud, Cherrier, Gauthier and Mathis (1994). The activity of Na-ZSM-5 in the oxidation of NO to NO_2 is very low compared to H-ZSM-5 (Fig. 2(c) and (d)). Halasz, Brenner and Simon (1995) also observed the activity of H-ZSM-5 in NO oxidation. The activity of H-ZSM-5 in NO oxidation to NO_2 was quite similar to Cu/H-ZSM-5 and Cu/Na-ZSM-5, but, surprisingly, the lag time of the appearance of NO_x in the system with Cu catalyst was much longer than the system with

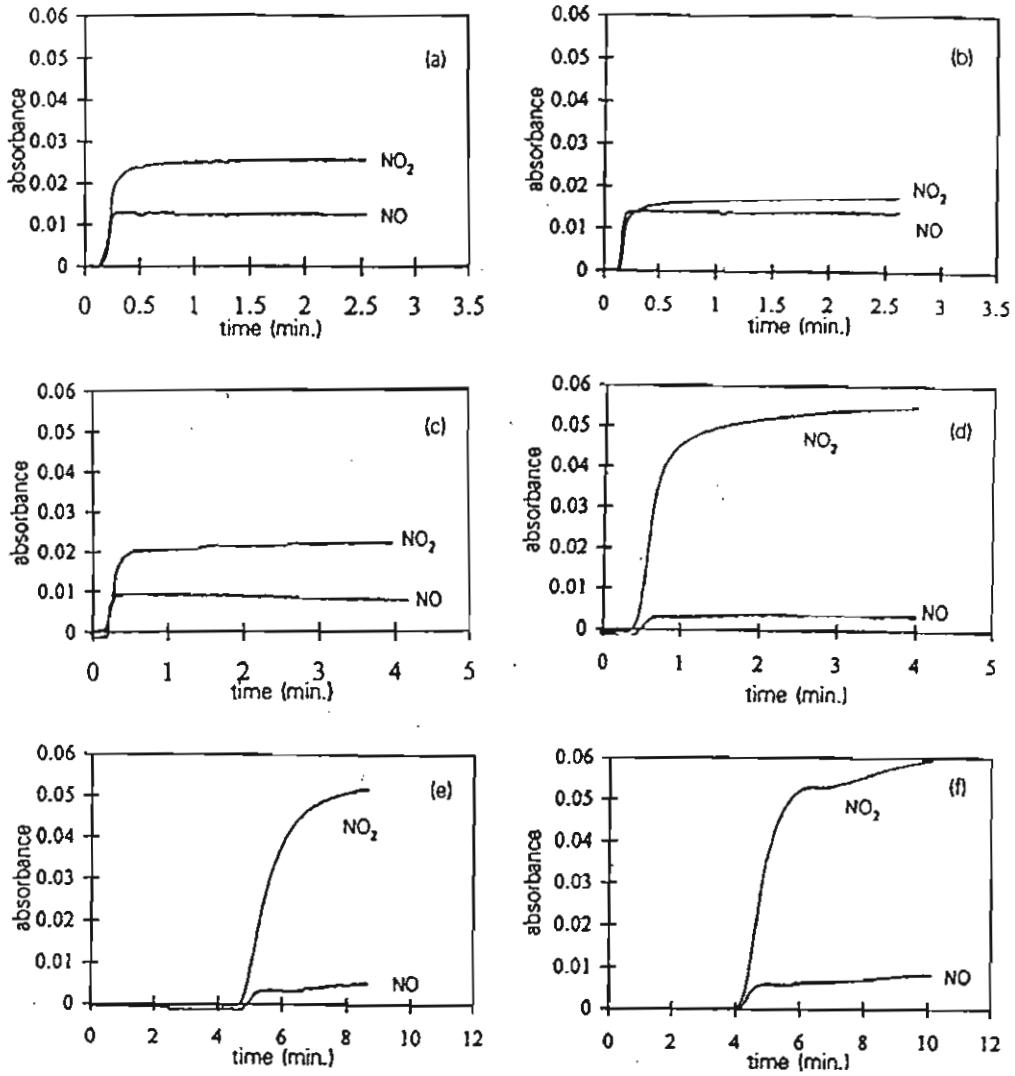

Fig. 2. Absorbance of gaseous species after switching from N_2 to 0.5% NO + 12% O_2 + N_2 at 350°C over (a) without catalyst at 30°C; (b) without catalyst at 350°C; (c) Na-ZSM-5 at 350°C; (d) H-ZSM-5 at 350°C; (e) Cu/Na-ZSM-5 at 350°C; (f) Cu/H-ZSM-5 at 350°C.

H-ZSM-5. NO_x signals in the experiment on H-ZSM-5 appeared, after switching, in about half a minute (Fig. 2(d)) whereas, in the Cu/ZSM-5 experiments, NO_x was first detected at around 4 min after switching (Fig. 2(f) and (e)). This indicates the high NO_2 adsorption capacity of Cu/ZSM-5.

The delay in the appearance of NO in Fig. 2(e) and (f) may be explained by the rapid oxidation of NO to NO_2 in the presence of O_2 in the feed. NO_2 appears only when the catalyst is saturated with NO_2. This condition interferes with NO oxidation allowing the appearance of some NO in the product gas. The lag of about 4 min in Fig. 2(e) and (f) compared to about 1 min in Fig. 1(d) and (e) is due to the concentration of NO in the feed. It is 1.2% in the latter and 0.5% in the former.

The slow rise in NO_2 in Fig. 1(d) and (e) appears to be due to the strong adsorption of NO_2 on the copper. Differences between Fig. 1(d) and (e) and Fig. 2(e) and (f) probably reflect the reduction of the Cu catalyst by NO when O_2 is not present in the feed.

Neither Na-ZSM-5 nor H-ZSM-5 is active in NO decomposition, but, in the case of the oxidation of NO by O_2, Na-ZSM-5 is not active whereas H-ZSM-5 is quite active. Possibly, the active site in H-ZSM-5 does not adsorb NO; instead it preferably adsorbs O_2. In NO oxidation over H-ZSM-5, we believe NO_2 was produced by the interaction between the adsorbed oxygen and NO in the gas phase. This hypothesis is supported by temperature-programmed desorption (TPD) measurements for NO. We did not find any desorption peak of NO during the temperature programming over Na-ZSM-5 and H-ZSM-5. Pirone et al. (1996) also noticed that H-ZSM-5 hardly adsorbed NO.

Absorbances of gases with time on stream shown in Fig. 3 were obtained from the experiments without oxygen in the feed gas over CU/H-ZSM-5 and

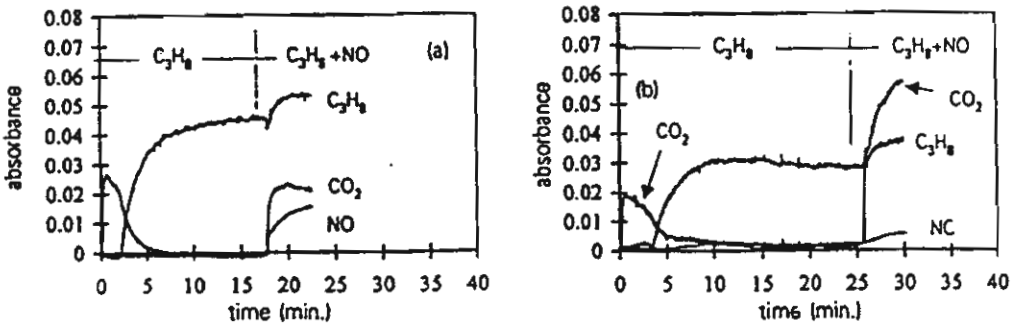

Fig. 3. Absorbance of gas products after switching from 0.4% C_3H_8 to 0.4% C_3H_8 + 0.5% NO at 400°C over (a) Cu/Na-ZSM-5, (b) Cu/H-ZSM-5.

Cu/Na-ZSM-5 zeolites. After switching from N_2 to C_3H_8, formation of CO_2 in the first few minutes after a step change from N_2 to C_3H_8 comes from the reaction between C_3H_8 and adsorbed oxygen or extra lattice oxygen in the catalyst (Valyon & Hall, 1993). When this oxygen was exhausted, the CO_2 signal disappeared. After CO_2 formation ended the response of the propane signal in the reactor outlet gradually increased until a constant level was reached after about 10 min. This could result from a chromatographic effect due to competitive adsorption of CO_2 and light hydrocarbon over Cu/ZSM-5 (Cho, 1995; Burch & Millington, 1993). After NO was added to the reactor feed, NO consumption and CO_2 production in the experiment over Cu/H-ZSM-5 was higher than for Cu/Na-ZSM-5. The C_3H_8 signal in the experimental over both catalysts is enhanced after addition of NO because NO adsorption competes with preadsorbed hydrocarbon and causes some hydrocarbon desorption. Hoost, Laframboise and Otto (1995) noticed that propane adsorption decreases in the presence of NO_x. CO, N_2O and NO_2 were not observed during NO reduction by propane in the absence of oxygen over both catalysts.

The first step of the reaction after introduction of NO would be the decomposition of NO (Burch & Scire, 1994). Oxygen generated will react further to form NO_2 or to oxidize propane. The NO_2 formed would be further reduced by propane to form CO_2, H_2O and N_2. NO_2 has been considered as the key intermediate of SCR of NO by hydrocarbon because it is more easily reduced by hydrocarbon than NO (Petunchi & Hall, 1993; Shelef, Montreuil & Jen, 1994; Chajar et al., 1994; Centi & Perathoner, 1996). Because for NO decomposition, Cu/H-ZSM-5 produces more NO_2 than Cu-Na-ZSM-5 (Fig. 1(d) and (e)), we believe that with propane in the feed, more NO_2 is formed and this leads to a higher rate of CO_2 formation over the Cu-H-ZSM-5 catalyst.

When the gas stream was changed from N_2 to a gas mixture of C_3H_8 and O_2, only CO_2 was observed with Cu/Na-ZSM-5 and Cu/H-ZSM-5 (Fig. 4(d) and 4(e)). This means that complete combustion took place. On the other hand, C_3H_8 and CO_2 signals appear with Na-ZSM-5 and H-ZSM-5 (Fig. 4(b) and 4(c)). The intensities of the absorbance of C_3H_8 and CO_2 in the experiment on Na-ZSM-5 are about the same as those for H-ZSM-5. The low-C_3H_8 conversion of H-ZSM-5 indicates low activity of the acid site in hydrocarbon oxidation at 350°C, which is in line with the report of Sasaki, Hamada, Kintaichi and Ito (1992). In comparison, propane is completely oxidized over Cu/Na-ZSM-5 and Cu/H-ZSM-5. The different oxidative performance between Cu/H-ZSM-5 and H-ZSM-5 must be the result of the presence of copper in the catalyst. Copper in zeolites is known to be very active in hydrocarbon oxidation (Neyestanaki, Kumar & Lindfors, 1995; Kucherov, Hubbard, Kucherova & Shelef, 1996). The pulse of the C_3H_8 signals on switching, observed in the experiments over Na-ZSM-5 and H-ZSM-5 (Fig. 4(b) and (c)), is due to the fluctuation of gas flow during switching rather than an adsorption phenomenon. Later, when NO is abruptly added to the feed, CO_2 formation rose rapidly and then gradually declined until a steady state was reached. This overshoot is observed in all zeolite runs (Fig. 4(b) to (e)). This is probably due to the competitive adsorption between NO_x and CO_2. The appearance of NO forces CO_2 on catalyst surface to desorb until a new balance of adsorption rate is reached. NO_2 was observed only in the experiment on Na-ZSM-5. NO and C_3H_8 were not detected in the experiment on Cu/H-ZSM-5 and Cu/Na-ZSM-5. In the H-ZSM-5 experiment, after NO was added into the system, C_3H_8 conversion increased enormously and NO signal was not observed. This observation indicates that NO reduction proceeds readily over the H-ZSM-5 samples. NO reduction, however, is not able to account for the drop in concentration of C_3H_8 leaving the reactor or for the large increase in CO_2 formation.

Even though the responses cannot be converted to concentrations because the IR signals were not calibrated, Fig. 4(c) can be analyzed by noting that the IR response at the low concentrations used is proportional to concentration. Stoichiometric considerations that 3 mol of CO_2 are formed per mol of C_3H_8 combusted mean that total oxidation of propane by O_2 over the

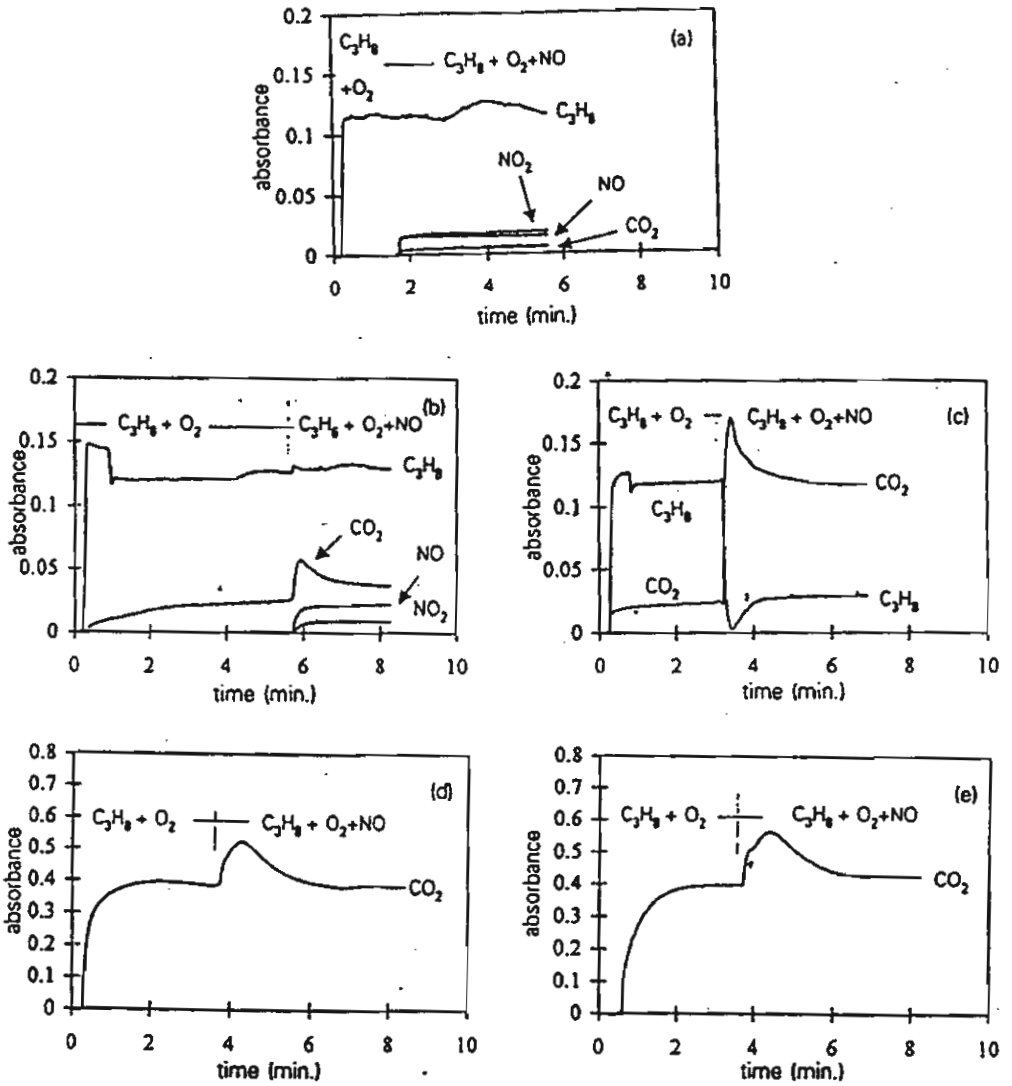

Fig. 4. Absorbance of gas products after switching from 0.4% C_3H_8 + 12% O_2 to 0.4% C_3H_8 + 12% O_2 + 0.5% NO over (a) without catalysts; (b) Na-ZSM-5 at 350°C; (c) H-ZSM-5 at 350°C; (d) Cu/Na-ZSM-5 at 300°C; (e) Cu/H-ZSM-5 at 300°C.

H-ZSM-5 sample must be promoted by the presence of NO in the reactor feed. Only this assumption can account for the response after NO introduction shown in Fig. 4(c). H-ZSM-5 is very active for NO oxidation by O_2 (see Fig. 2(d)) but does not adsorb NO strongly. Thus, we speculate that NO oxidation proceeds through

$$O_2\,(ad) + NO \rightarrow NO_2\,(ad) + O\,(ad)$$

In the presence of C_3H_8, the reactive O (ad) on the surface results in combustion. This is in addition to O_2 oxidation of the C_3H_8 that probably occurs at a different surface site. The promotion of hydrocarbon oxidation by O_2 in the presence of NO appears to have occurred for zeolite catalysts.

When activities between Cu/H-ZSM-5 and Cu/Na-ZSM-5 were compared in various transient experiments, it was found that Cu/H-ZSM-5 and Cu/Na-ZSM-5 have the same activity in the NO oxidation and NO reduction in the excess oxygen system. On the other hand, Cu/H-ZSM-5 is more active than Cu/Na-ZSM-5 in NO decomposition and NO reduction by propane without oxygen. The experiment with only NO in the feed produces more NO_2 for Cu/H-ZSM-5 than for Cu/Na-ZSM-5. More CO_2 was produced and more NO was converted in NO reduction by propane in the absence of oxygen over Cu/H-ZSM-5 than over Cu/Na-ZSM-5. However, the reactions are much faster with excess oxygen than in the absence of oxygen. The activity of both Cu/Na-ZSM-5 and Cu/H-ZSM-5 is nearly identical in NO oxidation.

The difference in the performance between Cu/Na-ZSM-5 and Cu/H-ZSM-5 observed in this study seems to be due to different residual cations, Na^+ or H^+, in the catalysts. Why this difference affects performance is

Table 3
Amount of Cu^{1+} in catalysts estimated by CO adsorption

Catalyst	Amount of CO Adsorbed (μmol/g.cat)	Number of Cu^{1+} ($\times 10^{19}$ site/g.cat)
Cu/Na-ZSM-5	1.121	1.35
Cu/H-ZSM-5	2.247	2.71

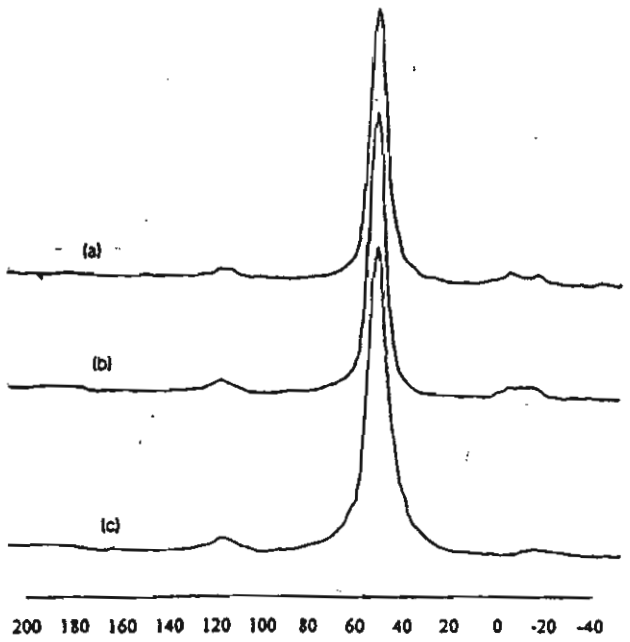

Fig. 5. Al-NMR spectra of (a) fresh H-ZSM-5; (b) spent H-ZSM-5 and (c) spent Cu/H-ZSM-5.

uncertain. It could be that these residual cations influence catalyst site directly. On the other hand, they may affect the Cu^{+}/Cu^{2+} ratio in the copper exchanged and calcined zeolites. Although the total copper content on both Cu/ZSM-5 zeolites was carefully controlled to be about the same, differences in the copper state may have occurred. It is generally accepted that several oxidation states of Cu can exist on Cu/ZSM-5 surface (Valyon & Hall, 1993; Gruinert, Hayes, Joyner, Shpiro, Siddiqui & Baeva, 1994). The residual cations could affect the distribution of states in each of the zeolite. Thus, the copper oxidation state was examined. CO adsorption is a simple method to determine the amount of Cu^{1+} (Iwamoto et al., 1991). The amount of CO adsorbed on the catalyst surface represents the amount of Cu^{1+}. Our measurements are shown in Table 3. The amount of Cu^{1+} in Cu/H-ZSM-5 appears to be about double in Cu/Na-ZSM-5. Since the total copper content of the two catalysts was equal, Cu/H-ZSM-5 had a higher Cu^{1+}/Cu^{2+} ratio. The difference in Cu^{1+}/Cu^{2+} could have an effect on the activity in the copper exchanged zeolites. One possibility for the different ratio is that the reducibility of Cu in the zeolites is affected by the residual cations.

Another explanation of the zeolite differences observed in our study is different extents of formation of Lewis acid sites through dealumination of the zeolite. This possibility was examined by carefully measuring the alumina content of our zeolite samples. Fig. 5 shows Al-NMR pattern of H-ZSM-5 and Cu/H-ZSM-5. Only one peak at around 50 ppm was observed in all samples. This peak is assigned to tetrahedral aluminum. The intensity of the peak was not reduced in spent catalysts indicating that dealumination did not occur in this study. This is supported by Torre-Abreu, Ribeiro, Henriques, Ribeiro and Delahay (1997). The dealumination of H-ZSM-5 and Cu/ZSM-5 was observed only in severely steamed samples (Tabata, Kokitsu, Okada, Nakayama, Yasumatsu & Sakane, 1994; Budi, Curry-Hyde & Howe, 1996). Therefore, dealumination of catalyst is not involved in the different activities observed among the zeolites in this study.

4. Conclusions

Among catalysts in this study, Na-ZSM-5 is not active in any reaction involving NO, O_2 and C_3H_8. H-ZSM-5 is not active in the decomposition of NO but is active in the oxidation of NO of NO_2. This probably implies that H-ZSM-5 does not adsorb NO but preferentially adsorbs O_2 which subsequently reacts with NO in the gas phase to form NO_2. The difference in activity between Cu/Na-ZSM-5 and Cu/H-ZSM-5 was not evident when oxygen was present in feed. When only NO was present, Cu/H-ZSM-5 produced more NO_2 but less N_2O than Cu/Na-ZSM-5. In addition, Cu/H-ZSM-5 was found to be more active than Cu/Na-ZSM-5 in the reduction of NO by propane in the absence of oxygen. NO_2 was produced more rapidly over Cu/H-ZSM-5 especially in the absence of oxygen compared with Cu/Na-ZSM-5. Promotion of O_2 oxidation of propane of H-ZSM-5 in the presence of NO was observed. The different activities of Cu/Na-ZSM-5 and Cu/H-ZSM-5 might be due to either the different residual cations or the Cu^{1+}/Cu^{2+} ratio on catalysts surface which was probably cause by these same cations. Differences in this ratio were found. Further study is needed to identify as to which of these explanations of the residual cations effect is correct.

Acknowledgements

These experiments were performed at The Reactor Engineering Laboratory of Prof. P.L. Silveston, Chemical Engineering Department, University of Waterloo. The research was supported financially by the Thailand Research Fund.

References

Budi, P., Curry-Hyde, E., & Howe, R. F. (1996). Stabilization of Cu/ZSM-5 NO_x reduction catalysts with lanthanum. *Catalysis Letters, 41*, 47–53.

Burch, R., & Millington, P. J. (1993). Role of propane in the selective reduction of nitrogen monoxide in copper-exchanged zeolites. *Applied Catalysis B. Environment, 2*, 101–116.

Burch, R., & Scire, S. (1994). Selective catalytic reduction of nitric oxide with ethene and methane on some metal exchanged ZSM-5 zeolite. *Applied Catalysis B. Environment, 3*, 295–318.

Centi, G., & Perathoner, S. (1996). Role and importance of oxidized nitrogen oxide adspecies on the mechanism and dynamics of reaction over copper-based catalysts. *Catalysis Today, 29*, 117–122.

Chajar, Z., Primet, M., Praliaud, H., Cherrier, M., Gauthier, G., & Mathis, F. (1994). Nitrogen dioxide effect in the reduction of nitric oxide by propane in oxidizing atmosphere. *Catalysis Letters, 28*, 33–40.

Cho, B. K. J. (1995). Nitric oxide reduction by ethylene over Cu-ZSM-5 under lean conditions: study of reaction dynamics by transient experiment. *Journal of Catalysis, 155*, 184–195.

Grunert, W., Hayes, N. W., Joyner, R. W., Shpiro, E. S., Siddiqui, R. H., & Baeva, G. N. (1994). Structure, chemistry, and activity of Cu-ZSM-5 catalysts for the selective reduction of NO_x in the presence of oxygen. *Journal of Physical Chemistry, 98*, 10832–10846.

Halasz, I., Brenner, A., & Simon Ng, K. Y. (1995). Active sites of H-ZSM-5 catalysts for the oxidation of nitric oxide by oxygen. *Catalysis Letters, 34*, 151–161.

Held, W., Konig, A., Richter, T., & Puppe, L. (1990). Catalytic NO_x reduction in net oxidizing exhaust gas. *SEA, 900496*, 13–19.

Hoost, T. E., Laframboise, K. A., & Otto, K. (1995). Co-adsorption of propane and nitrogen oxides on Cu-ZSM-5: An FTIR study. *Applied Catalysis B. Environment, 7*, 79–93.

Inui, T., Vamase, O., Fuguda, K., Itoh, A., Tarumoto, J., Morinage, N., Hagiwara, T., & Takegami, Y. (1984). *Proceedings of the Eighth International Congress on Catalysis*, Berlin, vol. 3, (p. 569).

Iwamoto, M. (1991). Copper ion-exchanged zeolites as active catalysts for direct decomposition of nitrogen monoxide. *Studies on Surface Science Catalysis, 60*, 327–334.

Iwamoto, M., & Hamada, H. (1991). Removal of nitrogen monoxide from exhaust gases through novel catalytic processes. *Catalysis Today, 10*, 51–71.

Iwamoto, M., Yahiro, H., Tanda, K., Mizuno, N., Mine, Y., & Kagawa, S. (1991). Removal of nitrogen monoxide through a novel catalytic process. 1. decomposition on excessively copper ion exchanged ZSM-5 Zeolites. *Journal of Physical Chemistry, 95*, 3727–3730.

Iwamoto, M., Mizuno, N., & Yahiro, H. (1992). Selective catalytic reduction of NO by hydrocarbon in oxidizing atmosphere. *Proceedings of the 10th International Congress on Catalysis*, Budapest (pp. 213–215).

Iwamoto, M. (1994). Heterogenous catalyst for removal of NO in excess oxygen: Progress in 1994. *Catalysis Today, 29*, 29–35.

Khodadadi, A. A. (1994). *Transient studies of the Fisher–Tropsch synthesis over a cobalt catalyst*. Ph.D. thesis, Univ. of Waterloo, Waterloo, Ontario, Canada.

Kucherov, A. V., Hubbard, C. P., Kucherova, T. N., & Shelef, M. (1996). Stabilization of the ethane oxidation catalytic activity of Cu-ZSM-5. *Applied Catalysis B. Environment, 7*, 285–298.

Li, Y., & Hall, W. K. (1990). Stoichiometric catalytic decomposition of nitric oxide over Cu-ZSM-5 catalysts. *Journal of Physical Chemistry, 94*, 6145–6147.

Mongkolsiri, N. (1998). *Effect on remaining cations in copper ion exchanged ZSM-5 zeolite for selective reduction on nitric oxide*. Ph.D. Thesis Chulalongkorn Univ. Bangkok, Thailand (Contact authors for a copy).

Neyestanaki, A. K., Kumar, N., & Lindfors, L. -E. (1995). Catalytic combustion of propane and natural gas over Cu and Pd modified ZSM-5 zeolite catalysts. *Applied Catalysis B. environment, 7*, 95–111.

Petunchi, J. O., & Hall, W. K. (1993). On the role of nitrogen dioxide in the mechanism of the selective reduction of NO_x over Cu-ZSM-5 zeolite. *Applied Catalysis B. Environment, 2*, L17–L26.

Pirone, R., Ciambelli, P., Morrette, G., & Russo, G. (1996). Niric oxide decomposition over Cu-exchanged ZSM-5 with high Si/Al ratio. *Applied Catalysis B. Environment, 8*, 197–207.

Sasaki, M., Hamada, H., Kintaichi, Y., & Ito, T. (1992). Role of oxygen in selective reduction of nitrogen monoxide by propane over zeolite and alumina-based catalysts. *Catalysis Letters, 15*, 297–304.

Shelef, M., Montreuil, C. N., & Jen, H. W. (1994). NO_2 formation over Cu/ZSM-5 and the selective catalytic reduction of NO. *Catalysis Letters, 26*, 277–284.

Shelef, M. (1995). Selective catalytic reduction of NO_x with N-free reduction. *Chemical Review, 95*, 209–225.

Tabata, T., Kokitsu, M., Okada, O., Nakayama, T., Yasumatsu, T., & Sakane, H. (1994). Deterioration mechanism of Cu/ZSM-5 as a catalyst of selective reduction of NO_x by hydrocarbons from the exhaust of stationary natural gas-fueled engine. *Studies on Surface Science and Catalysis, 88*, 409–417.

Torre-Abreu, C., Ribeiro, M. F., Henriques, C., Ribeiro, F. R., & Delahay, G. (1997). Deactivation of Cu-MFI catalysts under NO selective catalytic reduction by propane: influence of zeolite form, Si/Al ratio and copper content. *Catalysis Letters, 43*, 31–36.

Valyon, J., & Hall, W. K. (1993). Studies of species formed NO on copper zeolites. *Journal of Physical Chemistry, 97*, 1204–1212.

Zhang, Y., Leo, K. M., Salofim, A. F., & Hu, Z. (1995). Preparation effects on the activity of Cu-ZSM-5 catalyst for NO decomposition. *Catalysis Letters, 31*, 75–89.

Influence of Fe or Zn Loading Method on the Toluene Methylation over MFI-Type Zeolite Catalysts

*Suphot Phatanasri, Piyasan Praserthdam, and Thana Punsupsawat

Petrochemical Engineering Laboratory, Department of Chemical Engineering, Faculty of Engineering, Chulalongkorn University, Bangkok 10330, Thailand.

Fax: (+662)2186890, (+662)6390449, e-mail: suphot@thaibeginner.com

ABSTRACT Toluene methylation with methanol was investigated on MFI-type zeolite catalysts containing Fe or Zn within the range of 0 - 2 % by weight as an active component. The catalytic performances were compared on catalysts to which Fe or Zn was introduced by different methods, i.e. ion-exchanged and incorporation methods. The prepared catalysts were characterized by XRD, XRF, BET, FTIR and pyridine adsorption technique on in-situ FTIR. The results showed that the incorporated samples, H-Fe,Al-silicate(Si/Fe=150) and H-Zn,Al-silicate(Si/Zn=150), exhibited catalytic activity and xylene selectivities approximately equivalent to those from the ion-exchanged samples, Fe(0.8)/H-MFI and Zn(1.0)/H-MFI, containing nearly the same amount of Fe or Zn. The higher *p*-xylene selectivity was achieved with H-Fe,Al-silicate (Si/Fe=150) and H-Zn,Al-silicate (Si/Zn=150) because of the Brönsted acid strengths weaker than Fe(0.8)/H-MFI and Zn(1.0)/H-MFI. Therefore, the isomerization of *p*-isomer produced primarily was suppressed on the incorporated catalysts better than the ion-exchanged ones.

Running Title: Influence of metal loading methods on toluene methylation over MFI zeolites

Keywords: ion-exchange method, incorporation method, modified MFI zeolites, toluene methylation, characterization

---

* *To whom correspondence should be made.*

INTRODUCTION

MFI zeolites are known as a noteworthy material which have been used as catalysts in many commercial processes. Among their properties, shape selectivity, the presence of strong acid sites, and the resistance to deactivation by coking are the main causes of the unique catalytic behavior. The alkylation of benzene or toluene with light hydrocarbons over acidic catalysts for production of alkylaromatics is an important industrial process [Weitkamp, 1982]. The alkylation over solid catalysts usually has been employed. Initially, protonated or rare earth exchanged faujasites were used in the alkylation of benzene with various olefins [Venuto et al., 1966]. For instance, Yashima et al. [Yashima et al., 1981] focused attention on the distribution of xylene isomers produced by alkylation of toluene with methanol over a variety of cation exchanged Y-zeolites. Consequently, MFI has been used as an alkylation catalyst for the methylation of toluene with methanol [Kaeding et al., 1981]. Many researchers tried to modify MFI in order to alter the selectivities of the alkylaromatics products. Kaeding et al. [Kaeding et al., 1984] proposed that the higher para-selectivity was achieved with MgO, P_2O_5, B_2O_3 or SiO_2 modified MFI. Papa ratto et al. [Papa ratto et al., 1989] reported that the improvement in para-selectivity by the modification of MFI was due to the inactivation of the acid sites on the external surfaces. Sotelo et al. [Sotelo et al., 1993] reported that the impregnation of MFI with Mg or Ni also increases the para-selectivity.

The influence of the preparation methods, however, i.e. ion-exchange or incorporation method on the location of loading metals and their role for the catalytic properties were only briefly reported so far [Yashima et al., 1981, Inui et al., 1992, Parikh et al., 1992]. Therefore, we tried to obtain a more specific relation between the structural properties and the catalytic activity of the modified H-MFI catalysts in

toluene methylation with methanol. To this end, we investigated the catalytic activity of Fe- and Zn-MFI zeolites which were prepared by applying various loading methods in an attempt to change the location of the metals.

EXPERIMENTAL SECTION

Catalyst Preparation

The MFI-type catalysts were prepared by adopting the rapid crystallization method [Inui, 1989] using TPABr as a template. The Na-form MFI-type obtained was converted to its protonated form by four times ion-exchange with 1 M NH_4NO_3 solutions at 80 °C for 1 h, then washed with distilled water, dried overnight at 110 °C, and finally calcined in air at 540 °C for 3.5 h.

H-MFI zeolites incorporated with Fe or Zn, H-Fe,Al-silicate or H-Zn,Al-silicate were prepared by the rapid crystallization method similar to H-MFI synthesis but adding both Al and Fe or Zn during the stage of gel formation before crystallization.

H-MFI materials ion-exchanged with Fe or Zn, Fe/H-MFI or Zn/H-MFI catalyst were prepared by ion-exchange H-MFI with an aqueous solution of $Fe(NO_3)_3.9H_2O$ or $Zn(NO_3)_2.6H_2O$ followed by drying at 110 °C and calcined in air at 350 °C for 2 h. The loading amount of Fe and Zn was in the range of 0-2 % by weight. All the catalysts were tableted, crushed and sieved to 8-16 mesh for the reaction.

Catalyst Characterization

The prepared catalysts were characterized by employing the techniques of XRD (SIEMENS D5000 diffractometer) to confirm MFI framework structure; BET measurement (micromeritics ASAP2000 analyzer) to determine catalyst surface areas;

XRF (Fisons ARL-8410 spectrometer) to determine bulk compositions; FTIR (Nicolet Impact 400 spectrometer) to determine the vibrational modes in the structure sensitive region; and pyridine adsorption on in-situ FTIR to determine the zeolite acidities.

Pyridine adsorption technique on in-situ FTIR was described as following procedure: The prepared catalysts were pressed into self-supporting wafer, mounted in a vacuum apparatus containing cell for IR measurements fitted with potassium bromide windows. The wafer was pretreated by heating to 300 °C for 1 h under vacuum. Then, pyridine was allowed to expose the wafer for 2 h at room temperature. The wafer was then evacuated at 50 °C for 10 min and heated from 50 °C to 450 °C at a heating rate of 5 °C/min to desorb pyridine. In order to measure acid concentration and compare acid strength, the spectra were collected in the temperature range 150-450°C. Infrared spectra were collected on the spectrometer stated above with a resolution of 4 cm^{-1} and typically 500 interferograms were used as an average value.

Catalysis

The toluene methylation with methanol was carried out in a fixed bed tubular quartz reactor under atmospheric pressure. A portion of 0.25 g catalyst was packed in 6.0 mm inner diameter quartz reactor. The feed mixture of toluene and methanol was vaporized before it was contacted with the catalyst bed. The products were analyzed by a SHIMADZU GC-14A gas chromatograph using the flame ionization detector with silicon OV-1 and bentone column. The product selectivities were calculated on the carbon number basis.

RESULTS AND DISCUSSIONS

Catalyst Characterization

The X-ray diffraction (XRD) patterns of the prepared catalysts are shown in Fig. 1. All the prepared catalysts had substantially the structure identical to MFI-type zeolite. The MFI-type framework structure has been further confirmed by FTIR spectra using the KBr technique (0.5 % by weight catalyst) for studying vibrational modes in the structure-sensitive region [Karge, 1998]. As shown in Fig. 2, all the prepared catalysts provided the similar asymmetric stretching vibrations at 1220-1230 and 1100-1110 cm^{-1}; symmetric stretching vibration at 795-800 cm^{-1}; double ring vibration at 540-555 cm^{-1}; and the T-O stretching vibration at 440-450 cm^{-1}. Metal loading did not significantly affect the structure and shape of crystals. BET surface areas and other physical properties of catalysts are shown in Table 1.

From Table 1, the loading of Fe or Zn on H-MFI with incorporation method provided BET surface areas and external surface areas approximately the same as H-MFI. On the other hand, in case of small amounts loading of metal, Fe(0.2)/H-MFI, and Zn(0.2 %)/H-MFI , the external surface areas decreased and micropore areas increased when compared with those of H-MFI. By contrast, the external surface areas increased and micropore areas decreased with the high amounts loading of metal, Fe(0.8)/H-MFI and Zn(1.0)/H-MFI. This suggests that the aggregation of Fe and Zn on the external surface preferably occurred in case of the high amount loaded samples and only small amounts of Fe and Zn could be ion-exchanged with H^+. The aggregation of Fe and Zn on the external surface of catalyst may hinder the passage of N_2 and its adsorption on micropore areas resulting to the lower micropore areas in case of Fe(0.8)/H-MFI and Zn (1.0)/H-MFI.

The pyridine adsorption technique on in-situ FTIR was adopted for the assessment of Brönsted and Lewis acidities. The bands at about 1540 cm^{-1} and 1450 cm^{-1} were reportedly assigned to pyridine adsorbed on Brönsted and Lewis acid sites, respectively [Connerton et al., 1995, Campbell et al., 1996, Karge 1998]. The FTIR spectra of pyridine adsorbed on the prepared catalysts are shown in Fig. 3. The Brönsted and Lewis acid site concentrations of each zeolite sample were determined by measurement of peak areas of these bands at the reference temperature of 150 °C while the relative acid strengths were determined by measurement of the temperature required for reduce a half of pyridine adsorbed; the higher the temperature, the stronger the acid strength. The results are summarized in Table 2.

Effect of Metal Loading Amount in Fe/H-MFI and Zn/H-MFI Catalysts

The catalytic performances on toluene methylation with methanol of Fe/H-MFI and Zn/H-MFI catalysts containing Fe or Zn within the range of 0-2 wt.% loading are shown in Figs. 4 and 5. These data reveal that H-MFI ion-exchanged with 0.8 wt% of Fe, Fe(0.8)/H-MFI, and H-MFI ion-exchanged with 1.0 wt% of Zn, Zn(1.0)/H-MFI, exhibited the best aromatics and xylene selectivities. On the other hand, Fe(0.2)/H-MFI and Zn(0.2)/H-MFI provided the best *p*-xylene selectivity but exhibited the lowest toluene conversion and xylene selectivities. Of all xylene produced, the amount of *o*-xylene was almost constant while the amount of *p*-xylene was inversely related with that of *m*-xylene and toluene conversion. This can be explained by considering that isomerization of *p*-xylene proceeds as the secondary reaction and plays an important role on xylene selectivities [Yashima et al., 1981, Olson et al., 1984, Kaeding, 1985, Sotelo et al., 1993].

Effect of Metal Loading by Incorporation and Ion-exchange

For comparison, H-MFI incorporated with Fe or Zn, H-Fe,Al-silicate or H-Zn,Al-silicate were prepared. The comparative results are shown in Table 3. The thermodynamic compositions of xylene isomers at reaction temperature are given in parentheses.

From Table 3, both H-Fe,Al-silicate (Si/Fe=150) and H-Zn,Al-silicate (Si/Zn=150) exhibited catalyst activity and xylene selectivities approximately equivalent to Fe(0.8)/H-MFI and Zn(1.0)/H-MFI containing nearly the same amount of Fe or Zn. However, *p*-xylene selectivities obtained from toluene methylation with methanol on Fe(0.8)/H-MFI and Zn(1.0)/H-MFI were close to those expected from the thermal equilibrium. A further comparison of *p*-xylene to *m*-xylene and *p*-xylene to *o*-xylene ratios between Fe(0.8)/H-MFI and H-Fe,Al-silicate (Si/Fe=150); Zn(1.0)/H-MFI and H-Zn,Al-silicate (Si/Zn=150) at various reaction temperatures is given in Fig. 6.

The higher *p*-xylene selectivity was achieved with H-Fe,Al-silicate (Si/Fe=150) and H-Zn,Al-silicate (Si/Zn=150) at any reaction temperatures and hence less *p*-xylene isomerization than did Fe/H-MFI and Zn/H-MFI. Moreover, H-Fe,Al-silicate and H-Zn,Al-silicate can be prepared in only one-step crystallization and need no post-synthesis treatment by ion-exchange. This suggests that the modification of the catalytic properties of MFI-type zeolite by loading Fe or Zn as an active component by incorporation method is rather suitable for toluene methylation with methanol than ion-exchanged method because of the high selectivity of *p*-xylene obtained and the convenience of one-step preparation. In addition, it should be noted that the *p*-xylene selectivity decreased while *m*-xylene and *o*-xylene selectivities increased with the increasing reaction temperature.

Regarding the results in Table 2 it has been found that the increasing order of Brönsted acid strength in Fe-containing MFI was Fe(0.2)/H-MFI < H-Fe,Al-silicate (Si/Fe=150) < Fe(0.8)/H-MFI, and that in Zn-containing MFI was Zn(0.2)/H-MFI < H-Zn,Al-silicate (Si/Zn=150) < Zn(1.0)/H-MFI. The order of Brönsted acid strength was inversely related to *p*-xylene selectivity obtained from toluene methylation reaction. This suggests that the Brönsted acid strength plays a more important role to *p*-xylene selectivity than amount of Brönsted acid sites. Either Fe, Zn ion-exchanged or incorporated in H-MFI caused the decrease in amount and strength of Brönsted acid sites and the increase in amount of Lewis acid sites. It has been found that Zn-containing MFI catalysts especially the high amount loading samples exhibited the higher strength of Lewis acid sites than H-MFI which was consistent with the study of Berndt et al. [Berndt et al., 1996].

CONCLUSION

The different metal loading methods, i.e. incorporation and ion-exchanged ones, affect the structural properties and catalytic activity of the modified H-MFI zeolites. The variation in acidic properties between the incorporated catalysts and the ion-exchanged ones reflects the different location of metal in H-MFI zeolites. According to the results obtained, it is worthy to note that the strength of Brönsted acid sites plays a more important role to *p*-xylene selectivity than the amount of Brönsted acid sites. The higher *p*-xylene selectivity obtained on H-MFI zeolites containing Fe or Zn via incorporation method was attributed to the moderate Brönsted acid strength by which the isomerization of *p*-isomer was considerably suppressed.

ACKNOWLEDGEMENT

The authors would like to express their appreciation to the Thailand Research Fund (TRF) which partly supports this work.

REFERENCES

Berndt, H., Lietz, G. and Volter, "Zinc Promoted HZSM-5 Catalysts for Conversion of Propane to Aromatics", *J. Appl. Catal. A.*, **146**, 351 (1996).

Campbell, M., Bibby, M., Coddington, M., Howe, F. and Meinhold, H., "Dealumination of HZSM-5 Zeolites", *J. Catal.*, **161**, 358 (1996).

Connerton, J., Joyner, R. and Padley, M., "Characterisation of the Acidity of Well Defined Cu-ZSM-5 Catalysts Using Pyridine as a Probe Molecule", *J. Chem. Soc. Faraday Trans.*, **91**, 1841 (1995).

Inui, T., "Mechanism of Rapid Zeolite Crystallizations and Its Applications to Catalyst Synthesis", *ACS. Symp.*, 480 (1989).

Inui, T., Nagata, H., Okazumi, F., and Matsuda, H., "Catalytic Properties of Metallosilicates Containing Iron Group Metals in Light-Olefin Conversions", *Catal. Lett.*, 13, 297 (1992).

Kaeding, W.W., "Shape-Selective Reactions with Zeolite Catalyst V. Alkylation or Disproportionation of Ethylbenzene to Produce p-Diethylbenzene", *J. Catal.*, 95, 512 (1985).

Kaeding, W.W., Chu, C., Young, L.B., Weistein and Butter, S.A., "Selective Alkylation of Toluene with Methanol to Produce *p*-Xylene", *J. Catal.*, 67, 159 (1981).

Kaeding, W.W., Chu, C. and Young, L.B., "Shape-Selective Reactions with Zeolite Catalysts IV. Alkylation of Toluene with Ehylene to Produce p-Ethyltoluene", *J. Catal.*, 89, 267 (1984).

Karge, H.G., "Characterization by Infrared Spectroscopy", *Microporous Materials*, 22, 547 (1998).

Olson, D.H. and Haag, W.O., "Catalytic Materials Relationship Between Structure and Reactivity", *ACS. Symp.*, 248, 275 (1984).

Paparatto, G., de Alberti, G., Leofanti, G. and Padovan, M., "Toluene Ethylation on ZSM-5 Zeolites", *Stud. Surf. Sci. Catal.*, 41, 225 (1989).

Parikh, P.A., Subamanyum, N., Bhat, Y.S., and Halgeri, A.B., "Toluene Ethylation over Metallosilicates of MFI Structure", *Catal. Lett.*, 14, 107 (1992).

Sotelo, J.L., Uguina, M.A., Valverde, J.L. and Serrano, D.P., "Kinetics of Toluene Alkylation with Methanol over Mg-Modified ZSM-5", *J. Ind. Eng. Chem. Prod. Res.*, 32, 2548 (1993).

Venuto, P.B., Hamilton, L.A. and Landis, P.S., "Organic Reactions Catalyzed by Crystalline Aluminosilicates II. Alkylation Reactions", *J. Catal.*, 5, 484 (1966).

Weitkamp, "Isomerization of Long-Chain n-Alkanes on a Pt/CaY Zeolite Catalyst", *J. Ind. Eng. Chem. Prod. Res.*, 21, 550 (1982).

Yashima, T., Sakaguchi, Y. and Namba, S., "Selective Formation of *p*-Xylene by Alkylation of Toluene with Methanol on ZSM-5 Type Zeolites", *Stud. Surf. Sci. Catal.*, 7, 739 (1981).

Table 1. BET surface area of MFI catalysts prepared here

Catalyst	Ext. surf. area (m^2/g)	Micropore area (m^2/g)	BET surf. area (m^2/g)	Avg. pore dia. (^oA)
H-MFI	160.07	215.65	375.72	17.49
Fe(0.2)/H-MFI	138.93	247.55	386.48	19.82
Fe(0.8)/H-MFI	190.66	189.83	380.48	17.97
H-Fe,Al-silicate (Si/Fe=150)	156.74	221.38	378.11	17.76
Zn(0.2)/H-MFI	130.04	238.63	368.67	19.93
Zn(1.0)/H-MFI	225.39	160.38	385.76	17.63
H-Zn,Al-silicate (Si/Zn=150)	161.16	217.62	378.78	19.53

* All the prepared catalysts have bulk Si/Al ratio in the range of 31-35.

Table 2. Brönsted and Lewis acidities on catalysts

Catalyst	A_B	A_L	$T_{B/2}$ (°C)	$T_{L/2}$ (°C)
H-MFI	82.8	39.2	366	242
Fe(0.2)/H-MFI	36.8	90.1	320	241
Fe(0.8)/H-MFI	60.1	63.5	354	200
H-Fe,Al-silicate (Si/Fe=150)	79.6	61.9	348	208
Zn(0.2)/H-MFI	36.7	73.1	255	234
Zn(1.0)/H-MFI	54.9	66.0	320	262
H-Zn,Al-silicate (Si/Zn=150)	46.0	93.6	298	260

* A_B and A_L refer to areas by weight of band at 1540 cm^{-1} due to Brönsted acid sites and at 1450 cm^{-1} due to Lewis acid sites, respectively. $T_{B/2}$ and $T_{L/2}$ refer to temperature required for reduce a half of pyridine adsorbed on Brönsted and Lewis acid sites, respectively.

Table 3. Comparison of catalytic performances of different catalysts

(450 °C, GHSV 6000 h^{-1}, 1.5 h on stream, Methanol/Toluene feed ratio 2.5-3.5:1 by wt.)

Catalyst	H-MFI	Fe-containing MFI			Zn-containing MFI		
		(0.2)	(0.8)	(150)	(0.2)	(1.0)	(150)
Fe or Zn Observed (wt %)	0.00	0.25	0.46	0.50	0.19	0.74	0.76
Conversion (%)							
Methanol	90.7	73.1	93.5	94.0	77.7	93.3	93.9
Toluene	66.0	55.1	71.7	70.6	55.5	70.2	72.0
Products Distribution (wt %)							
C1-C4	40.1	49.4	31.7	31.8	46.7	29.9	27.4
C5-C8	2.0	2.1	2.5	4.0	7.7	3.6	1.8
Benzene	2.2	0.2	1.0	0.5	0.2	1.1	1.0
Toluene	14.6	17.2	12.4	13.3	17.4	14.3	12.2
Ethylbenzene	0.2	0.2	0.3	0.3	0.2	0.3	0.4
Xylene	30.3	20.7	33.6	31.6	22.5	33.9	37.0
Ethyltoluene	8.4	6.8	14.3	13.5	7.5	13.2	16.3
Others	2.2	3.5	4.1	5.2	3.9	3.6	4.0
Xylene Composition (%)							
p-xylene (21.56)	30.5	44.7	26.3	34.4	45.1	26.7	29.0
m-xylene (53.33)	46.8	32.0	51.2	45.3	32.5	51.7	49.3
o-xylene (25.11)	22.6	23.3	22.5	20.3	22.4	21.6	21.7

* Fe(0.2), Fe(0.8), Fe(150), Zn(0.2), Zn(1.0) and Zn(150) refer to Fe(0.2)/H-MFI, Fe (0.8)/H-MFI, H-Fe,Al-silicate(Si/Fe=150), Zn(0.2)/H-MFI, Zn(1.0)/H-MFI and H-Zn,Al-silicate(Si/Zn=150), respectively.

Fig. 1 XRD patterns of the prepared catalysts

Fig. 2 FTIR spectra of the prepared catalysts

(a) H-MFI, (b) Fe(0.8)/H-MFI, (c) H-Fe,Al-silicate (Si/Fe=150), (d) Zn(1.0)/H-MFI, and (e) H-Zn,Al-silicate (Si/Zn=150)

Fig. 3 FTIR spectra of pyridine adsorbed on the prepared catalysts

(a) H-MFI, (b) Fe(0.2)/H-MFI, (c) Fe(0.8)/H-MFI, (d) H-Fe,Al-silicate (Si/Fe=150), (e) Zn(0.2)/H-MFI, (f) Zn(1.0)/H-MFI, and (g) H-Zn,Al-silicate (Si/Zn=150)

Fig. 4 Catalytic performances of Fe/H-MFI with different amounts of Fe on toluene methylation with methanol

(a) Toluene conversion, Product selectivities; (b) Xylene selectivities

Reaction conditions: 450 °C, 6000 h^{-1} GHSV, 1.5 h on stream, methanol/toluene feed ratio 2.5-3.5:1 by wt.

Fig. 5 Catalytic performances of Zn/H-MFI with the different amounts of Zn on toluene methylation with methanol

(a) Toluene conversion, Product selectivities; (b) Xylene selectivities

Reaction conditions: 450 °C, 6000 h^{-1} GHSV, 1.5 h on stream, methanol/toluene feed ratio 2.5-3.5:1 by wt.

Fig. 6 (a) Xylene selectivities on

(i) Fe(0.8)/H-MFI and (ii) H-Fe,Al-silicate (Si/Fe=150)

(b) Xylene selectivities on

(i) Zn(1.0)/H-MFI and (ii) H-Zn,Al-silicate (Si/Zn=150)

Reaction conditions: 350-550 °C, 6000 h^{-1} GHSV, 1.5 h on stream, methanol/toluene feed ratio 2.5-3.5:1 by wt.

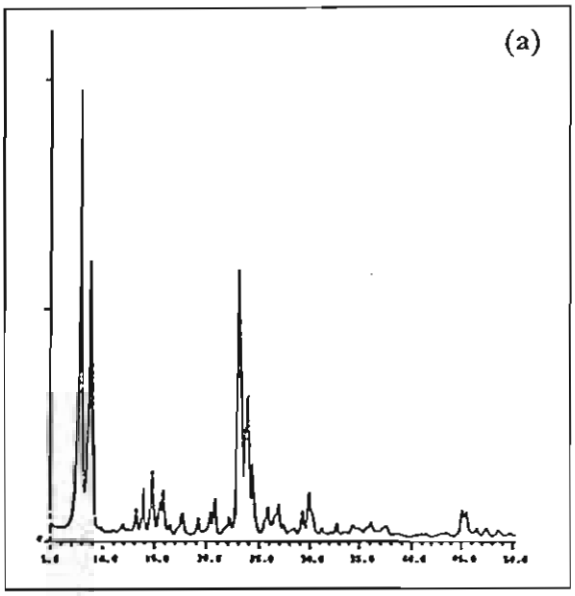
(a)

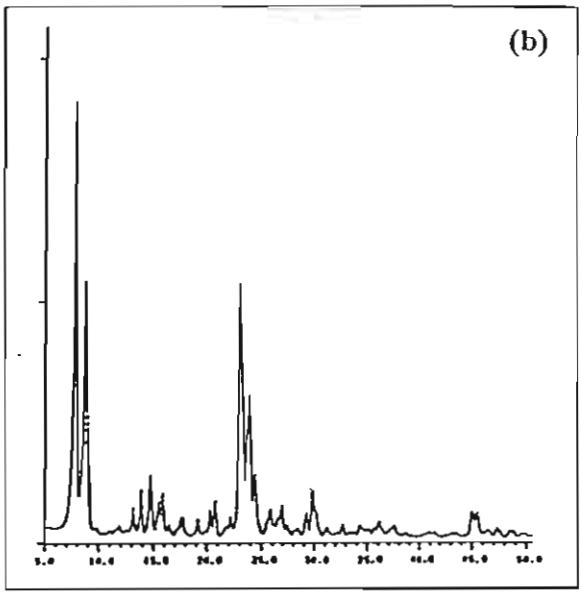
(b)

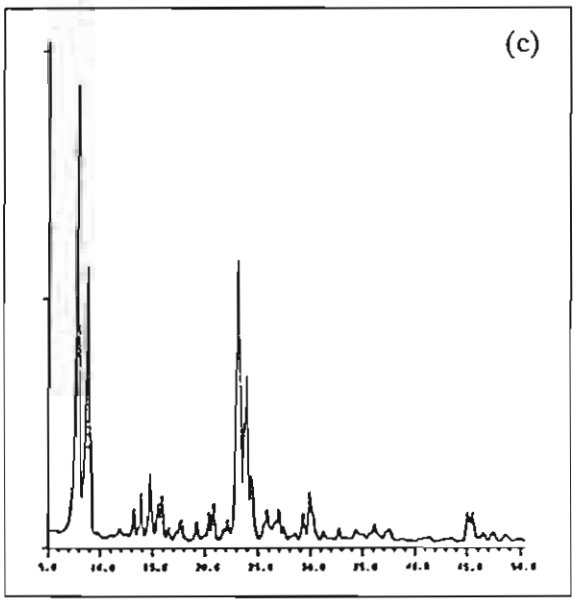
(c)

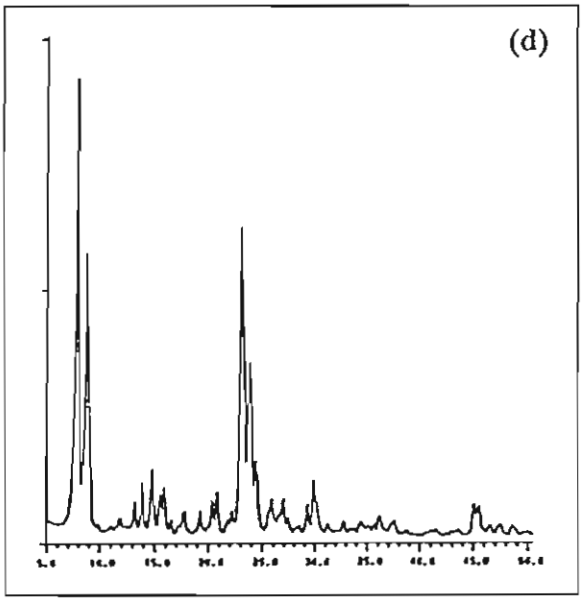
(d)

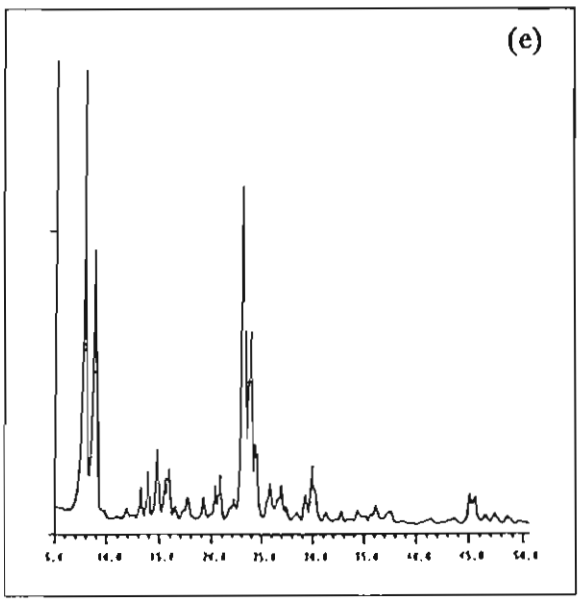
(e)

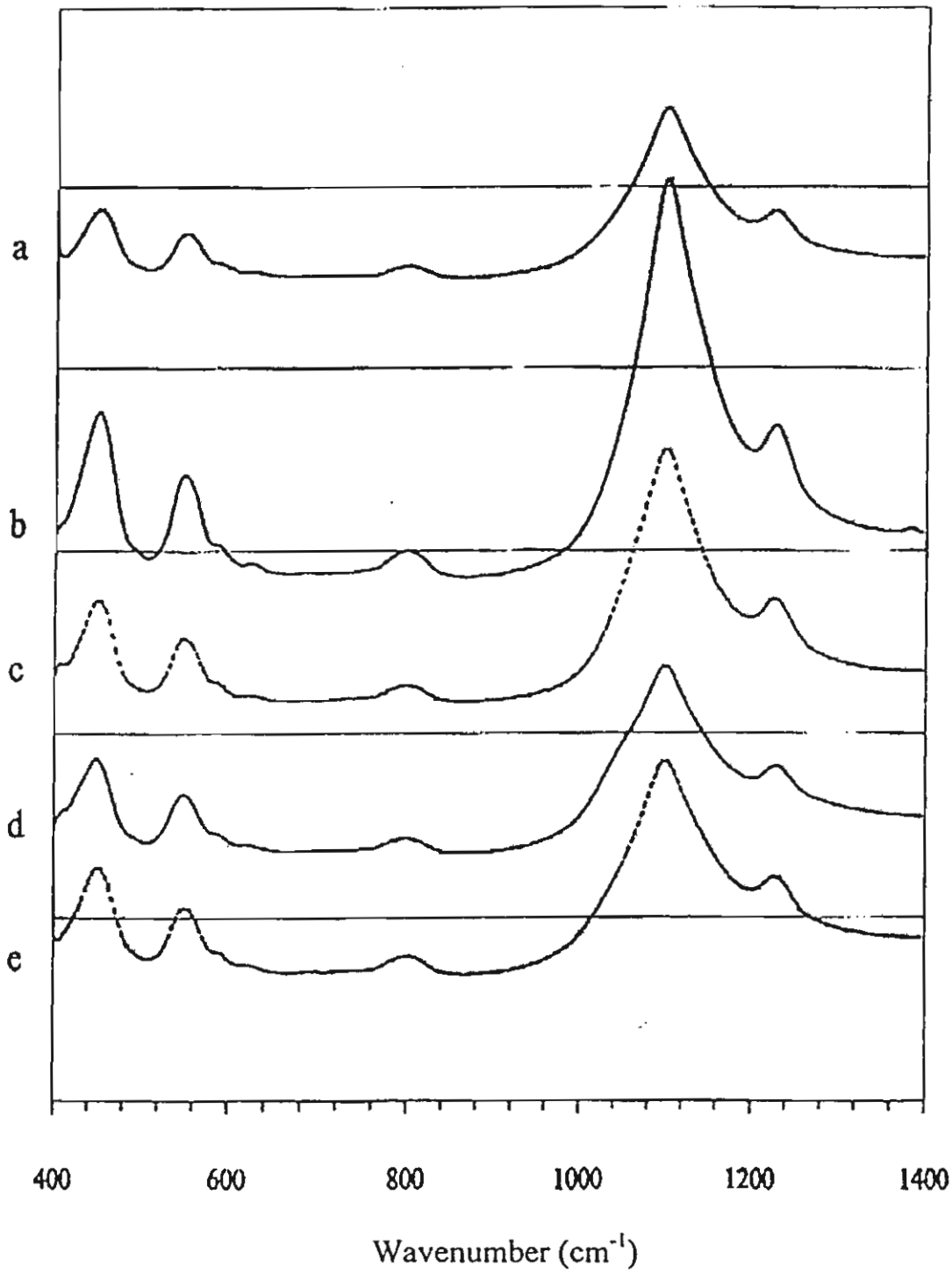
a
b
c
d
e
400
600
800
1000
1200
1400
Wavenumber (cm-1)

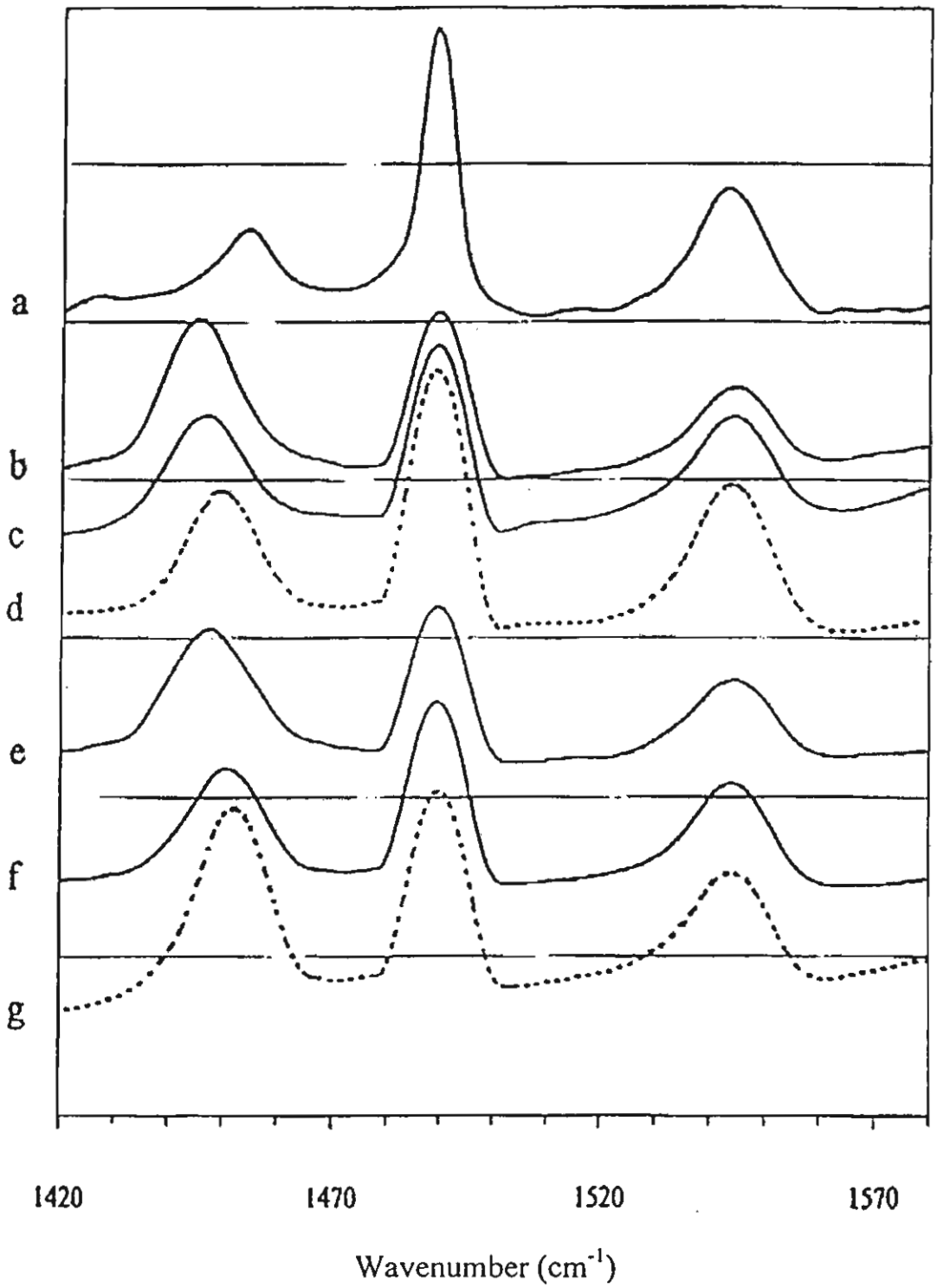
a
b
c
d
e
f
g
1420
1470
1520
1570
Wavenumber (cm-1)

4(a)

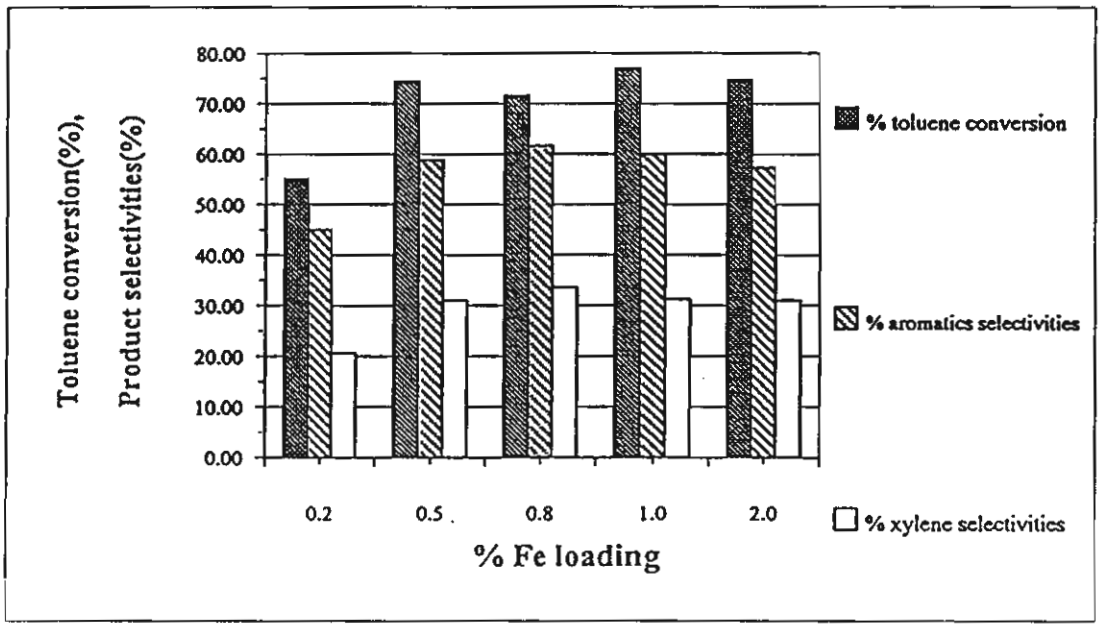
Toluene conversion(%), Product selectivities(%)
80.00
70.00
60.00
50.00
40.00
30.00
20.00
10.00
0.00
0.2
0.5
0.8
1.0
2.0
% Fe loading
% toluene conversion
% aromatics selectivities
% xylene selectivities

4(b)

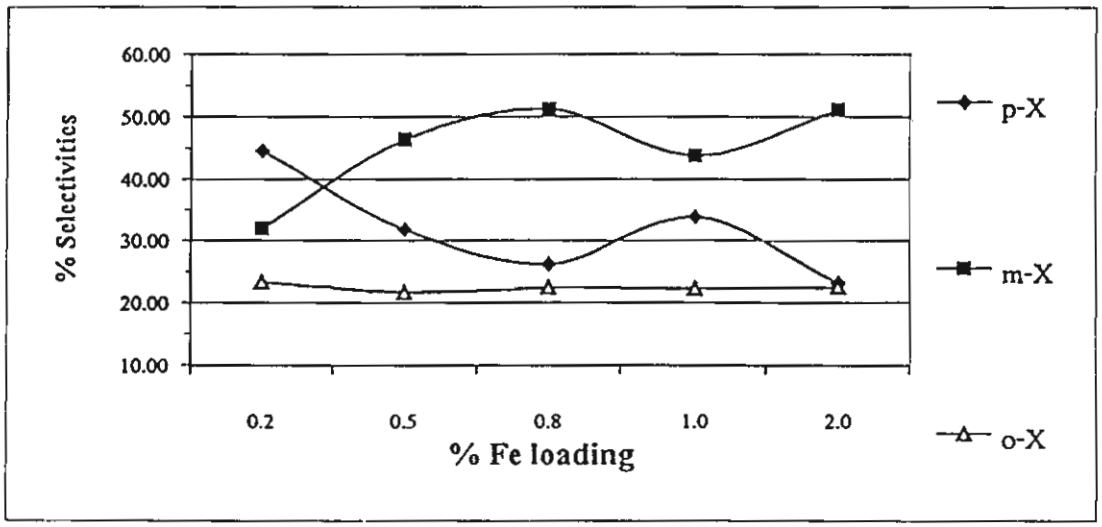
% Selectivities
60.00
50.00
40.00
30.00
20.00
10.00
0.2
0.5
0.8
1.0
2.0
% Fe loading
p-X
m-X
o-X

5(a)

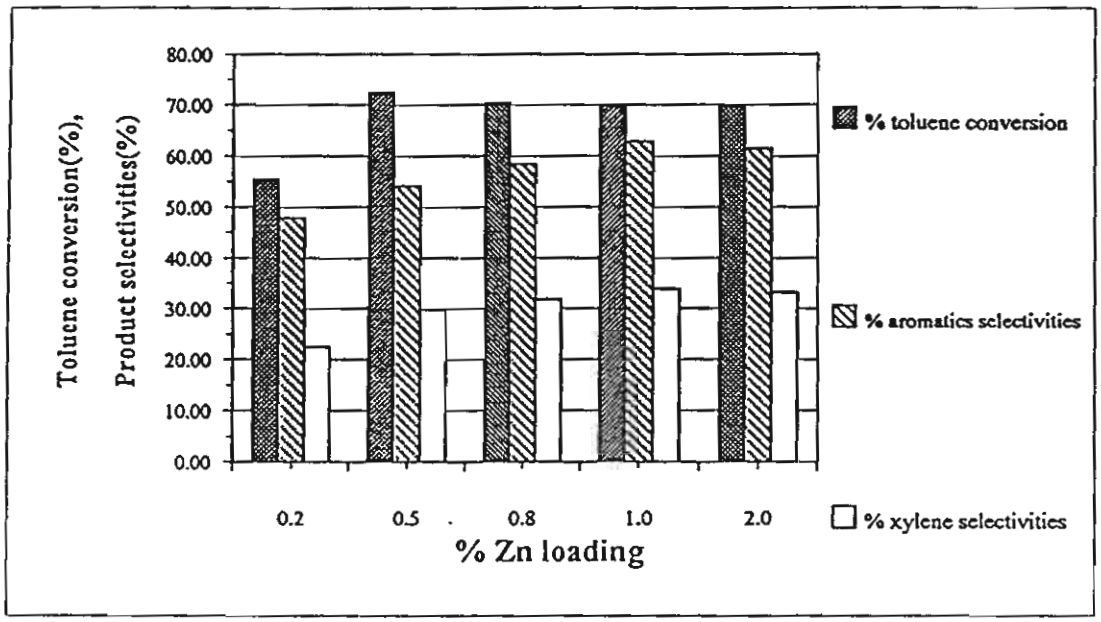
80.00
70.00
60.00
50.00
40.00
30.00
20.00
10.00
0.00
Toluene conversion(%), Product selectivities(%)
0.2
0.5
0.8
1.0
2.0
% Zn loading
% toluene conversion
% aromatics selectivities
% xylene selectivities

5(b)

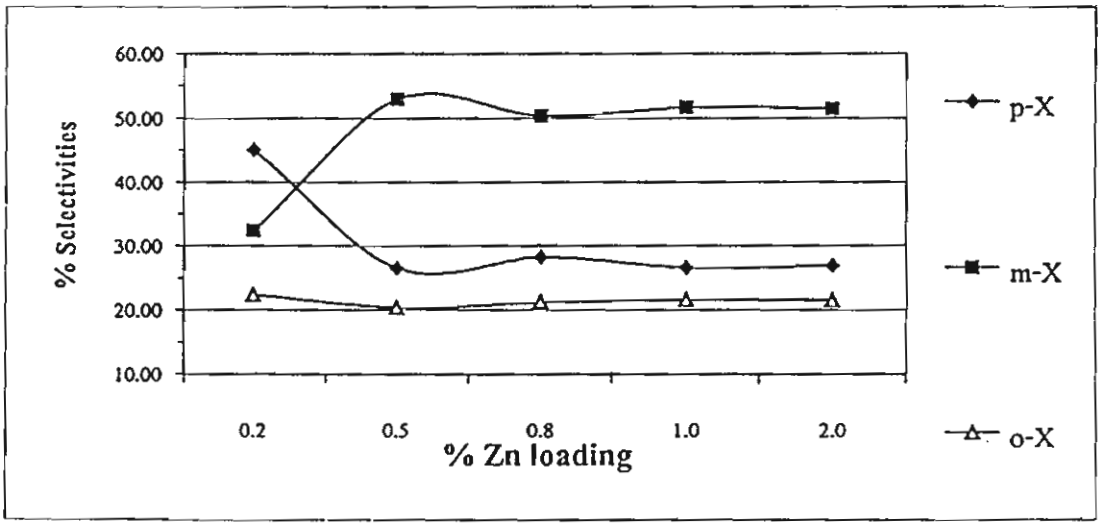
60.00
50.00
40.00
30.00
20.00
10.00
% Selectivities
0.2
0.5
0.8
1.0
2.0
% Zn loading
p-X
m-X
o-X

6(a)

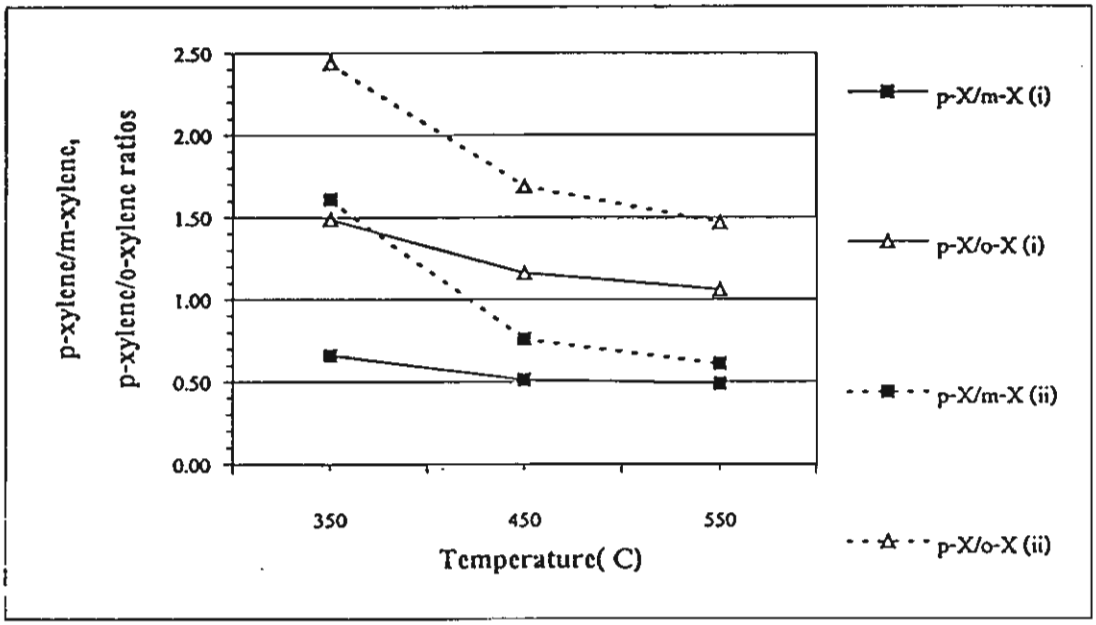
p-xylene/m-xylene,
p-xylene/o-xylene ratios
2.50
2.00
1.50
1.00
0.50
0.00
350
450
550
Temperature(C)
p-X/m-X (i)
p-X/o-X (i)
p-X/m-X (ii)
p-X/o-X (ii)

6(b)

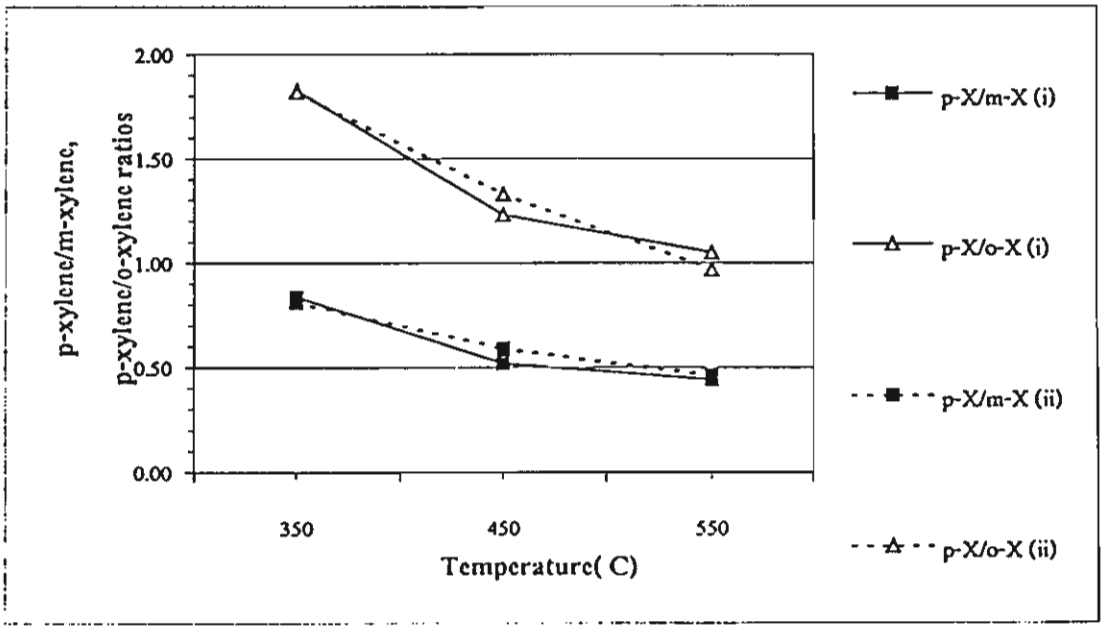
p-xylene/m-xylene,
p-xylene/o-xylene ratios
2.00
1.50
1.00
0.50
0.00
350
450
550
Temperature(C)
p-X/m-X (i)
p-X/o-X (i)
p-X/m-X (ii)
p-X/o-X (ii)

ACTIVATION OF Pd-Ag CATALYST FOR SELECTIVE HYDROGENATION OF ACETYLENE VIA NITROUS OXIDE ADDITION

*Piyasan Praserthdam, Suphot Phatanasri, Jumpod Meksikarin

Petrochemical Engineering Research Laboratory, Department of Chemical Engineering, Chulalongkorn University, Bangkok 10330, Thailand

Abstract

Hydrogenation of acetylene in the presence of a large excess of ethylene has been investigated on the Pd-Ag catalyst under 60°C and a space velocity of 2,000 h^{-1}. It was found that an enhancement in the performance of Pd-Ag catalyst can be obtained by pretreatment with N_2O. It is suggested that added N_2O on the catalyst before use not only augments the sites associated with ethylene production from acetylene but also depletes the sites responsible for direct ethane formation.

Keywords: Selective hydrogenation, Acetylene, Silver promoted palladium catalyst, N_2O pretreatment

INTRODUCTION

The selective hydrogenation of acetylene over supported palladium catalysts is a process widely used to purify the ethylene produced by steam cracking of hydrocarbons. The ethylene to acetylene ratio in the stream to be treated is generally higher than seventy [1]. At present all such catalysts are based on palladium supported on alumina carrier. Palladium-based catalysts promoted by a second metal are now available [2]. The promoter improves selectivity or stability of the catalyst. A. Sarkany et al. [3] have clearly demonstrated that the addition of copper to palladium causes a significant decrease in the overall rate of ethane

* Corresponding author. E-mail : Piyasan.p@chula.ac.th

formation and at the same time there is a decrease in the catalyst activity as well as a marginal decrease in oligomer selectivity. Recently, it has been discovered that the catalyst comprising elements of group IB and transition metals could be activated with N_2O before use [4]. Thus it is an objective of the study to pretreat the Pd-Ag catalyst before being used on the selective hydrogenation of acetylene.

EXPERIMENTAL

A 0.04 wt% Pd-Ag/γAl_2O_3 (Ag:Pd = 4:1) was prepared by the serial impregnation method. The order of catalyst impregnation was the deposition of palladium followed by silver, respectively. Alumina support was Al_2O_3 (CS-303) supplied by United Catalyst Incorporation (UCI), USA. Palladium nitrate and silver nitrate were used as sources for Pd and Ag, respectively. The calcination temperatures for palladium and silver were 300°C and 370°C, respectively.

0.2 g of the catalyst was packed into the 0.6 cm-ID quartz reactor and heated from room temperature to 100°C in Ar, then replaced Ar with H_2 and maintained at this temperature for 2 h. After reduction, the reactor was cooled down to 60°C under argon flow and held for 10 minutes. Then a gas mixture of 0.3% C_2H_2, 0.8%H_2 and C_2H_4 balanced was switched to replace Ar with the flow rate of 30 ml/min. Consequently, the gas mixture was reacted under catalytic hydrogenation, i.e., C_2H_2 was selectively hydrogenated to C_2H_4. However, in the case of N_2O treatment, the reactor was cooled down from 100°C to 90°C under Ar flow and held for 10 minutes before N_2O injection. Then the temperature was reduced to 60°C and the reaction was started. The products were analysed by SHIMADZU FID GC 14B equipped with Carbosieve column s-2.

The active sites of the catalysts were determined by CO adsorption technique and the BET surface areas by a Micromeritic Surface Area Analyser (model ASAP 2000).

The following terms used herein are defined as:

$$\text{Acetylene conversion (\%)} = \frac{\text{acetylene in feed - acetylene in product}}{\text{acetylene in feed}} \times 100$$

$$\text{Ethylene selectivity (\%)} = \frac{\text{ethylene in product - ethylene in feed}}{\text{acetylene converted}} \times 100$$

RESULTS AND DISCUSSION

From several previous investigations (Al-Ammar et al. [5-7], Margitfalvi et al. [8,9], Moses et al. [10], and Weiss et al. [11]), it has

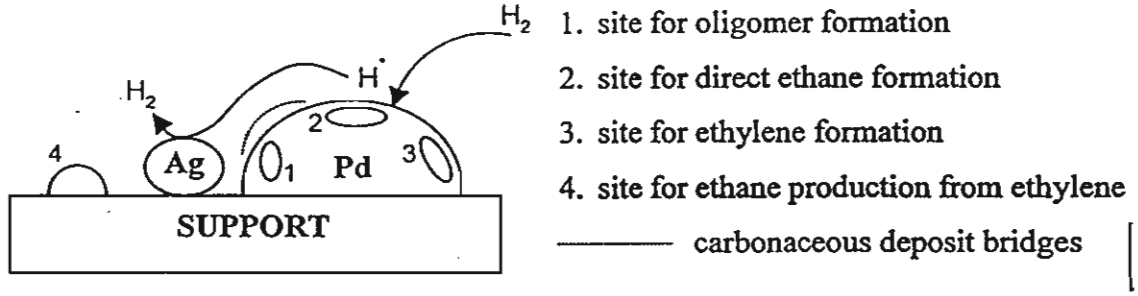

Figure 1 Conceptual model demonstrating four main types of surface sites on Al_2O_3-supported Pd catalyst and the role of Ag promoter as desorption site for transferred H_2

been generally accepted that four main types of surface sites are involved in the alumina-supported Pd catalyst. Three types of which, locating on the Pd metal surface, are responsible for selective conversion of acetylene to ethylene, direct ethane production from acetylene, and oligomer formation from acetylene as shown in Fig. 1. Another site accounting for the hydrogenation of ethylene to ethane is on the surface of alumina

support. It has been reported from some researchers [3,12] that the decrease in ethylene selectivity (i.e. increase in ethylene hydrogenation) during aging has been related to the amount of carbonaceous adsorbate on the catalyst surface. In other words, the carbonaceous deposit acts as hydrogen bridge for the hydrogen spillover from Pd to support. To prove this, the experiment was designed to obtain the set of data at an early period (5 min on stream), or set A, during which the negligible amount of coke was formed. Another one was the set of data at 44 h on stream, or set B, during which the considerable amount of coke was presumably formed though the exact amount of coke deposit was not determined.

As shown in Table 1, the substantial amount of ethane obtained for 0.04% Pd/Al_2O_3 of set A should be produced directly from acetylene, and the ethylene hydrogenation to ethane should be negligible with the

Table 1

Product distribution in C wt% of three kinds of catalysts.

Reaction conditions: 60°C, GHSV 2000h^{-1}

Set	Catalyst	TOS	Feed					
			0.2099	99.7708	0.0121	0.0072		
			Product					
			C_2H_2	C_2H_4	C_2H_6	CH_4	C_2H_2 Conv.(%)	C_2H_4 Selectivity(%)
A	Base[a]	5 min	0.0037	99.8568	0.1321	0.0074	98.23	41.71
	Untreated[b]		0.0065	99.8566	0.1294	0.0074	96.90	42.18
	Treated[c]		0.0015	99.8784	0.1126	0.0073	99.28	51.63
B	Base[a]	44 h	0.0192	99.8338	0.1396	0.0074	90.85	33.04
	Untreated[b]		0.0156	99.8465	0.1305	0.0073	92.56	38.96
	Treated[c]		0.0059	99.8731	0.1134	0.0075	97.18	50.15

[a] 0.04% Pd/Al_2O_3

[b] 0.04% $Pd\text{-}Ag/Al_2O_3$

[c] 0.04% $Pd\text{-}Ag/Al_2O_3$ treated with 0.1 cc of N_2O

assumption that no carbonaceous deposit bridge was formed. When the base catalyst was promoted with Ag, the amount of ethane significantly decreased and so did the acetylene conversion while the amount of

ethylene was almost constant. This implies that the alumina-supported Pd catalyst promoted by Ag may reduce the sites responsible for direct ethane formation from acetylene which is consistent with the previous investigation [12]. In case of the N_2O treatment for set A, both acetylene conversion and ethylene selectivity markedly increased and the amount of ethane was further decreased. This means that the addition of nitrous oxide augments the sites responsible for ethylene formation from acetylene as described above, and advantageously reduces the sites accounting for direct ethane formation as well. As for set B, the amount of ethylene obtained for 0.04% Pd/Al_2O_3 was considerably less than that of the corresponding catalyst for set A, and so did the acetylene conversion. The carbonaceous deposit on the catalyst surface should be responsible for the decrease in acetylene conversion. It is interesting to note that the amount of ethane formed on the base catalyst for set B was higher than that for set A even with less acetylene conversion. This means the substantial amount of ethane was formed via the ethylene hydrogenation on the support sites, with aid of carbonaceous deposit acting as H_2 bridge, rather than the direct ethane formation from acetylene on Pd sites. Sarkany [13,14] has found that the hydrocarbonaceous deposit on Pd/Al_2O_3 catalyst may enhance the over-hydrogenation of 1,3-butadiene and permits the hydrogenation of propene in the presence of 1,3-butadiene due to transport hindrance of 1,3-butadiene. Thus, the over-hydrogenation of acetylene and hydrogenation of ethylene in the presence of acetylene can also be interpreted by transfer limitation of acetylene caused by the presence of carbonaceous deposits. With the Ag-promoted catalyst, the increase in amount of ethylene and acetylene conversion was obtained while the amount of ethane declined. This also implies that the ethylene hydrogenation was reduced by Ag promotion, and the direct ethane formation from acetylene on Pd sites

covered with carbonaceous deposit was negligible. Thus it has been suggested that Ag may hinder the hydrogen spillover from the metal surface to alumina support probably by providing the desorption sites for transferred hydrogen as illustrated in Fig. 1. With the N_2O treatment, both acetylene conversion and ethylene selectivity significantly increased while the amount of ethane was further decreased as similar to those obtained for set A. The improved results achieved on N_2O-treated Pd-Ag/Al_2O_3 catalyst for both sets of data essentially contend that the addition of N_2O increases the sites responsible for ethylene formation from acetylene and decreases the sites involving direct ethane formation as mentioned above. Table 2 shows the results of BET surface area of the catalysts. It has been found that the BET surface area of the N_2O-treated catalyst was slightly higher than that of the untreated one. This reflects that two silver atoms may move closely to one oxygen atom to form Ag_2O. This phenomenon can expose the active palladium sites which normally locate under the surface of metal cluster as modeled in Fig. 2. Table 3 shows the metal active sites of catalysts measured by co adsorption. It has been found that the Ag-Promoted Pd catalyst exhibited less amount of active sites than that of the unpromoted one. This may be due to the alloy formation between both metals. The addition of N_2O to

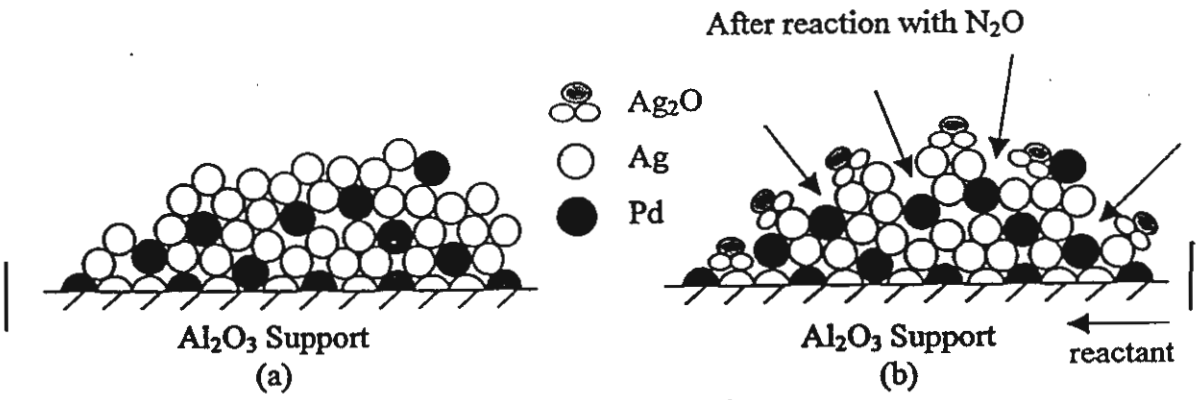

Figure 2 Proposed model illustrating the effect of N_2O addition on enhancing the accessible sites of active Pd responsible for acetylene hydrogenation to ethylene.

Table 2

BET surface area of three catalysts

Catalyst	BET (m^2/g)
0.04% Pd/Al_2O_3	4.74
0.04% $Pd-Ag/Al_2O_3$ (untreated)	4.36
0.04% $Pd-Ag/Al_2O_3$ (treated)	4.98

Table 3

The metal active sites of catalysts measured by CO adsorption

Catalyst	Metal active sites (sites/gram of catalyst)
0.04% Pd/Al_2O_3	3.30×10^{17}
0.04% $Pd-Ag/Al_2O_3$	2.52×10^{17}
0.04% $Pd-Ag/Al_2O_3$ (0.02 cc of N_2O)	3.14×10^{17}
0.04% $Pd-Ag/Al_2O_3$ (0.035 cc of N_2O)	3.22×10^{17}
0.04% $Pd-Ag/Al_2O_3$ (0.05 cc of N_2O)	3.70×10^{17}
0.04% $Pd-Ag/Al_2O_3$ (0.10 cc of N_2O)	4.04×10^{17}
0.04% $Pd-Ag/Al_2O_3$ (0.15 cc of N_2O)	3.37×10^{17}
0.04% $Pd-Ag/Al_2O_3$ (0.33 cc of N_2O)	3.18×10^{17}

the silver-promoted catalyst was found to enhance the amount of active sites, and the highest amount of which was achieved with the injection of 0.1 cc of N_2O. Though N_2O addition may cause the formation of both silver oxide and palladium oxide on the surface of Al_2O_3 support corresponding to the reproduction and destruction of active sites, respectively, the highest amount of active sites obtained with 0.1 cc injection of N_2O may be attributed to the predominant reproduction of Pd active sites.

CONCLUSION

It might be concluded that N_2O treatment could improve the catalytic performance of the silver-promoted palladium catalyst by enhancing the accessible sites of active Pd responsible for ethylene production from

acetylene, and meanwhile decreasing the sites involving the direct ethane formation from acetylene.

ACKNOWLEDGEMENTS

The financial support of this research by The Thailand Research Fund (TRF) is gratefully acknowledged.

REFERENCES

1. G.C. Battiston, L. Dallord, G.R. Tauszik: *Appl. Catal.*, 2, 1 (1982).
2. J.P. Boitianx, J. Cosyn, M. Derrien, and G. Leger: *Hydrocarbon Processing*, March, 51 (1985).
3. A. Sarkany, and L. Guczi: *Appl. Catal.*, **10**, 369 (1984).
4. P. Praserthdam, U.S. Patent 5,849,662, Dec. 15, 1998.
5. Al-Ammar A.S., and G. Webb: *J.C.S. Faraday*, **174**, 195 (1978).
6. Al-Ammar A.S., and G. Webb: *J.C.S. Faraday*, **174**, 657 (1978).
7. Al-Ammar A.S., and G. Webb: *J.C.S. Faraday*, **175**, 1900 (1978).
8. J. Margitfalvi, L. Guczi, and A.H. Weiss, *J. Catal.*, **72**, 185 (1981).
9. J. Margitfalvi, L. Guczi: *React. Kinet. Catal. Lett.*, **15**, 475 (1980).
10. J.M. Moses, A.H. Weiss, K. Matsusek, and L. Guczi: *J. Catal.*, **86**, 417 (1984).
11. A.H. Weiss, S. Leviness, V. Nau, L. Guczi, A. Sarkany, and Z. Schay: *Proc. 8th Int. Congr. Catal.*, **5**, 591 (1984).
12. S. Leviness, V. Nau, A.H. Wiess, Z. Schay, and L. Guczi: *J. Mol. Catal.*, **25**, 131 (1984).
13. A. Sarkany: *J. Catal.*, **180**, 149 (1998).
14. A. Sarkany: *Appl. Catal.*, **175**, 245 (1998).

Reprinted from

THE CHEMICAL ENGINEERING JOURNAL

An International Journal of Research and Development

Chemical Engineering Journal 77 (2000) 215–219

Short communication

Coke formation over Pt–Sn–K/Al_2O_3 in C_3, C_5–C_8 alkane dehydrogenation

P. Praserthdam [a,*], N. Grisdanurak [b], W. Yuangsawatdikul [a]

[a] *Petrochemical Engineering Laboratory, Department of Chemical Engineering, Chulalongkorn University, Bangkok 10330, Thailand*

[b] *Department of Chemical Engineering, Khon Kaen University, Khon Kaen 40002, Thailand*

Received 9 October 1998; received in revised form 20 February 1999; accepted 1 September 1999

ELSEVIER

CHEMICAL ENGINEERING JOURNAL

An International Journal of Research and Development

Aims and Scope

The *Chemical Engineering Journal* provides an international forum for the presentation of original research, interpretative reviews and discussion of new development in chemical and biochemical engineering. Papers which describe novel theory and its application to practice are welcome, as are those which illustrate the transfer of techniques from other disciplines. Reports of carefully executed experimental work which is soundly interpreted are also welcome.

Publication information: Chemical Engineering Journal (ISSN 1385-8947). For 2000, volume(s) 78–80 are scheduled for publication. Subscription prices are available upon request from the Publisher or from the Regional Sales Office nearest you or from this journal's website (http://www.elsevier.nl/locate/cej). Further information is available on this journal and other Elsevier Science products through Elsevier's website: (http://www.elsevier.nl). Subscriptions are accepted on a prepaid basis only and are entered on a calendar year basis. Issues are sent by standard mail (surface within Europe, air delivery outside Europe). Priority rates are available upon request. Claims for missing issues should be made within six months of the date of dispatch.

USA mailing notice: – *Chemical Engineering Journal* (ISSN 1385-8947) is published *monthly* by Elsevier Science S.A. (P.O. Box 211, 1000 AE Amsterdam, The Netherlands). Annual subscription price in the USA US$ 1731.00 (valid in North, Central and South America), including air speed delivery. Application to mail at periodical postage rate is pending at Jamaica, NY 11431.

USA POSTMASTER: Send address changes to Chemical Engineering Journal, Publications Expediting, Inc., 200 Meacham Avenue, Elmont, NY 11003.

AIRFREIGHT AND MAILING in the USA by Publication Expediting Inc., 200 Meacham Avenue, Elmont, NY 11003..

Orders, claims and product enquiries: please contact the Customer Support Department at the Regional Sales Office nearest you:

New York: Elsevier Science, P.O. Box 945, New York, NY 10159-0945, USA. Tel.: (+1) 212-633-3730 [Toll free number of North American customers: 1-888-4ES-INFO (437-4636)], Fax: (+1) 212-633-3680, E-mail: usinfo-f@elsevier.com

Amsterdam: Elsevier Science, P.O. Box 211, 1000 AE Amsterdam, The Netherlands. Tel.: (+31) 20-485-3757, Fax: (+31) 20-485-3432, E-mail: nlinfo-f@elsevier.nl

Tokyo: Elsevier Science, 9-15 Higashi-Azabu 1-Chome, Minato-ku, Tokyo 106-0044, Japan. Tel.: (+81) 3-5561-5033, Fax: (+81) 3-5561-5047, E-mail: info@elsevier.co.jp

Singapore: Elsevier Science, No. 1 Temasek Avenue, #17-01 Millenia Tower, Singapore 039192. Tel.: (+65) 434-3727, Fax: (+65) 337-2230, E-mail: asiainfo@elsevier.com.sg

Rio de Janeiro: Elsevier Science, Rua Sete de Setembro 111/16 Andar, 20050-002 Centro, Rio de Janeiro-RJ, Brazil; Tel.: (+55) (21) 509 5340; fax.: (+55) (21) 507 1991; e-mail: elsevier@campus.com.br [Note (Latin America): for orders, claims and help desk information, please contact the Regional Sales Office in New York as listed above]

Advertising Information

The paper used in this publications meets the requirements of ANSI/NISO Z39.48-1992 (Permanence of Paper).

Printed in The Netherlands

Chemical Engineering Journal 77 (2000) 215–219

Chemical Engineering Journal

www.elsevier.com/locate/cej

Short communication

Coke formation over Pt–Sn–K/Al_2O_3 in C_3, C_5–C_8 alkane dehydrogenation

P. Praserthdam [a,*], N. Grisdanurak [b], W. Yuangsawatdikul [a]

[a] *hemical Engineering Laboratory, Department of Chemical Engineering, Chulalongkorn University, Bangkok 10330, Thailand*

[b] *Department of Chemical Engineering, Khon Kaen University, Khon Kaen 40002, Thailand*

Received 9 October 1998; received in revised form 20 February 1999; accepted 1 September 1999

actants on coke formation during dehydrogenation (DH) over 0.3 wt.%Pt–0.3 wt.%Sn–0.6 wt.%K/Al_2O_3 was investigated. e carried out in the temperature range 200–600°C at 1 atm with pairs of alkanes and alkenes (C_3, C_5–C_8). The carbonaceous during the process were analyzed using the temperature-programmed oxidation (TPO) technique. With the same amount profiles of the short alkane and alkene (C_3) did not match completely, while those of the larger chain alkanes and alkenes tually identical. From these results, a simple model of coke formation has been proposed. Short alkane DH provides coke er alkane DH generates coke in series and consecutive modes.

dehydrogenation; TPO; Coking

n

of catalysts by carbonaceous deposits is a equently encountered in the petrochemical has far-reaching applications and consent years, it has received increasing attention, the rapidly growing number of publications is topic.

ition (DH) of alkanes is one of the most tions in increasing chemical feedstocks. onditions needed for this process, high temw pressure, result in the formation of coke t, which leads to a short catalyst lifetime. s have been conducted to improve the catalyst . Lin et al. [1] showed that Pt–Sn/Al_2O_3 can gth of chemisorption of the hydrocarbon on nd the carbon precursor can then migrate to ily. This process reduced coke accumulation s. Recent work reported that the addition of –Sn/Al_2O_3 for propane DH can extend the e by decreasing the amount of coke on the

author. Fax: +43-362240.

iyasan@pioneer.netserv.chula.ac.th (P. Praserthdam).

Several research groups have published mechanisms and kinetic models of coke formation [3–5]. A recent mechanism was proposed by Hughes [6], which explained the formation of coke by using a series and parallel model. However, the model did not explain the effect of different reactants with respect to coke formation. Since feedstocks contain mixtures of a variety of paraffins, it is important to know the effects of different paraffin components upon the activity, selectivity and stability of the catalyst. The outcomes could help to decide possible uses of a cut with a certain hydrocarbon composition.

Several techniques have been used to study carbonaceous residues, e.g. Fourier transform infrared (FTIR) [7], transmission electron microscopy (TEM) [8], nuclear magnetic resonance (NMR) [9], Auger electron spectroscopy (AES) [10], temperature-programmed oxidation (TPO) [11–13] etc. All of these techniques give different types of information on coke deposition. A technique widely used to characterize coke deposits is the temperature-programmed technique. This technique supplies information about the location and general structure of coke accumulation over the catalyst surface.

This paper presents the results obtained when a Pt–Sn–K/Al_2O_3 catalyst was used to dehydrogenate pure paraffins. This includes the analysis of the coke and a proposed coke formation model.

7(99)00169-2

2. Experimental details

2.1. Materials

High-purity alumina type NKH-3 (Sumitomo Aluminium Smelting, Japan) was used as the support. Chloroplatinic acid (Wako Pure Chemical I, Japan), stannous chloride dihydrate (Fluka Chemie AG, Switzerland) and potassium nitrate (KNO_3) (E. Merck, USA) were used to prepare the 0.3%Pt–0.3%Sn–0.6%K/Al_2O_3 catalyst. A gas mixture (TIG, Thailand) containing propane, pentane, hexane or octane was used as reaction feed. Diluted oxygen (1 vol%) in helium (TIG, Thailand) was used as an oxidant in the TPO process.

2.2. Catalyst

Alumina support was ground to a mesh size of 60/80, followed by washing with distilled water and then dried at 100°C overnight. The support was then calcined in air at 300°C for 3 h. The impregnation method was used to prepare a catalyst with a calcination step for each addition of the three active chemicals, Pt, Sn and K. Our full report describes this in more detail [14].

2.3. Apparatus and methodology

The apparatus used was an ordinary atmospheric flow system consisting of a quartz reactor. The reactor temperature was controlled by an electric furnace. A schematic diagram of the apparatus is shown in Fig. 1. A variety of gases, shown in Table 1, were used as feed. C_3 was fed directly into the reactor, while C_5–C_8 were vaporized in a saturator at a particular temperature. Nitrogen gas was carried along with the vapour in order to maintain the same concentration of carbon before being introduced into the reactor.

Table 1
Concentration and control temperature of reactants

Reactant	vol% in N_2	Control temperature in the saturator (°C)
Propane	20	–
Propene	20	–
n-Pentane	12	−14.2
1-Pentene	12	−19.5
n-Hexane	10	10.2
1-Hexene	10	5.6
n-Heptane	8.6	32.4
1-Heptene	8.6	28.1
n-Octane	7.5	52.9
1-Octene	7.5	48.8

In each run, 0.1 g of fresh catalyst was placed in the isothermal zone inside the reactor. It was then reduced by hydrogen for 1 h at a flow rate of 30 $cm^3\,min^{-1}$ at 500°C, and then cooled to the required temperature before the reaction. Afterwards, reactant gas was fed into the reactor with a GHSV of 20 000 h^{-1}. The reaction products were analyzed between 5 min and 2 h during the process with a Shimadzu GC-14B flame ionization detector (FID) gas chromatograph (GC). Two kinds of GC columns were used for analysis. The first type was a capillary column. The temperature was initially programmed at 35°C and then followed by a 10°C min^{-1} ramp up to 140°C. The second GC column was a VZ-10 column with an initial temperature set at 65°C followed by an increase of 10°C min^{-1} to 80°C.

The coke formation over each spent catalyst was characterized by a TPO process. The carrier gas containing oxygen in helium was fed into the sample cell at a constant flow rate of 30 $cm^3\,min^{-1}$ under ambient conditions. The temperature was increased linearly from 50 to 700°C at a heating rate of 5°C min^{-1}. At the end of the TPO process, the coke deposits were completely removed. The reaction products were analyzed by an on-line TCD GC with a packed column (Porapack QS). The column temperature was maintained isothermal at 90°C for the entire analysis.

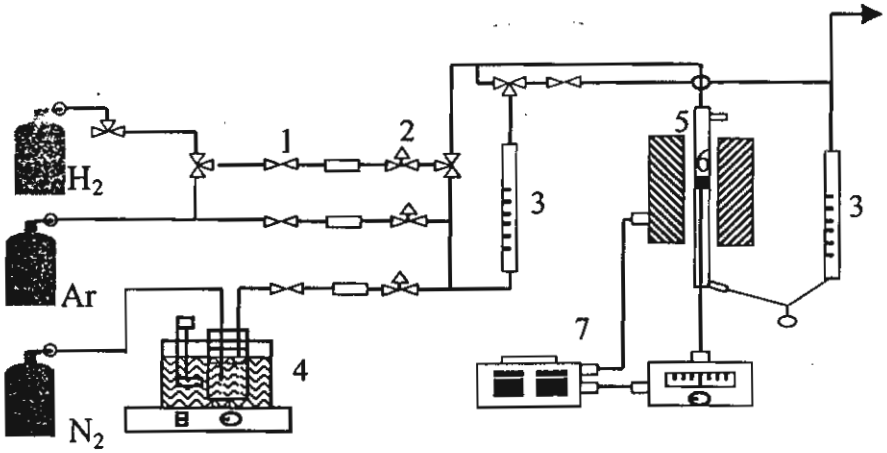

Fig. 1. Schematic diagram of the flow reactor: (1) on–off valve; (2) needle valve; (3) flow meter; (4) saturator; (5) reactor; (6) catalyst bed; (7) temperature control set.

ne reaction selectivity of coke formation was defined as ows:

$$\text{Selectivity of coke formation} = \frac{\text{Atoms of carbon deposited on catalyst} \times 100}{\text{Atoms of carbon feed converted averaged with time}}$$

Results and discussion

was apparent that the products of straight chain alkane would be the parent alkane, the corresponding alkene hydrogen. To better understand the mechanism of coke ation, the corresponding alkenes needed to be investi- d for DH as well. Therefore, normal paraffins and olefins C_3 and C_5–C_8 were used as feeds.

he process for each feed in the absence of a catalyst was ed out to evaluate whether thermal cracking affected It was found that thermal cracking occurred at 500°C; side-reaction was quite significant, especially for high cular weight hydrocarbons, accounting for 5–30% con- ion for C_5–C_8 and almost none for C_3.

reduce the effect of thermal cracking for higher molec- weight hydrocarbons, it was necessary to decrease the ating temperature. The experiments using C_5, C_6, C_7 C_8 alkanes and alkenes showed insignificant thermal cing at 350, 300, 250 and 200°C, respectively, and so experiments were performed at these temperatures. The ity and the selectivity are presented below.

Activity and coke selectivity

propane and propene DH, as shown in Fig. 2, the ac- of propane DH is higher than that of propene DH. The ts corresponded with those of the thermodynamic calcu- ns. However, the activity declined markedly for propane The major products from propane DH were propene, gen and a moderate amount of propadiene. When propene as a feed, more propadiene was produced. idering the percentage of coke produced in the same

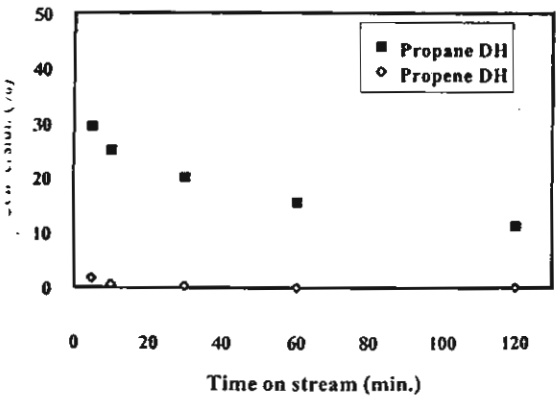

ig. 2. Conversion as a function of time for C_3 DH at 500°C.

Table 2
Coke content and coke selectivity for 2 h time on stream over 0.3 wt.%Pt–0.3 wt.%Sn–0.6 wt.%K/Al_2O_3 operated with a variety of reactants

Reactant	Reaction temperature (°C)	Coke (%)	Selectivity of coke formation (%)
Propane	500	0.80	0.002
Propene	500	2.30	0.185
n-Pentane	350	2.35	0.922
1-Pentene	350	1.93	0.006
n-Hexane	300	1.61	0.393
1-Hexene	300	1.64	0.010
n-Heptane	250	0.22	0.080
1-Heptene	250	0.31	0.016
n-Octane	200	0.16	0.020
1-Octene	200	0.12	0.002

reaction period, it was found that propene DH produced more coke than did propane DH. Therefore, coke selectivity via propene DH was higher than via propane DH, as shown in Table 2. Since propadiene by nature is extremely reactive towards other chemicals, it was reasonable to assume that propadiene would be one of the important precursors for coke formation in low molecular weight alkane DH.

For higher molecular weight hydrocarbons, the activity results are reversed from those of C_3 DH. As shown in Figs. 3–6, the activities of alkene DH are higher than those

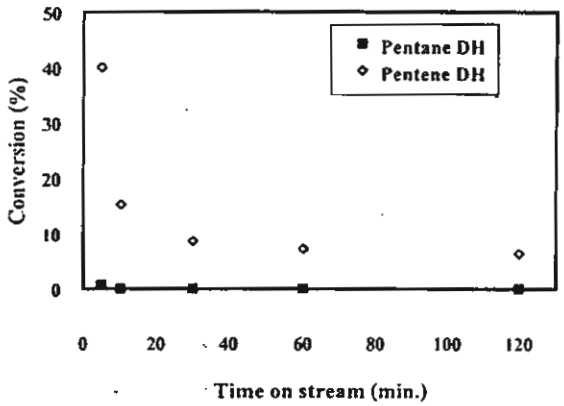

Fig. 3. Conversion as a function of time for C_5 DH at 350°C.

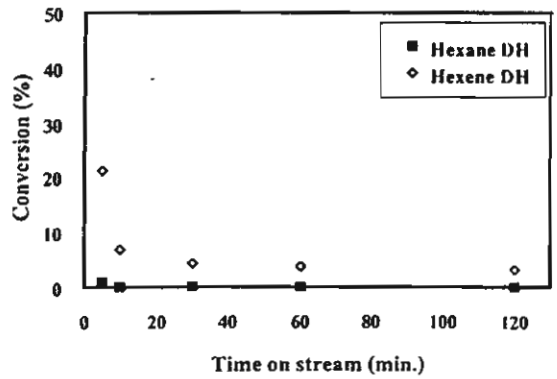

Fig. 4. Conversion as a function of time for C_6 DH at 300°C.

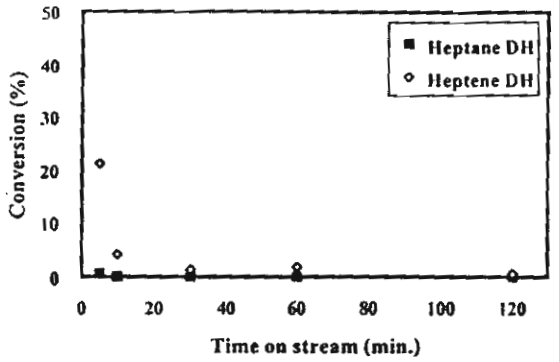

Fig. 5. Conversion as a function of time for C_7 DH at 250°C.

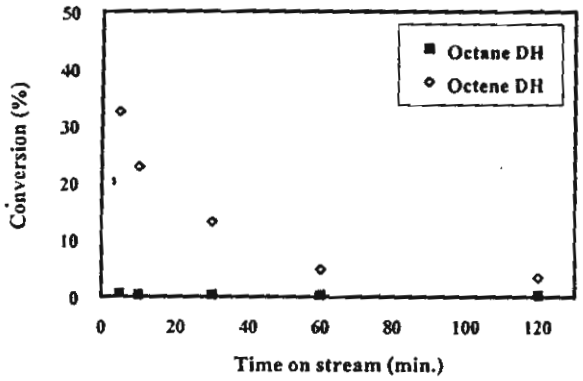

Fig. 6. Conversion as a function of time for C_8 DH at 200°C.

of the corresponding alkane DH. In the early stages, the chromatogram of alkene DH showed a variety of products, including dienes and cycloalkane, while these products were not observed from alkane DH. When the reaction time was increased, 120 min time on stream, both alkane and alkene DH provided similar products. This implied that higher alkane DH over Pt–Sn–K/Al_2O_3 would perform not only DH but also polymerization, cyclization and catalytic cracking. Coke analysis indicated that the percentage of coke was similar for each pair of alkane–alkene DH. The percentage of coke selectivity of the catalyst for alkane DH was higher than that for alkene DH as shown in Table 2. From a thermodynamic viewpoint, reaction through a cyclopentane pathway is one of the most favourable pathways. The experimental results also supported this, as the chromatograms for each feed (C_5–C_8) showed a peak for C_5. Moreover, this indicates that C_5 should be considered as an important coke precursor for high molecular weight hydrocarbons. This result is similar to the study of Beltramini et al. [15]. As shown in Table 2 for the results of pentane through octane, it was found that the higher molecular weight hydrocarbons produced a lower percentage of coke. This confirms that intermediate C_5 is the coke precursor.

Considering the percentage of coke for every reaction studied, it was found that propene DH gave a higher percentage of coke than propane DH, while in the case of large

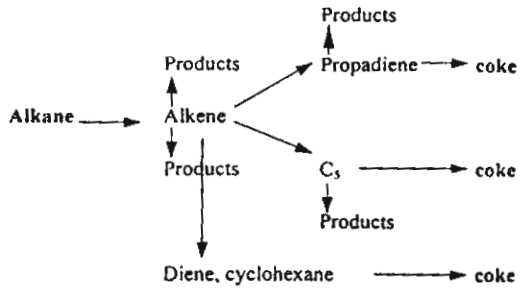

Fig. 7. Schematic representation of coke formation in C_3–C_8 alkane DH.

hydrocarbons, both alkane and alkene DH created an equal percentage of coke. The results suggest that coke formation from different kinds of alkanes occurs via different mechanisms. A schematic diagram of the coke formation mechanism is shown in Fig. 7. This shows that alkanes with a low molecular weight deposit coke via a series mode, while for high molecular weight hydrocarbons, coke formation over catalysts occurs via both consecutive and parallel modes. This also suggests that the coke amount and formation are not directly related to the molecular weight of the hydrocarbon, but related to the structure of the reactants and products, which is similar to the results of Beltramini's work [15].

3.2. Coke analysis

It is accepted that the low temperature peak of the TPO spectrum (280–370°C) corresponds to coke deposited on or in contact with metal sites. The intermediate temperature peak at 445°C is associated with the coke on acid sites close to the metal. The 570°C peak is produced by coke on acid sites far away from any metal sites, called high temperature coke. The aim of this section is to understand the development of coke deposition [16,17].

Fig. 8 shows the TPO patterns of spent catalysts from propane and propene DH, which operated at 500°C after 2 h time on stream. The propene DH spectrum contains two peaks. In contrast, the propene TPO pattern has only one

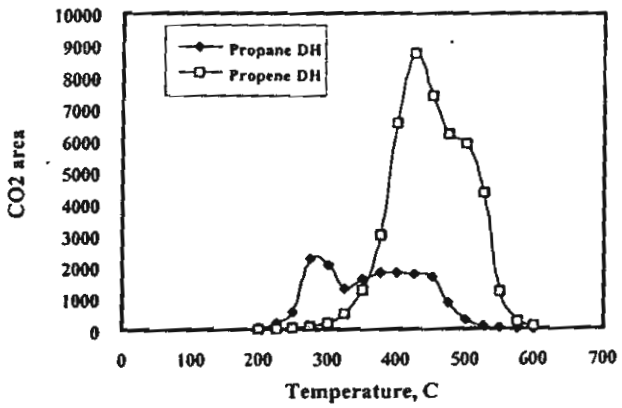

Fig. 8. TPO spectra for C_3 DH operated at 500°C and 2 h time on stream.

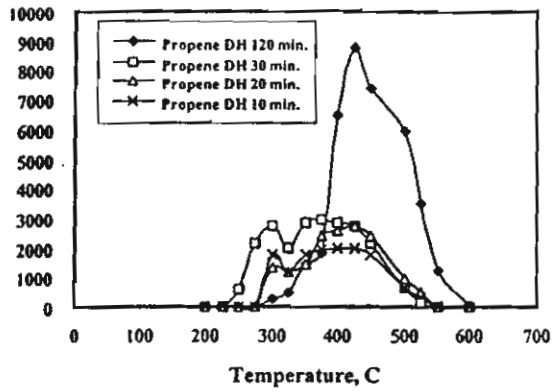

. 9. TPO spectra for propene DH as a function of time on stream.

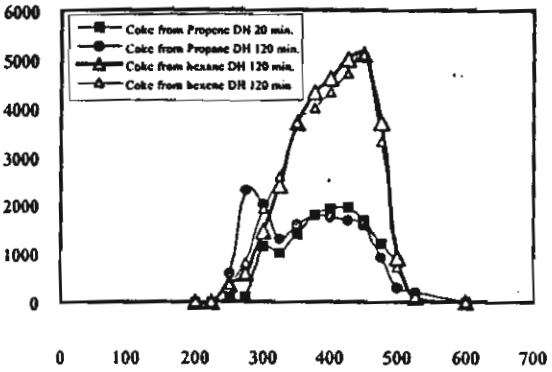

0. TPO spectra for the same amount of coke from C_3 and C_6 DH.

. The coke deposited via propane DH is a low temper- coke and contains a simple structure, while the coke ture obtained from propene DH may be more complex. nderstand the process of development of coke on cat- ; and the content of the coke from propene DH, TPO ra as a function of time were studied, as shown in 9. Two peaks are observed at the initial time interval 30 min). The first peak in the spectrum gradually shifts ime on stream and eventually becomes one peak. This s that coke becomes more complex in structure with ased time on stream. It was therefore theorized that, 120 min, coke was hard to deposit on a small site of . The structure also increased in molecular weight and d to deposit over supports close to metal sites [18].

. 10 presents the TPO patterns obtained from spent st from propane–propene DH at 500°C. The results that both propane and propene DH produce the same nt of coke at 120 min for propane DH and at 20 min opene DH. It was found that both patterns did not etely match. In contrast, TPO patterns of coke by hexane–hexene DH at 300°C were perfectly matched. There was only one peak in the TPO pattern at 445°C and no peak was observed at 280°C. Comparing the amount of coke between C_3 and C_5 (area under the TPO pattern) at 120 min time on stream, C_5 DH had a higher coking rate than C_3 DH.

4. Conclusions

The effect of reactants on coke formation in hydrocarbon DH was investigated over 0.3 wt.%Pt–0.3 wt.%Sn–0.6 wt.% K/Al_2O_3 using the TPO technique. A reactant having three carbon atoms produced coke in a series pathway, while reactants with five to eight carbon atoms produced coke in series and parallel pathways. Propadiene is a coke precursor for C_3 DH and C_5 is a coke precursor for C_5 or higher hydrocarbon DH. Coke increases in molecular weight and prefers to cover the supports rather than the metal sites.

Acknowledgements

Funding provided by the Thailand Research Fund for this study is gratefully acknowledged.

References

[1] L. Lin, Z. Tao, Z. Jingling, X. Zhusheng, Appl. Catal. 67 (1990) 11–23.
[2] N. Lim, Effect of promoters on coke formation on metal site of propane DH catalysts, M.Eng. Thesis, Chulalongkorn University, Thailand, 1996.
[3] N. Daisuke, S. Tomoya, Ind. Eng. Chem. Res. 31 (1992) 14–19.
[4] C.A. Querini, S.C. Fung, Appl. Catal. A: Gen. 117 (1994) 53–74.
[5] K. Liu, S.C. Fung, T.C. Ho, D.S. Rumschitzki, Catalyst Deactivation (1997) 625–638.
[6] R. Hughes, Deactivation of Catalyst, ACS Series, 1984.
[7] C.L. Pieck, E. Jablonsky, E. Parera, J.M. Parera, R. Frety, F. Lefebre, Ind. Eng. Chem. Res. 31 (1992) 1017.
[8] R.A. Cabrol, A. Oberlin, J. Catal. 89 (1984) 256.
[9] F. Diez, B.C. Gates, J.T. Miller, F.J. Sajkowski, S.G. Kukes, Ind. Eng. Chem. Res. 31 (1992) 1017.
[10] J. Niemantsverdiert, A.D. Langeveld, Fuel 65 (1986) 1396.
[11] P. Praserthdam, C. Chaisuk, P. Kanchanawanichkun, Res. Chem. Intermed. 24 (1998) 605–612.
[12] N.S. Figoli, J.N. Beltramini, E.E. Martinelli, J.M. Parer, Appl. Catal. 5 (1983) 19.
[13] C.A. Querini, S.C. Fung, J. Catal. 141 (1993) 389.
[14] W. Yuangsawatdikul, Effect of reactants on coke formation in dehydrogenation, M. Eng. Thesis, Chulalongkorn University, Thailand, 1996.
[15] J.N. Beltramini, E.E. Martinelli, E.J. Churin, N.S. Fogoli, J.M. Parera, Pt–Sn–Cl/Al_2O_3 in pure hydrocarbon reforming, Appl. Catal. 5 (1983) 43–55.
[16] J. Barbier, Catalyst Deactivation (1987) 1–17.
[17] S.C. Fung, C.A. Querini, J. Catal. 138 (1992) 240–254.
[18] J. Barbier, Appl. Catal. 23 (1986) 225–243.

Guide for Authors

Submission of Papers

Papers for *Chemical Engineering Journal* should be submitted to the Editor, Dr R.C. Darton or the Reviews Editor or to one of the Associate Editors.

Addresses of the Editors may be found on the inside cover of the journal.

Submission of a manuscript implies it is not being simultaneously considered for publication elsewhere and that the authors have obtained the necessary authority for publication.

All paper will be independently refereed.

Types of Contribution

Original papers–these should be complete and authoritative accounts of work which has a special significance and must be presented clearly and concisely.

Review articles – these will normally be commissioned by the Editor or the Reviews Editor. Prospective authors of a review article should consult with either Editor to check the suitability of their topic and material before submitting their review.

Short communications – will be accepted for the early communication of important and original advances. Such accounts may be of a preliminary nature but should always be complete and should not exceed the equivalent of 3000 words, including figures and tables.

Letters to the Editor – Letters commenting on work published in the journal shold be sent to the Editor.

The journal will also publish *Book reviews.*

Language

The principle language of the Journal is English, but papes in French are also published.

Authors in Japan please note: upon request, Elsevier Science Japan will Provide authors with a list of people who can check and improve the English of their paper (*before submission*). Please contact our Tokyo office: Elsevier Science Japan, 1-9-15 Higashi-Azabu, Minato-ku, Tokyo 106-0044, Japan. Tel: (03) 5561 5032; Fax: (03) 5561 5045.

Manuscript Preparation

Three copies should be provided in double-space typing on numbered pages of uniform size with a wide margin to the left.

Correspondence address

The name, complete postal address, telephone number, fax number and e-mail address of the corresponding author should be given on the first page of the manuscript.

Abstract

A brief summary (50-200 words) of the contents and conclusions of the paper and an indication of the relevance of new material should be included at the beginning of the paper. Authors of papers in French should provide a translation of the Abstract in English.

References

These should be indicated by numerals in square brackets, introduced consecutively in the text and must be listed at the end of the paper in numerical order. Journal titles should be abbreviated according to the Chemical Abstracts Service Source Index, 1970 edition, and supplements. The abbreviated title should be followed by the volume number, year (in parentheses) and page numbers.

Equations

These should be numbered (1), (2) etc.

Illustrations

It is imperative that authors supply the original and two copies of each illustration. Artwork should be supplied as black ink tracings or as high contrast black and white glossy photographs. High quality computer graphics are also acceptable. Because artwork will generally be reduced in size before printing, any lettering must be sufficiently large (3–5 mm) to be ligible after reduction. All illustrations should preferably require the same degree of reduction and must be clear numbered. Legends to illustrations must be submitted on a separa list. Illustrations can be printed in colour when they are judged t the Editor to be essential to the presentation. Further informatk concerning colour illustrations and the costs to the authors can b obtained from the publisher.

Units

The use of SI units is preferred.

Referees

When submitting a paper authors many suggest up to 3 referee supplying the full name and address in each case. However, the fin choice of referees will remain entirely with the Editor.

Accepted articles on disk

The final and accepted text should be submitted on a 3.5 in diskette (addition to a hard copy with original figures). Double density (D or high density (HD) diskettes formatted for MS-DOS or Apple Ma intosh compatibility are acceptable, but must be formatted to the capacity before the files are copied on to them. The files should b saved in the native format of the word processing program used. Mo popular wordprocessor file formats are acceptable. It is essential th the name and version of the word processing program, type of cor puter on which the text was prepared, and format of the text files a clearly indicated.

Copyright Transfer

All authors must sign the 'Transfer of Copyright' agreement before a article can be published. This transfer agreement enables Elsevi Science to protect the copyrighted material for the authors, but doe not relinquish the author's proprietary rights. The copyright transf covers the exclusive rights to reproduce and distribute the articl including reprints, photographic reproductions, microform or a other reproductions of similar nature and translations, and include the right to adapt the article for use in conjunction with computer sy tems and programs, including reproduction or publication machine-readable form and incorporation in retrieval system Authors are responsible for obtaining from the copyright hold permission to reproduce any figures for which copyright exists.

Proofs

Corresponding authors will receive proofs of their paper. (Authors w not receive proofs of Letters, in order to achieve rapid publicatio They are requested to return corrected proofs as soon as possibl No new material may be inserted in the text at the time of proof rea ing. A "note added in proof" will be accepted only if permission ha been obtained from the Editor.

Offprints

Twenty-five offprints are provided free of charge. Further copies ca be ordered at prices shown on the offprint order form which accon pany the proofs.

Page charges

There are no page charges.

Further Information

All questions arising after the acceptance of manuscripts, especiall those relating to proofs, should be directed to: Elsevier Science Irelan Ltd, Elsevier House, Brookvale Plaza, East Park, Shannon, Co. Clar Ireland. Tel.: +353(61) 709600, Fax: +353(61) 709113. The full and com plete Instructions to Authors can be found on the World Wide Wel access under http://www.elsevier.nl or http://www.elsevier.com.

J. Chin. Inst. Chem. Engrs., Vol. 31, No. 1, 19-25, 2000

Oxidative Coupling of Methane in a Ceramic Membrane Reactor: Uniform Oxygen permeation Pattern

Suttichai Assabumrungrat[1] **and Piyasan Praserthdam**
Petrochemical Research Laboratory, Department of Chemical Engineering, Faculty of Engineering, Chulalongkorn University
Bangkok 10330, Thailand

Shigeo Goto
Department of Chemical Engineering, Nagoya University
Chikusa, Nagoya 464-8603, Japan

Abstract — This paper models the oxidative coupling of methane in a porous ceramic membrane reactor. The catalyst is packed in the tube side of a membrane reactor where the reaction takes place. Methane and oxygen are fed to the tube side and shell side of the membrane, respectively. The membrane controls the distribution of oxygen from the shell side to the tube side and, hence, improves the yield to C_2 hydrocarbon products. The side products such as carbon dioxide and water are suppressed because a low concentration of oxygen in the tube side is maintained. The performance of the membrane reactor is compared with a plug flow reactor where both reactants are fed together to the catalyst bed. It is found that the membrane reactor provides much higher selectivity to C_2 hydrocarbons than the plug flow reactor. Moreover, the membrane reactor is superior to the plug flow reactor in yield when the CH_4/O_2 ratio and the oxygen feed side pressure are high. There is a minimum membrane thickness in which complete permeation occurs for each operating condition. In addition, there is an optimum membrane thickness in which the yield is maximized.

Key Words: Oxidative Coupling of Methane, Membrane Reactor, Optimization and Ceramic Membran

INTRODUCTION

Membrane reactor is one of the fastest expanding subjects of researches in chemical reaction engineering. The concept can be traced back for a few decades. Various types of inorganic membranes have been used in the high-temperature applications. Most of the earlier studies on membrane reactors have focused on overcoming equilibrium by selective removal of one of reaction products from a reaction zone through a membrane. As a result, it can drive equilibrium-limited reactions continuously towards the product side and results in higher than equilibrium conversions, thus limiting the need for high temperature and reducing recycle and downstream separation requirements. This process has often been applied to dehydrogenation reactions (Zeika et al., 1993, Collin et al., 1996; Szegner et al., 1997). Another main field of applications of the membrane reactors is to use the membrane to introduce a reactant in a controlled manner. The membrane is not necessary to be selective but acts as a barrier to separate two streams of reactants. Its applications are, for example, for a reaction which is so highly exothermic that reactants should not be mixed in the same feed inlet, and for a selective oxidation of hydrocarbons where excessive oxygen in the reaction zone should be avoided due to the favorable complete oxidation to carbon dioxide and water. Oxidative coupling of methane to C_2 hydrocarbons, with which this work is concerned, is an example of this case.

The oxidative coupling of methane to C_2 hydrocarbons has become the topic of interest after the pioneering work of Keller and Bhasin (1982). This reaction is important as it represents one of the most effective way to convert methane, the most abundant component of natural gas, to more useful products. Now most of the effort has focused on catalyst characterization, reaction mechanism, catalyst screening and reactor configurations. From the kinetics study it was found that high ratio of methane to oxygen throughout the reactor should favour the desired C_2 formation reaction (Lane and Wolf, 1988). The operation under high oxygen atmosphere enhances the formation of side products, CO_2 and water, leading to a low selectivity to the C_2 hydrocarbons. Taking into account this feature, a series of reactor configurations such as plug flow reactor with discrete feed points of

[1] * To whom all correspondence should be addressed

oxygen (Choudhary et al., 1989), counter-current moving bed chromatographic reactor (Tonkovich and Carr 1995), fluidized-bed reactor (Edwards et al., 1992), riser simulator reactor (Pekediz and de Lasa, 1994) and membrane reactor has been developed. The first and the last reactor configurations are based on the concept of distributing oxygen to the reaction zone discretely and continuously, respectively, along the reactor length. Choudhary et al. (1989) compared a fixed bed reactor with co-feeding of oxygen and methane and a reactor with discrete oxygen feed points along the reactor length. They found that with a fixed overall ratio of methane to oxygen, the C_2 yield increased as the number of oxygen feed points increased in the tubular reactors. However, some researchers found that by splitting the feed of oxygen at various discrete feed points along the reactor length did not significantly improve the C_2 yield (Schweer et al., 1994; Campbell and Ekstrom, 1993). They concluded that the effectiveness of the distributed feed of oxygen depended mainly on the applied catalysts.

Various types of membranes have been used in membrane reactors for the oxidative coupling of methane. Most of them are solid oxides such as yttria-stabilized zirconia (YSZ), PbO or Ag. These membranes are capable of conducting either ionic oxygen or protons and, hence, they are very selective to oxygen. However, because the flux of oxygen obtained is generally low due to its low permeability, the hydrocarbon yield is usually small (Lafarga et al., 1994) and a conversion per pass is low (Omata et al. 1989). Recently membranes with much higher permeability such as modified alumina membrane and porous Vycor glass have been studied. The transport mechanisms include laminar flow and Knudsen diffusion, rather than solid state ionic diffusion. Since the oxygen flows to the reaction side at rates controlled by the applied pressure difference, it results in significantly higher hydrocarbon yield. Lu et al. (1997) compared the oxidative coupling of methane in membrane reactors with various reactor configurations. The overall methane to oxygen feed ratio was optimized such that the C_2 yield at the reactor outlet was maximized. They found that distributed feed oxygen could give rise to much higher C_2 yields than the co-feeding reactor. They also considered the case of a two-membrane reactor where one membrane was used for oxygen feed and the other for C_2 product removal. It was found that the selectivity of the second membrane played an important role on the performance of the reactor. Alternative way to improve the C_2 yield of the oxidative coupling process is to separate C_2 either by a cryogenic method or by adsorption and recycle the unconverted methane (Sofranko and Jubin, 1989).

In this paper the modelling of the oxidative coupling of methane in a ceramic membrane reactor was investigated. Kinetics data of 34 wt% lead oxide catalyst impregnated on γ-alumina (Hinsen et al., 1985) and data on permeation rate of gases through a commercial "Membralox" membrane with 4 nm pore size (Assabumrungrat and White, 1996) were used in the modelling. The performance of the membrane reactor was compared with a plug flow reactor. Particular interest was to investigate the optimum thickness of the membrane in which maximum yield to C_2 hydrocarbons was obtained.

MODELLING OF A MEMBRANE REACTOR

The membrane reactor in this study is a double tubular reactor; the inner tube is made of an alumina membrane, and the outer shell of an impermeable wall. The catalyst is packed in the tube side where a feed of methane is introduced. Oxygen is fed to the shell side. The membrane is exploited to distribute oxygen to the reaction chamber. The model can be simplified by the following assumptions.

(1) The flow in the system is at steady state.
(2) The reaction is operated at isothermal conditions.
(3) The ideal gas law can be used to determine gas properties.
(4) There is a constant pressure in both the shell and the tube side.
(5) The interfacial mass transfer resistance between the gas and the surface of membrane is small compared with the internal mass transfer resistance in the membrane.
(6) Axial diffusion is negligible and all species are ideally mixed in the radial direction.
(7) The membrane is not catalytically active.

Figure 1 illustrates the membrane configuration used in this study. It is operated under cocurrent flow pattern. By performing the material balance across a small distance dz, the following differential equations can be obtained.

For tube side:

$$\frac{d}{dz}N_i = \frac{\pi}{4}D_t^2 r_i + \pi D_t q_i \tag{1}$$

For shell side:

$$\frac{d}{dz}Q_i = -\pi D_t q_i \tag{2}$$

The transport of gas phase through a porous membrane can be taken place by many mechanisms, namely, viscous bulk flow, Knudsen diffusion, surface diffusion, capillary condensation and molecular sieving. Viscous flow (or Poiseuille flow) takes place when the membrane pores are larger than the mean free path of the permeating gas molecules. This mechanism is non-separative and undesired for gas separation process. The transport rate can be described by the Hagen-Poiseuille equation. Knudsen

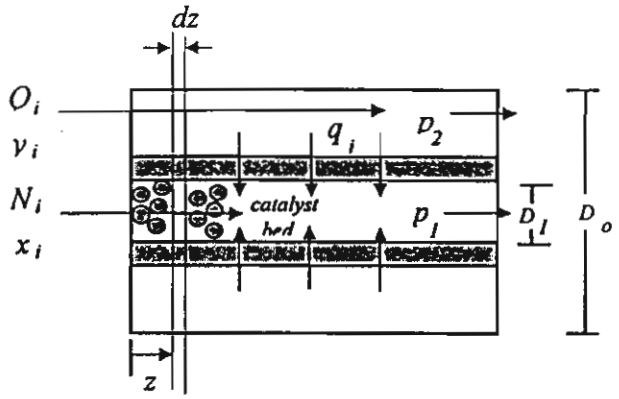

Fig. 1. The membrane reactor configuration.

flow regime predominates when the pore diameter is smaller than the mean free path of gases to be separated. The permeation flux is inversely proportional to the square root of molecular weight. The permeation data used in this study is based on the permeation data of gases through a commercial "Membralox" membrane. The membrane consists of a porous α-alumina support and a separative layer of γ-alumina with pore size of 4 nm and thickness of 5 μm. It was found that both Knudsen and viscous flow mechanisms are important for the permeation of gas through the membrane and the permeation flux of specie i can be expressed as follows (Assabumrungrat and White, 1996).

$$q_i = \frac{a}{t_m\sqrt{M_i}}(p_2 y_i - p_1 x_i) + \frac{b y_i}{t_m \mu}(p_2^2 - p_1^2) \qquad (3)$$

where

$$a = \frac{\epsilon d_p}{3RT\tau}\sqrt{\frac{8RT}{\pi}} \qquad (4)$$

$$b = \frac{\epsilon d_p^2}{64\tau RT} \qquad (5)$$

$$x_i = \frac{N_i}{\Sigma N_i} \qquad (6)$$

and

$$y_i = \frac{Q_i}{\Sigma Q_i} \qquad (7)$$

It should be noted that surface diffusion is unlikely in this study because the reaction is carried out at high temperatures and that the permeation flux is inversely proportional to the thickness.

In the model, the kinetics data of 34 wt% lead oxide catalyst impregnated on γ-alumina was used (Hinsen et al., 1985). The chemical reactions and the rate expressions are given as follows:

$$CH_4 + 2\,O_2 \rightarrow CO_2 + 2\,H_2O \qquad -r_{CH_4} = 15.0 \exp(-6134/T)\, C_{CH_4}^{0.4} \cdot C_{O_2}^{0.5} \qquad (8)$$

$$CH_4 + 1/4\,O_2 \rightarrow 1/2\,C_2H_6 + 1/2\,H_2O \qquad -r_{CH_4} = 1.2 \times 10^3 \exp(-11908/T)\, C_{CH_4}^{0.8} \cdot C_{O_2}^{1} \qquad (9)$$

$$C_2H_6 + 1/2\,O_2 \rightarrow C_2H_4 + H_2O \qquad -r_{C_2H_6} = 1.0 \times 10^{-1} \exp(-722/T)\, C_{C_2H_6}^{0.8} \cdot C_{O_2}^{0} \qquad (10)$$

$$C_2H_4 + 3\,O_2 \rightarrow 2\,CO_2 + 2\,H_2O \qquad -r_{C_2H_4} = 1.0 \times 10^{-13} \exp(26461/T)\, C_{C_2H_4}^{0.8} \cdot C_{O_2}^{6} \qquad (11)$$

It should be noted that the C_2 formation reaction has a lower reaction order in O_2 and a higher reaction order in methane than CO_2 formation. Hence, the selectivity to the C_2 production can be maximized by operating the reactor using high methane concentration and low oxygen concentrations.

Since the obtained system of ordinary differential equations from the cocurrent operation leads to an initial value problem, the Runge-Kutta method is used to integrate the initial value case with the following initial conditions

$$\text{at} \quad z = 0 \qquad N_i = N_i^0$$

and

$$\text{at} \quad z = 0 \qquad Q_i = Q_i^0$$

RESULTS AND DISCUSSION

In this study, the effect of oxygen feed pressure and CH_4/O_2 ratio (defined as the inlet flow rate of CH_4 divided by that of O_2) were investigated. In addition, the membrane thickness was optimized to maximize the yield. The numerical values of the parameters used in the simulations are summarized in Table 1.

Partial pressure profiles at the standard condition

Figures 2 and 3 show partial pressure profiles of all species in the tube and shell sides, respectively, under the standard condition with shell side pressure of 607.8 kPa and CH_4/O_2 ratio of 2. It can be seen that using the membrane reactor the partial pressure of oxygen in the tube size is kept at small value and that there is only a small amount of methane and the reaction products permeating through the membrane because of the high pressure in the shell side.

Figures 4, 5 and 6 compare the conversion, selectivity and yield of the membrane reactors at different values of oxygen feed pressure and CH_4/O_2 ratios with those of the plug flow reactor. It should be noted that the pressure in the reaction side of both plug flow and membrane reactors is the same at 101.3 kPa.

The conversion, selectivity and yield are defined as follows:

$$\text{Conversion} = (N_{CH_4}^0 - N_{CH_4} - Q_{CH_4})/N_{CH_4}^0$$

Table 1. Summary of the values of parameters at standard condition.

Parameters	value	unit
Temperature	1,023	K
Tube side pressure	101.3	kPa
Catalyst bed density	1,500	kg/m^3
Mole fraction of methane in tube side	1	-
Mole fraction of oxygen in shell side	1	-
Membrane inner diameter	0.006	m
Reactor length	0.05	m
Membrane thickness	5×10^{-6}	m
Catalyst weight/molar flow rate of methane (W/F)	50	kg-cat.s/mol
Knudsen parameter (a)	1.26×10^{-12}	$s.(mol/kg)^{1/2}$
Viscous flow parameter (b)	1.30×10^{-22}	$s^2.mol/kg$
Viscosity of pure oxygen	4.55×10^{-5}	kg/(m.s)

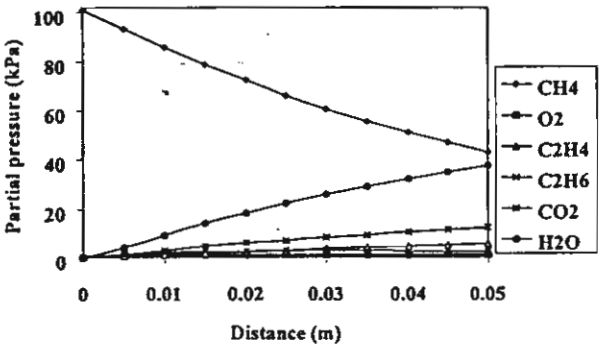

Fig. 2. Partial pressure of all species in the tube side.

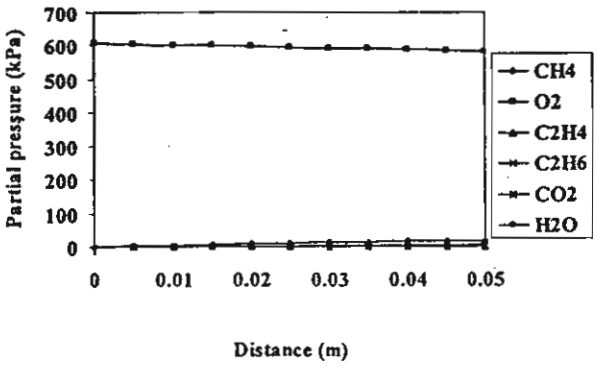

Fig. 3. Partial pressure of all species in the shell side.

$$\text{Selectivity} = 2\,(N_{C_2\text{hydrocarbons}} + Q_{C_2\text{hydrocarbons}})/(N_{CH_4}{}^0 - N_{CH_4} - Q_{CH_4})$$

$$\text{Yield} = (\text{conversion}) \times (\text{selectivity})$$

where $N_{CH_4}{}^0$ and N_{CH_4} are molar flow rates of methane in the tube side at the feed and the exit, respectively. Q_{CH_4} is the molar flow rates of methane in the shell side at the exit. $N_{C_2\text{hydrocarbon}}$ and $Q_{C_2\text{hydrocarbon}}$ are molar flow rates of C_2 hydrocarbons at the exit of the tube side and the shell side, respectively. For the

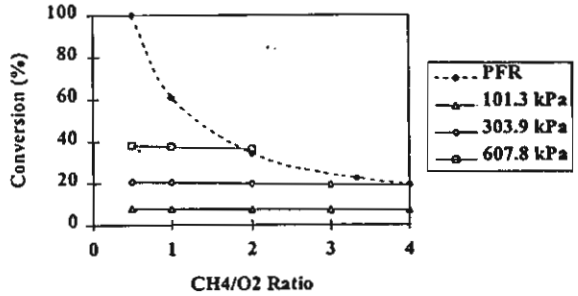

Fig. 4. Conversion versus CH_4/O_2 ratio at different oxygen feed pressures.

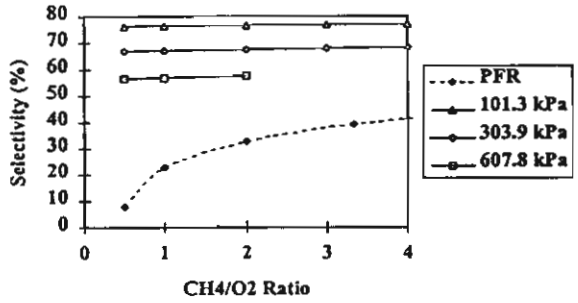

Fig. 5. Selectivity versus CH_4/O_2 ratio at different oxygen feed pressures.

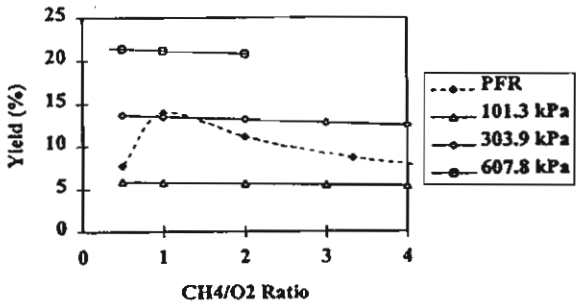

Fig. 6. Yield versus CH_4/O_2 ratio at different oxygen feed pressures.

plug flow reactor $Q_{C_2 hydrocarbon}$ is equal to zero.

The plug flow reactor without the shell side was simulated by the feed mixture of CH_4 and O_2 at 101.3 kPa of total pressure in the tube side. Considering only the effect of CH_4/O_2 ratio, it is obvious that the conversion, selectivity and yield of the plug flow reactor are highly dependent on the CH_4/O_2 ratio while that of the membrane reactors are not. The decrease in the CH_4/O_2 ratio of the plug flow reactor results in the increase in conversion and the decrease in selectivity. This is because at high oxygen partial pressures the undesired complete oxidation to CO_2 and H_2O is favorable (Lane and Wolf, 1988). From Fig. 6, it should be noted that there is an optimum CH_4/O_2 ratio for the plug flow reactor in which the yield to C_2 hydrocarbons is maximized. However, at that optimum ratio the selectivity is only around 22%. For membrane reactor, it was found that selectivity is much higher than that of the plug flow reactor and that the CH_4/O_2 ratio does not significantly affect the conversion, selectivity and yield of the reactor. It is because the membrane controls the supply of oxygen from the shell side to the tube side and, hence, the oxygen partial pressure is maintained at low values throughout the reactor length.

One way to control the supply of oxygen to the tube side is to adjust the oxygen feed pressure in the shell side. From the same figure, it can be found that the oxygen feed pressure in the shell side of the membrane reactor significantly affects the performance of the reactors. When the oxygen feed pressure in the shell side increases, the conversion is higher but the selectivity is lower. This is because more oxygen passes through the membrane and reacts with methane. Even though the selectivity is lower, the selectivity of the membrane reactor is still much higher than that of the plug flow reactor. From Fig. 6, it can be seen that the yield of the membrane reactor is higher than that of the plug flow reactor when the oxygen feed pressure is higher than 303.9 kPa.

Optimizing the maximum yield

Another way to control the oxygen permeation rate is to control the membrane thickness because the permeation flux is inversely proportional to the membrane thickness. Consequently, in order to obtain the maximum yield an optimum membrane thickness should be chosen. Figures 7 and 8 show the selectivity and yield of the membrane reactor at different values of oxygen feed pressure. The CH_4/O_2 ratio is fixed at 2. The dotted lines show the corresponding values of the plug flow reactor. It should be noted that the left end of each curve (different oxygen feed pressures) represents its minimum membrane thickness at which the complete permeation of gases from the shell side to the tube side occurs . It can be seen

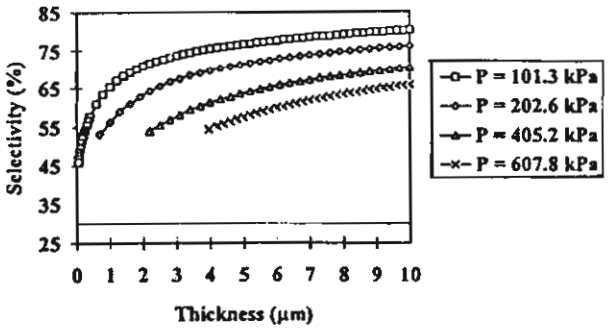

Fig. 7. Selectivity versus membrane thickness at different oxygen feed pressures.

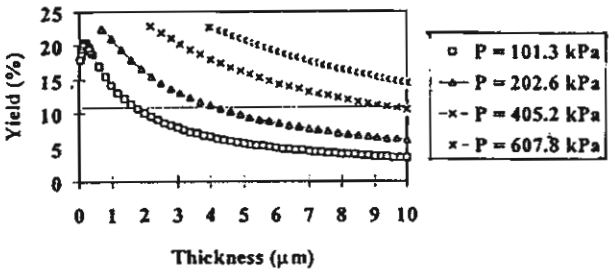

Fig. 8. Yield versus membrane thickness at different oxygen feed pressures.

from the figures that as the membrane thickness is thinner, the selectivity decreases while the yield increases. The increase of the yield means that the increase of the reaction conversion is more significant than the decrease of the selectivity. However, with the oxygen feed pressure of 101.3 kPa when the membrane thickness is thinner, the yield increases until reaching its maximum value and then starts decreasing. The decrease of the yield means that the decrease of the selectivity is more pronounced than the increase of the reaction conversion. This behaviour is similar to the plug flow reactor presented earlier in that there is an optimum CH_4/O_2 in which the yield is maximized. It is obvious from Figs. 7 and 8 that the optimum membrane thickness varies with the oxygen feed pressure; however, the maximum yields obtained from the membrane reactor for the membrane reactor are the same (around 22%) and higher than that of the plug flow reactor (only 11%). In addition, the selectivity of the membrane reactor at the maximum yield is 52% compared to only 30% from the plug flow reactor. It should be noted that the yield of the membrane reactor can be maximized by either adjusting the oxygen feed pressure or choosing an appropriate membrane thickness or by considering both of them together.

Figures 9 and 10 show the selectivity and yield of the membrane reactor at different CH_4/O_2 ratios. The oxygen feed pressure was fixed at 607.8 kPa. Dotted lines in the figures are used to indicate the location of minimum membrane thickness where com-

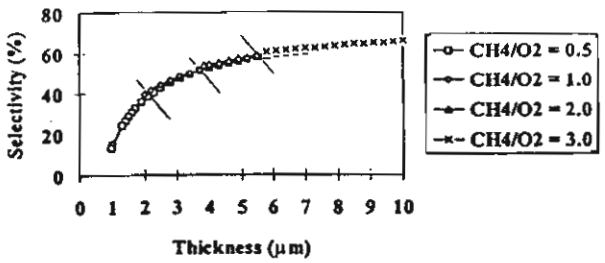

Fig. 9. Selectivity versus membrane thickness at different feed ratios.

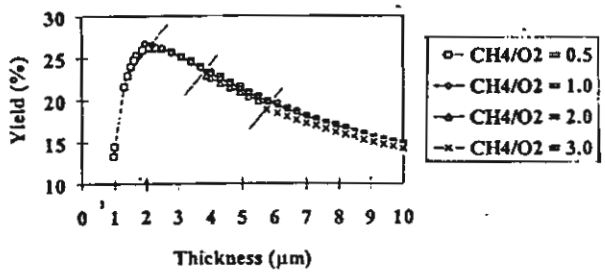

Fig. 10. Yield versus membrane thickness at different feed ratios.

plete permeation of gases in the shell side takes place for different CH_4/O_2 ratios. It can be seen from the figures that the trends of the selectivity and yield of the membrane reactor with the membrane thickness for different values of CH_4/O_2 ratio are similar to those for different values of oxygen feed pressure. However, the minimum membrane thickness and the obtained maximum yield are different for the different CH_4/O_2 ratios. When the CH_4/O_2 ratio is smaller, the more oxygen can be supplied to the reaction system and, hence, thinner membrane thickness can be used. It should be noted that even though the yield increases with the decrease of CH_4/O_2 ratio, the selectivity becomes worsen. From Figs. 7, 8, 9 and 10 it can be concluded that the optimum membrane thickness which gives the maximum yield depends on the operating pressure and the CH_4/O_2 ratio.

It should be noted that in this paper the effects of pressure drop, non-isothermal condition and radial dispersion are not considered. The results from the simulations may slightly deviate from the real values; however, they are still able to represent the benefits of applying the membrane to distribute the oxygen to the reactor for the oxidative coupling of methane.

CONCLUSION

Oxidative coupling of methane in a membrane reactor was modelled using the kinetics and permeation data from the literatures. It was found that the membrane reactor shows much higher selectivity and yield than the plug flow reactor. In addition, for the plug flow reactor there is an optimum CH_4/O_2 ratio that gives the maximum yield while for the membrane reactor there is an optimum membrane thickness that gives the maximum yield. The optimum membrane thickness depends on the operating pressure and the CH_4/O_2 ratio. In addition, for the membrane reactor there is also a minimum membrane thickness in which the complete permeation of gases from the shell side to the tube side occurs for each operating condition.

ACKNOWLEDGMENT

This research was supported by the Thailand Research Fund.

NOMENCLATURE

a	Knudsen parameter defined as Eq. (4), s. $(mol/kg)^{1/2}$
b	viscous flow parameter defined as Eq. (5), $s^2.mol/kg$
C_i	gas concentration of species i, mol/m^3
D_I	inner diameter of membrane reactor, m
D_o	outer diameter of membrane reactor, m
d_p	membrane pore diameter, m
L	length of the reactor, m
M_i	molecular weight, kg/mol
N_i	molar flow rate of species i in the tube side, mol/s
p	pressure at any distance in membrane, Pa
p_i	partial pressure of species i, Pa
p_1	pressure in the tube side, Pa
p_2	pressure in the shell side, Pa
Q_i	molar flow rate of species i in the shell side, mol/s
q_i	molar flow flux of specie i across the membrane, $mol/s.m^2$
r_i	rate of formation of component i, mol/kg-catalyst.s
R	universal gas constant (= 8.314J/(mol.K))
T	temperature, K
t_m	thickness of the separative membrane layer, m
x_i	composition of species i in the tube side
y_i	composition of species i in the shell side
z	axial distance, m

Greek Letters

ε	porosity of membrane, –
μ	viscosity of gas mixture, kg/(m.s)
ρ	density of the catalyst bed, kg/m^3

τ toutorsity factor of membrane, –

REFERENCES

Assabumrungrat, S. and D. A. White, "Permeation of Ethanol and Methanol Vapours through a Porous Alumina Membrane," *Chem. Eng. Sci.*, **51**, 5241, (1996).

Cambell, I. and A. Ekstrom, "Methane Oxidative Coupling in a Pressurized Distributed Feed Reactor," *Symposium on Methane Activation, Conversion and Utilization*, Australia, (1993).

Choudhary, V.R., S.T. Chaudhari, A.M. Rajput and V. H. Rane, "Beneficial Effect of Oxygen Distribution on Methane Conversion and C_2 Selectivity in Oxidative Coupling of Methane to C_2 Hydrocarbon Over Lanthanum-promoted Magnesium Oxide," *J. Chem. Soc., Chem. Commun.*, **20**, 1526, (1989).

Collins, J.P., R.W. Schwartz, R. Sehgal, T. L. Ward, C.J. Brinker, G. P. Hagen and C. A. Udovich, "Catalytic Dehydrogenation of Propane in Hydrogenation Permselective Membrane Reactors," *Ind. Eng. Chem. Res.*, **35**, 4398, (1996).

Edwards, J.H., K.T. Do and R.J. Tyler, "The Catalytic Oxidative Coupling of Methane: I. Comparison of Experimental Performance Data from Various Types of Reactor," *Methane Conversion by Oxidative Process: Fundamental and Engineering Aspects: Wolf, E.E., Ed.; Catalyst Series;* Van Nostrand Reinhold: New York, 429, (1992).

Hinsen, W., W. Bytyn and M. Baerns, "Oxidative Dehydrogenation and Coupling of Methane," *Proceedings of the 8th International Congress on Catalysis, Verlag Chemie: Weinheim, Germany*, 3, 581, (1985).

Keller, G.E. and M.M. Bhasin, "Synthesis of Ethylene via Oxidative Coupling of Methane I. Determination of Active Catalyst," *J. Catal.*, **73**, 9, (1982).

Lane, G.S. and E.E. Wolf, "Methane Utilization by Oxidative Coupling: I. A Study of Reaction in the Gas Phase during the Cofeeding of Methane and Oxygen," *J. Catal.*, **113**, 144, (1988).

Larfarga, D., J. Santamaria and M. Menendez, "Methane Oxidative Coupling using Porous Membrane Reactor I. Reactor Development," *Chem. Eng. Sci.*, **49**, 2005, (1994).

Lu, Y., A.G. Diixon, W.R. Moser and Y.H. Ma, "Analysis and Opitmization of Cross-Flow Reactors for Oxidative Coupling of Methane," *Ind. Eng. Chem. Res.*, **36**, 559, (1997).

Omata, K.S., S. Hashimoto, H. Tominaga and K. Fujimoto, "Oxidative Coupling of Methane Using a Membrane Reactor," *Appl. Catal.*, **52**, L1, (1989).

Pekediz, A. and H.L. de Lasa, "Methane Oxidative Coupling in a Novel Riser Simulator Reactor," *Chem. Eng. Sci.*, **49**, 4759, (1994).

Sofranko, J.A. and J.C. Jubin, Natural Gas to Gasoline: the ARCO GTG Process. Paper 165. Preprints, *Pacifichem* 89, Honolulu, HI, 152, (1989).

Schweer, D., L. Mleczko and M. Bauerns, M. "Oxidative Coupling of Methane in a Fixed-Bed Reactor: Limits and Perspectives," *Catal. Today*, **21**, 357, (1994).

Szegner, J., K. L. Yeung and A. Varma, "Effect of Catalyst Distribution in a Membrane Reactor: Experiments and Model," *AIChE*, **43**, 2059, (1997).

Tonkovich, A. L. Y. and R. W. Carr, "Modeling of the Simulated Counter-Current Moving-Bed Chromatographic Reactor Used for the Oxidative Coupling of Methane," *Chem. Eng. Sci.*, **49**, 4657, (1995).

Ziaka, Z.D., R.G. Minet and T.T. Tsotsis, "A High Temperature Catalytic Membrane Reactor for Propane Dehydrogenation," *J. Mem. Sci.*, **77**, 221, (1993).

(Manuscript Received March 4, 1999)

Kinetics for Dehydrogenation of Propane on Pt-Sn-K/γ-Al_2O_3 Catalyst

SUTTICHAI ASSABUMRUNGRAT[1],
WIROJ JHORALEECHARNCHAI[1],
PIYASAN PRASERTHDAM[1] AND SHIGEO GOTO[2]
[1]*Petrochemical Engineering Laboratory, Department of Chemical Engineering, Chulalongkorn University, Bangkok 10330, Thailand*
[2]*Department of Chemical Engineering, Nagoya University, Nagoya 464-8603, Japan*

Reprinted from
JOURNAL OF
CHEMICAL ENGINEERING
OF
JAPAN
Vol. 33, No. 3 (2000)
Pages 529–532

ırnal of Chemical Engineering of Japan, Vol. 33, No. 3, pp. 529–532, 2000

:inetics for Dehydrogenation of Propane on Pt-Sn-K/γ-Al_2O_3 Catalyst

SUTTICHAI ASSABUMRUNGRAT[1],
WIROJ JHORALEECHARNCHAI[1],
PIYASAN PRASERTHDAM[1] AND SHIGEO GOTO[2]
[1]*Petrochemical Engineering Laboratory, Department of Chemical Engineering, Chulalongkorn University, Bangkok 10330, Thailand*
[2]*Department of Chemical Engineering, Nagoya University, Nagoya 464-8603, Japan*

:ywords: Dehydrogenation, Propane, Propene, Kinetics, Platinum-Based Catalyst

The performance of three catalysts, namely Pt/γ-Al_2O_3, Pt-Sn/γ-Al_2O_3 and Pt-Sn-K/γ-Al_2O_3 for dehy-ogenation of propane is discussed. All catalysts are found to be highly selective towards propene. Pt-ı-K/γ-Al_2O_3 appears to be the most stable and suitable catalyst for the dehydrogenation of propane. Pt-n/γ-Al_2O_3 is also found to be superior to Pt/γ-Al_2O_3. In the kinetic study, the reaction rate constants ısed on the number of active sites are calculated from the apparent reaction rate constants and the ımber of metal active sites. The reaction rate constants for Pt/γ-Al_2O_3, Pt-Sn/γ-Al_2O_3 and Pt-Sn-K/γ-l_2O_3 catalysts at 773 K are 0.48×10^{-25}, 0.67×10^{-25} and 2.98×10^{-25} mol/(site·s·Pa), respectively. In ddition, for Pt-Sn-K/γ-Al_2O_3, the frequency factor and the activation energy are 6.14×10^{-24} mol/(site·s·Pa) nd 62.7 kJ/mol, respectively.

ntroduction

The concept of membrane reactor has shown high ɔotential for applications in the fields of biological and hemical reaction engineering during the past several ecades. One of the major applications of membrane eactors is overcoming an equilibrium conversion by ombining reaction and separation in a single unit operation. The dehydrogenation of propane to propene is ɔne of the reactions of interest in this type of application. A number of researchers have studied this reaction using various types of membrane materials and atalysts. Sheintuch and Dessau (1996) used a Pd/Ru or Pd/Ag) membrane reactor packed with a supported t catalyst. They found that the yield was limited by eactivation of the catalyst due to the low partial pressure of hydrogen in the reaction side. Weyten *et al.* (1997) investigated the system using H_2-selective silica nembrane with a chromia/alumina catalyst, and found hat the propene yield was at least twice as high as the value obtained at thermodynamic equilibrium in a conentional reactor. Yildirim *et al.* (1997) evaluated the elative performance of three composite membranes; namely Pd/Ag, silica, and Pd-dispersed porous membranes. They found that the dense Pd-Ag composite ystem possessed higher performance levels. However, metal-dispersed porous systems had advantages due to their significantly higher contact surface-to-volume atio.

Received on September 9, 1999. Correspondence concerning this article should be addressed to S. Assabumrungrat.

Although significant research has been carried out in this area, there is little effort to investigate the reaction rate constants of propane dehydrogenation. This study is focused on kinetic determination for the dehydrogenation of propane. Three catalysts, namely Pt/γ-Al_2O_3, Pt-Sn/γ-Al_2O_3, and Pt-Sn-K/γ-Al_2O_3 were tested to find out the catalytic performance and the reaction rate constants were determined. These data are useful in the modeling of the dehydrogenation of propane in the membrane reactor.

1. Experiment

1.1 Catalyst preparation

0.3%Pt/γ-Al_2O_3 catalyst was prepared by impregnation of a γ-alumina support. γ-Alumina (produced by Sumitomo Alumina Smelting Co., Ltd., Japan) was ground to the desired mesh size, and then impregnated in a solution of chloroplatinic acid dissolved in de-ionized water. The catalyst was heated at the rate of 10 K per minute, and calcined at 773 K for 3 h. 0.3%Pt-0.3%Sn/γ-Al_2O_3 catalyst was prepared by using an impregnation solution with mixtures of chloroplatinic acid and $SnCl_2$ dissolved in de-ionized water. 0.3%Pt-0.3%Sn-0.6%K/γ-Al_2O_3 could be made by re-impregnation of the calcined 0.3%Pt-0.3%Sn/γ-Al_2O_3 catalyst with potassium nitrate solution.

1.2 Carbon monoxide chemisorption technique

The metal active sites of fresh and used catalyst were measured using a carbon monoxide chemisorption technique whose concept is based on the assumption that one molecule of carbon monoxide adsorbs onto

Table 1 Values of $N_{site,fresh}$, $N_{site,3min}$, $N_{site,120min}$ and conversions at 3 and 120 min for three catalysts

Time	0 min	3 min		120 min		
Catalyst	$N_{site,fresh} \times 10^{-21}$ [site/kg]	Conversion [%]	$N_{site,3min} \times 10^{-21}$ [site/kg]	Conversion [%]	$N_{site,120min} \times 10^{-21}$ [site/kg]	$N_{site,120min}/N_{site,fresh}$
$Pt/\gamma\text{-}Al_2O_3$	29.0	17.0	12.5	1.5	1.33	0.046
$Pt\text{-}Sn/\gamma\text{-}Al_2O_3$	18.2	17.1	8.2	1.8	0.82	0.045
$Pt\text{-}Sn\text{-}K/\gamma\text{-}Al_2O_3$	5.24	29.8	3.6	6.7	0.67	0.128

one metal active site (Burch *et al.*, 1994). Measurements were made using a pulse method. This technique involved pulsing a known volume of carbon monoxide over a catalyst sample at room temperature. The carbon monoxide that was not adsorbed was measured using a gas chromatography with a thermal conductivity detector. Pulses were continued until no further carbon monoxide adsorption was observed. The quantity of carbon monoxide adsorbed by the catalyst sample could then be calculated and hence the amount of metal active sites obtained.

1.3 Experiment

Dehydrogenation of propane was carried out in a micro reactor installed in a furnace with a temperature controller. The reactor was a quartz tube reactor whose inner diameter was 6.35 mm. The catalyst was packed in the middle of the quartz tube. Hydrogen gas was used to reduce the catalyst for 1 h, and then argon was used for purging hydrogen. The feed gas supplied by Thai Industrial Gases Limited was mainly a mixture of 3% propane in nitrogen. The experiment was performed at 773 K unless otherwise specified.

2. Kinetics

The rate equation for the dehydrogenation reaction can be expressed in the following simple form

$$-r_A = k_{app}\left(p_A - \frac{p_B p_C}{K}\right) = k_{app}\left(\frac{p_{Ao}(1-X_A)}{(1+y_{Ao}X_A)} - \frac{(p_{Bo}+p_{Ao}X_A)(p_{Co}+p_{Ao}X_A)}{(1+y_{Ao}X_A)^2 K}\right) \quad (1)$$

$$k_{app} = \frac{F_{Ao}}{W}\int_0^{X_A} \frac{dX_A}{\left(\frac{p_{Ao}(1-X_A)}{(1+y_{Ao}X_A)} - \frac{(p_{Bo}+p_{Ao}X_A)(p_{Co}+p_{Ao}X_A)}{(1+y_{Ao}X_A)^2 K}\right)} \quad (2)$$

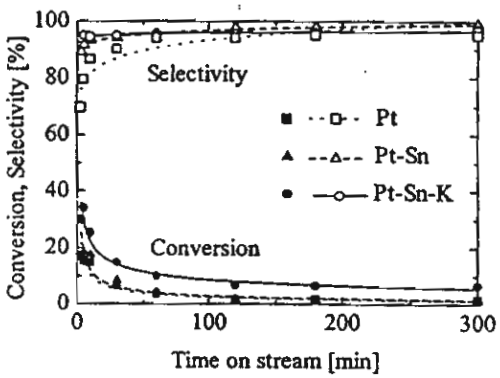

Fig. 1 Conversion and selectivity with time on stream: $F_{Ao} = 6.24 \times 10^{-7}$ mol/s, $T = 773$ K, $W = 0.1$ g, $y_{Ao} = 0.03$, $p_{Ao} = 3039$ Pa, $p_{Bo} = p_{Co} = 0$ Pa

By assuming a plug flow reactor, the apparent rate constant k_{app} can be determined as

The equilibrium constant, K can be calculated from Gibb's free energy data at different temperatures and correlated as the following expression.

$$K = 1.76 \times 10^{12} \exp(-15{,}521/T) \quad (3)$$

3. Results and Discussion

3.1 Comparison between catalysts

A set of experiment was carried out to compare the performance of $Pt/\gamma\text{-}Al_2O_3$, $Pt\text{-}Sn/\gamma\text{-}Al_2O_3$, and $Pt\text{-}Sn\text{-}K/\gamma\text{-}Al_2O_3$ catalysts. The conversion and selectivity to propene were measured as shown in **Fig. 1**. The propane molar flow rate was fixed at 6.24×10^{-7} mol/s, and the catalyst weight was 0.1 g.

All catalysts are highly selective towards propene, and the selectivities are higher than 95%. In addition, the conversions of all the catalysts decrease with time on stream, and reach the asymptotes after 120 min. Deactivation may be due to coke formation on the catalyst. The addition of Sn on $Pt/\gamma\text{-}Al_2O_3$ catalyst improves the conversion of $Pt/\gamma\text{-}Al_2O_3$ catalyst. This can be explained by the ensemble effect in which the addition of Sn results in an increase in Pt dispersion and, hence, the stability of the catalytic activity is improved from

Table 2 Values of k_{app} and k_{site} for three catalysts

Time	3 min		120 min		
Catalyst	$k_{app,3min} \times 10^7$ [mol/(kg·s·Pa)]	$k_{site,3min} \times 10^{28}$ [mol/(site·s·Pa)]	$k_{app,120min} \times 10^7$ [mol/(kg·s·Pa)]	$k_{site,120min} \times 10^{28}$ [mol/(site·s·Pa)]	$k_{site,average} \times 10^{28}$ [mol/(site·s·Pa)]
Pt/γ-Al_2O_3	5.3	0.42	0.59	0.44	0.43
Pt-Sn/γ-Al_2O_3	5.7	0.70	0.54	0.64	0.67
Pt-Sn-K/γ-Al_2O_3	11.0	3.09	1.9	2.86	2.98

the reduced amount of coke depositing on the metal active sites (Barias *et al.*, 1996; Krishnamurthy, 1998). Moreover, the addition of Sn can improve the selectivity to propene due to blocking or poisoning of acid sites on the support (Barias *et al.*, 1995). Figure 1 also shows that Pt-Sn-K/γ-Al_2O_3 catalyst gives the highest conversion. This may be explained by three reasons, i.e.; (1) alkali metals such as potassium enhance hydrogen spillover on the catalyst surface; (2) alkali metals reduce the amount of coke depositing on the active sites (Praserthdam *et al.*, 1997); and (3) alkali metals neutralize the acid sites of the alumina support (Demiguel *et al.*, 1995).

3.2 Kinetic studies

As preliminary experiments, operating conditions where the resistances of external mass transfer and internal mass transfer are negligible were searched to obtain intrinsic kinetics. In this study, only Pt-Sn-K/γ-Al_2O_3 catalyst with the highest activity was tested. To investigate the effect of external mass transfer on the conversions, the experiment was carried out by using the same value of time factor, W/F_{A0} = 160 s·kg/mol and the catalyst mesh size of 60–80 mesh. The feed flow rate was varied between 2.5–10.0 × 10^{-7} m^3(STP)/s. The resistance of external mass transfer could be neglected when the feed flow rate was higher than 7.5 × 10^{-7} m^3(STP)/s. Another set of experiment was carried out to investigate the effect of internal mass transfer on conversion. Three ranges of catalyst sizes, 60–80, 200–250 and 250–325 meshes, were tested under the same operating conditions such as the catalyst weight of 0.1 g, operating temperature of 773 K, and propane molar flow rate of 9.63 × 10^{-7} mol/s. The resistance of internal mass transfer was negligible for the catalyst size smaller than 60–80 mesh.

In order to determine the reaction rate constants, it was assumed that the decrease of catalyst activity was due to the formation of coke on metal active sites, and that the dehydrogenation of propane reached steady state within seconds (Larrson *et al.*, 1997, 1998). The experiment was carried out using 0.1 g of catalyst. The operating temperature was 773 K and the propane molar flow rate was 9.63 × 10^{-7} mol/s. **Table 1** summarizes the number of metal active sites of fresh catalysts and those of used catalysts after 3 and 120 min together with their corresponding conversions. The apparent reaction rate constants, k_{app} (calculated from Eq. (2)) at 3 and 120 min reaction times on stream are also presented in **Table 2**. It should be noted that the last column in Table 1 also provides some insight into the superior stability of the Pt-Sn-K/γ-Al_2O_3 catalyst by comparing the ratio of the metal active site of spent catalyst at 120 min (the values at the asymptotes) and of fresh catalysts, $N_{site,120min}/N_{site,fresh}$. It is clearly seen that the value of Pt-Sn-K/γ-Al_2O_3 catalyst is higher than the others. In other words, deactivation of the Pt-Sn-K/γ-Al_2O_3 catalyst is less than the other catalysts.

The reaction rate constants based on the number of active sites, k_{site}, is defined as follows.

$$k_{site} = k_{app}/N_{site} \tag{4}$$

The values of the reaction rate constants, k_{site}, can be determined from the number of available active sites, N_{site} in Table 1 and are also presented in Table 2. The average reaction rate constant of Pt-Sn-K/γ-Al_2O_3 ($k_{site,average}$ = 2.98 × 10^{-28} mol/(site·s·Pa)) is higher than those of Pt-Sn/γ-Al_2O_3 (0.67 × 10^{-28} mol/(site·s·Pa)) and Pt/γ-Al_2O_3 (0.43 × 10^{-28} mol/(site·s·Pa)). This implies that the presence of Sn does not significantly alter the strength of the metal active site while the presence of potassium increases the strength. This phenomena was also addressed previously by Demiguel *et al.* (1995), where it was found that the addition of alkali metals produced a modification of the characteristics of the metallic phase which involved an electronic modification of the metallic phase.

To confirm the value of reaction rate constant of Pt-Sn-K/γ-Al_2O_3, one experiment was carried out using the same conditions except for a 20% mixture of propane in nitrogen. The obtained reaction rate constant of 3.08 × 10^{-28} mol/(site·s·Pa)) agrees well with that of 3% propane (2.98 × 10^{-28} mol/(site·s·Pa)).

To complete the kinetics for Pt-Sn-K/γ-Al_2O_3 the reaction rate constants were determined at different temperatures from 723 to 873 K. The obtained results fit very well with Arrhenius's equation as shown in **Fig. 2**. The following expression can be determined.

$$k_{site} = 6.14 \times 10^{-24} \exp(-7{,}545/T) \tag{5}$$

The activation energy was 62.7 kJ/mol.

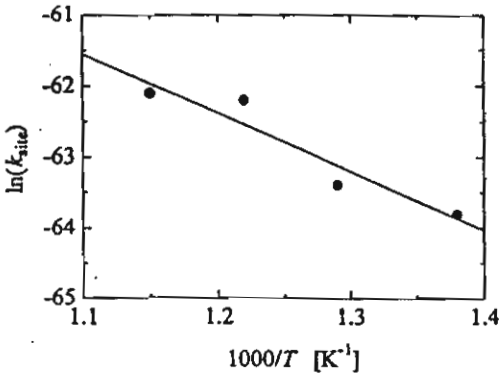

Fig. 2 Arrhenius plot for Pt-Sn-K/γ-Al_2O_3

Conclusion

The performance of Pt/γ-Al_2O_3, Pt-Sn/γ-Al_2O_3 and Pt-Sn-K/γ-Al_2O_3 catalysts were investigated. All catalysts exhibit the selectivity towards propene higher than 95%. Pt-Sn-K/γ-Al_2O_3 appears to be the most suitable catalyst for dehydrogenation of propane. The reaction rate constant based on the number of metal active site for Pt/γ-Al_2O_3, Pt-Sn/γ-Al_2O_3 and Pt-Sn-K/γ-Al_2O_3 catalysts at 773 K are 0.43×10^{-28}, 0.67×10^{-28} and 2.98×10^{-28} mol/(site·s·Pa), respectively. Arrhenius's equation can be determined by changing temperatures.

Acknowledgment

This research was financially supported by the Thailand Research Fund and TJTTP-OECF.

Nomenclature

F_{Ao}	=	feed flow rate of propane	[mol/s]
K	=	equilibrium constant	[Pa]
k_{app}	=	apparent reaction rate constant	[mol/(kg·s·Pa)]
k_{site}	=	reaction rate constant based on active site	[mol/(site·s·Pa)]
N_{site}	=	number of active site	[site/kg]
p_i	=	partial pressure of component i	[Pa]
$-r_A$	=	rate of reaction	[mol/(kg·s)]
W	=	catalyst weight	[kg]
X_A	=	reaction conversion	[—]
y_{io}	=	initial mole fraction of component i in the feed inlet	[—]

<Subscript>

A	=	propane
B	=	propene
C	=	hydrogen
o	=	condition at feed inlet

Literature Cited

Barias, O. A., A. Holmen and E. A. Blekkan; "Propane Dehydrogenation over Supported Platinum Catalysts—Effect of Tin as a Promoter," *Cat. Tod.*, 24, 361–364 (1995)

Barias, O. A., A. Holmen and E. A. Blekkan; "Propane Dehydrogenation over Supported Pt and Pt-Sn Catalysts: Catalyst Preparation, Characterization, and Activity Measurements," *J. Cat.*, 158, 1–12 (1996)

Burch, R., P. J. Millington and A. P. Walker; "Mechanism of the Selective Reduction of Nitrogen Monoxide on Platinum-Based Catalysts in the Presence of Excess Oxygen," *App. Cat. B: Envi.*, 4, 65–94 (1994)

Demiguel, S. R., A. A. Castro, O. A. Scelza and J. Soria; "Effect of the Addition of Alkali-Metals on the Metallic Phase of Pt/Al_2O_3 Catalysts," *Cat. Letts.*, 32, 281–291 (1995)

Krishnamurthy, K. R.; "Modifications in Supported Metal Catalysts: Effect of Promoters," *Recent Advances in Basic and Applied Aspects of Industrial Catalysis*, 113, 139–150 (1998)

Larrson, M., N. Henriksson and B. Andersson; "Estimation of Reversible and Irreversible Coke by Transient Experiments," *Catalyst Deactivation*, 111, 673–680 (1997)

Larrson, M., N. Henriksson and B. Andersson; "Investigation of the Kinetics of a Deactivating System by Transient Experiments," *App. Cat. A*, 166, 9–19 (1998)

Praserthdam, P., T. Mongkhonsi, S. Kunatippapong, B. Jaikaew and N. Lim; "Determination of Coke Deposition on Metal Active Sites of Propane Dehydrogenation Catalysts," *Catalyst Deactivation*, 111, 153–158 (1997)

Sheintuch, M. and R. M. Dessau; "Observations, Modeling and Optimization of Yield, Selectivity and Activity during Dehydrogenation of Isobutane and Propane in a Pd Membrane Reactor," *Chem. Eng. Sci.*, 51, 535–547 (1996)

Weyten, H., K. Keizer, A. Kinoo, J. Luyten and R. Leysen; "Dehydrogenation of Propane Using a Packed-Bed Catalytic Membrane Reactor," *AIChE J.*, 43, 1819–1827 (1997)

Yildirim, Y., E. Gobina and R. Hughes; "An Experimental Evaluation of High-Temperature Composite Membrane Systems for Propane Dehydrogenation," *J. Mem. Sci.*, 135, 107–115 (1997)

Dependence of Hydrogen Pressure on the Permeation Rate through Composite Palladium Membranes

SHIGEO GOTO[1], SUTTICHAI ASSABUMRUNGRAT[2], TOMOHIKO TAGAWA[1] AND PIYASAN PRASERTHDAM[2]

[1]*Department of Chemical Engineering, Nagoya University, Nagoya 464-8603, Japan*

[2]*Department of Chemical Engineering, Faculty of Engineering, Chulalongkorn University, Bangkok 10330, Thailand*

Reprinted from
JOURNAL OF CHEMICAL ENGINEERING OF JAPAN
Vol. 33, No. 2 (2000)
Pages 330–333

Journal of Chemical Engineering of Japan, Vol. 33, No. 2, pp. 330–333, 2000

Dependence of Hydrogen Pressure on the Permeation Rate through Composite Palladium Membranes

SHIGEO GOTO[1], SUTTICHAI ASSABUMRUNGRAT[2], TOMOHIKO TAGAWA[1] AND PIYASAN PRASERTHDAM[2]

[1]*Department of Chemical Engineering, Nagoya University, Nagoya 464-8603, Japan*

[2]*Department of Chemical Engineering, Faculty of Engineering, Chulalongkorn University, Bangkok 10330, Thailand*

Keywords: Membrane Reactor, Composite Palladium Membrane, Order, Permeation Rate Expression

A composite pailadium membrane consists of a thin film of palladium layer coated on a ceramic support. Two kinds of models are formulated for the direction of permeation through the composite membrane (CP mode and PC mode). The apparent order of hydrogen pressure is varied from 0.5 to 1.0 by the relative values between two resistances of palladium film and ceramic support for the hydrogen permeation rate through the composite membrane. The relation between the apparent order and the relative resistance is dependent on the operating conditions. Once the apparent order can be determined from the linearity of experimental data, we can estimate the relative resistance.

Introduction

A composite palladium membrane consists of a thin film of palladium layer coated on a ceramic support. Since the defectless palladium film in the composite membrane can be made much thinner on an asymmetric ceramic support than the normal dense membrane, the resulting permeation rate may be significantly improved. The ceramic support provides the mechanical strength for the membrane; however, the small pore diameter of such ceramic supports may affect the permeation rate. Nowadays, this type of composite membrane has become attractive for applications in the field of membrane reactors due to its superior permeability and permselectivity to hydrogen (Dittmeyer *et al.*, 1999).

There are two directions of hydrogen permeation through the composite palladium membrane, that is, CP mode (at first through the ceramic support and then through the palladium film) and PC mode (opposite manner). The permeation rate for CP mode is higher by 20% than that for PC mode in some cases (Goto *et al.*, to be submitted).

It is well-known through Sievert's law that the pressure dependence of hydrogen is half order through the palladium film. On the other hand, the pressure dependence of hydrogen is first order through the ceramic support due to Knudsen and molecular diffusions. In the composite membrane, the apparent order may be in the range between 0.5 and 1. For example, the values of 0.552–0.622 (Collins and Way, 1993), 0.68 (Hurlbert and Konecny, 1961), 0.76 (Umemiya *et al.*, 1991) and 0.80 (DeRosset, 1960) were reported as the apparent order. Umemiya *et al.* (1991) explained the reason for this discrepancy from Sievert's law in that hydrogen diffusivity might vary with the concentration of hydrogen.

In this work, the deviation of the apparent order from Sievert's law for the permeation of hydrogen through the composite membrane is illustrated by relating the apparent order with the relative resistances of the palladium film and the ceramic support.

Received on October 14, 1999. Correspondence concerning this article should be addressed to S. Goto (E-mail address: goto@park.nuce.nagoya-u.ac.jp).

1. Mathematical Model

The permeation rate of hydrogen through a composite membrane may be expressed by an apparent order, n as follows:

$$Q_H = \alpha_{H,app}\left\{\left(p_{H,R} / p_0\right)^n - \left(p_{H,S} / p_0\right)^n\right\} \quad (1)$$

1.1 CP mode

Performing the material balance of hydrogen, a set of equations can be obtained. Let $p_{H,M}$ be the pressure of hydrogen at the membrane interface between the palladium film and ceramic support. Since transport through the support may mainly be governed by the first order of pressure of hydrogen, the permeation rate, Q_H can be expressed as

